CONDITION MONITORING OF SQUIRREL CAGE INDUCTION GENERATORS IN WIND TURBINES

by

IAN RADCLIFFE KUILER

Thesis submitted in fulfilment of the requirements for the degree

Master of Engineering: Electrical Engineering

in the Faculty of Electrical, Electronic and Computer Engineering

at the Cape Peninsula University of Technology

Supervisor: Dr M Adonis
Co-supervisor: Dr A Raji

Bellville
March 2017

DECLARATION

I, Ian Radcliffe Kuiler, declare that the contents of this thesis represent my own unaided work, and that the dissertation/thesis has not previously been submitted for academic examination towards any qualification. Furthermore, it represents my own opinions and not necessarily those of the Cape Peninsula University of Technology.

Signed	**Date**

ABSTRACT

Globally governments are faced with challenges in the energy sector which are exacerbated by uncertain financial markets and resource limitations. The over utilization of fossil fuels for electricity generation has had a profound impact on the climatic conditions on earth. Coal power stations release carbon dioxide (CO_2) during the combustion process and studies show that concentrations have sharply risen in the atmosphere. Adverse environmental conditions like global warming exist as a result of high greenhouse gas (GHG) emissions in particular CO_2.

In 2015 Eskom constructed Sere Wind farm with a supply capability of 100 MW. Due to the lack of technical expertise and skills with regard to the new technology within Eskom, Siemens was offered a 5 year maintenance contract. Siemens also provides training on basic operation and maintenance (O&M) of the wind farm to Eskom staff. This excludes specialised training on Siemens Turbine Condition Monitoring (TCM) systems which is a critical part to develop optimum maintenance strategies.

This shortage of specialised skills in the application of condition monitoring techniques within Eskom is a major concern. If the most cost effective maintenance strategies during the contract period are implemented, the long term plant health and design life of Sere wind farm will be reduced. There is a need to develop new condition monitoring techniques to complement or address the shortcomings of the existing systems. Developing these skills will increase the understanding of the technology and improve the operating and maintenance of Sere wind farm.

ACKNOWLEDGEMENTS

I wish to thank:

DEDICATION

To God be the Glory!

TABLE OF CONTENTS

LIST OF FIGURES

LIST OF TABLES

GLOSSARY

AEP	Annual Energy Production
AP	Active Power
ANOVA	Analysis of Variance
AT	Ambient Temperature
CF	Capacity Factor
CO_2	Carbon dioxide
CO_2eq	Carbon dioxide equivalent
DFIG	Double fed Induction Generator
DoE	Department of Energy
EU	European Union
EWEA	European Wind Energy Association
FFT	Fast Fourier Transform
GHG	Greenhouse Gasses
GW	Gigawatt
GWEC	Global Wind Energy Council
GWh	Gigawatt-hour
GUI	Graphical User Interface
HAWT	Horizontal Axis Wind Turbines
IEA	International Energy Agency
IPCC	Intergovernmental Panel on Climate Change
IRENA	International Renewable Energy Agency
IRP	Integrated Resource Plan
kWh	Kilowatt hour
LCOE	Levelised cost of electricity
MCSA	Motor Current Signal Analysis
MLR	Multiple Linear Regression
MTBF	Mean Time Between Failure
Mtoe	Million tonnes oil equivalent
MW	Megawatt
NT	Nacelle Temperature
O&M	Operating and Maintenance
OCGT	Open cycle gas turbine
ppm	Parts per million
ppmv	Parts per million volume
PV	Photovoltaic
PWM	Pulse Width Modulation
PWh	Petawatt hours
PWh/y	Petawatt hours per year
REIPPPP	Renewable Energy Independent Power Producer Procurement Program
REN21	Renewable Energy Policy Network for the 21st Century
SCADA	Supervisory Control and Data Acquisition
SCIG	Squirrel Cage Induction Generator
SR	Stepwise Regression
TSR	Tip Speed Ratio
TWh	Terawatt hours
TWh/y	Terawatt hours per year
USD	United States Dollars
VAWT	Vertical Axis Wind Turbine
WEC	Wind Energy Converter
WT	Wind Turbine

CHAPTER ONE
STUDY OVERVIEW

1.1   Introduction

Economic development and social welfare are mainly supported by reliable and cost effective energy systems. The inter relationships between energy; food and water are becoming more critical as resources become depleted, scarce and expensive. Forecasts are that energy demand will double in the next 30 years while food and water needs will increase by half worldwide [1]. These challenges are further aggravated by unstable financial systems and degrading environmental conditions.

Africa is blessed with abundant renewable energy sources, minerals and rich fossil fuels supplies. In South Africa, electrification rates are high and only 15% of its population are without electricity supply [2]. South Africa has the second largest energy demand of 141 Mtoe behind Nigeria and is the only African country which per capita energy demand is higher than the global mean [3]. As the largest electricity producer and carbon dioxide emitter on the African continent [4], South Africa can benefit through the deployment of renewable energy technologies.

In 2010 the Department of Energy (DoE) released its Integrated Resource Plan (IRP) which aims to diversify the current coal dominated energy mix by incorporating renewable energy technologies like wind and solar energy. The objective of the IRP (2010) was to add 42 % of the new power generating capacity from wind and solar energy technologies by 2030 [5]. The planned wind energy capacity is 8.4 GW as stipulated in the IRP (2010). There are already 15 wind farm projects in full commercial operation, adding just over 1 GW of wind power to the national grid [6]. These projects were implemented through the Renewable Energy Independent Power Producer Procurement Programme (REIPPPP) which was established by the DoE.

1.2   Background

The Intergovernmental Panel on Climate Change (IPCC) recommends that GHG emissions in the atmosphere settle between 445 – 490 ppm CO_2eq to limit the rise in mean global temperature to 2 °C above preindustrial levels [7]. All GHG emissions have increased over time more noticeable the CO_2 levels which was 396 ppmv in 2013 in comparison to the stable level of 280 ppmv during the pre-industrial area [8].

Figure 1 [8] shows how the combustion of fossil fuels used for electricity generation over the decades changed CO_2 concentrations in the atmosphere.
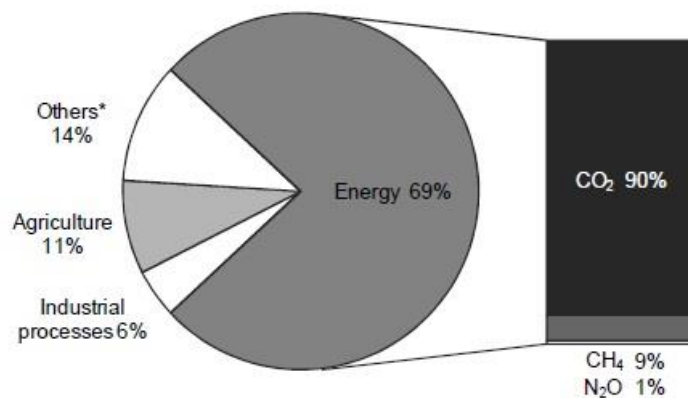
Figure 1: Worldwide contributions of human related GHG in 2010

Matured renewable energy technologies like wind and solar photovoltaic (PV) are less resource intensive compared to conventional power systems. Wind energy systems produce no greenhouse gasses and use no water during power generation. Renewable energy sources have made a significant contribution towards global energy consumption in the last 10 years as shown by **Figure 2** [9].
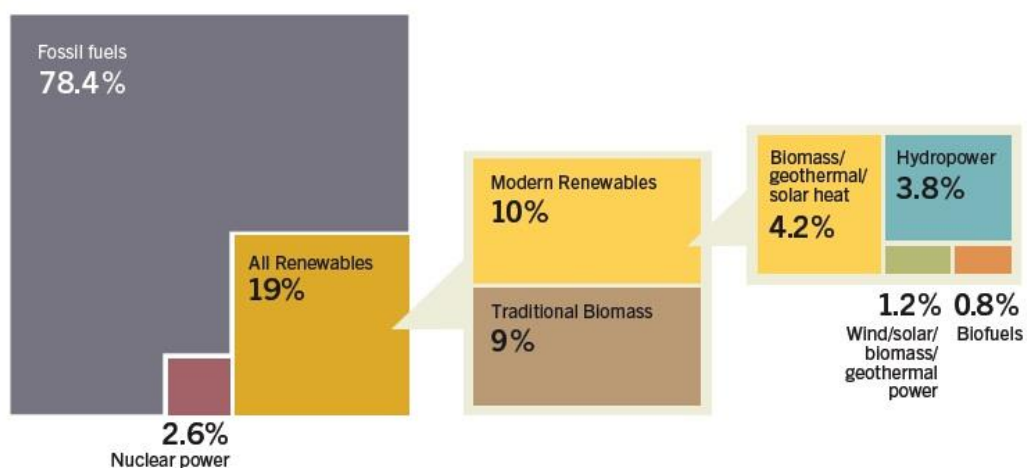
Figure 2: Renewable energy percentage of global final energy consumption 2013

The Department of Energy (DoE) is responsible for providing reliable, cost effective and sustainable energy systems that support the socio-economic development of South Africa. The DoE has implemented the Renewable Energy Independent Power Producer Procurement Program (REIPPPP) in 2011 to execute various renewable energy targets as captured in major policy documents such as:

- White Paper on Renewable Energy (2003);
- National Development Plan (NDP 2011);
- Integrated Resource Plan (IRP 2010).

During 2014 wind and solar PV projects saved an estimated R3.7 billion in diesel and coal fuel expense while the benefit to the economy for not experiencing load shedding amounted to R1.6 billion [10]. The fuel cost savings from wind energy alone was 1.62 R/kWh compared to the tariff of 1.38 R/kWh for the 1st bidding window in the REIPPPP [10].

The following energy sources are used by Eskom to generate electricity with their respective net output [11]:

- Coal (34 952 MW);
- Nuclear (1 830 MW);
- Hydro and Pumped-hydro (2 000 MW);
- OCGT (2 426 MW);
- Wind (100 MW).

New build power stations currently under construction are Medupi and Kusile coal power stations each rated at 4800 MW as well as Ingula Pumped-hydro scheme which has a capacity of 1 332 MW. All these power stations are running behind schedule and are not fully commissioned. Eskom also imports hydro power (1 500 MW) from Cahora Bassa hydro-electric scheme via Mozambique.

Since November 2013 until June 2015 the REIPPPP produced 4 294 GWh of renewable energy [12] which stabilized the grid during unavailable base load coal power generation. Wind energy's contribution was 1 991 GWh and together with solar PV produced 15% of the total energy demand during peak load [12].

1.3   Project statement and objectives

Eskom diversified its carbon based power generation plant and constructed their largest renewable power generating facility called Sere wind farm. Sere wind farm produces 100 MW of wind energy from 46 Siemens manufactured wind turbines. The wind power facility started commercial operation in the beginning of 2015. Because of the huge capital infrastructure investment and the skills shortage on this new technology Eskom decided to sign an O&M contract with Siemens for 5 years. Siemens is therefore accountable to ensure that the wind farm produces cheap wind power while meeting the performance criteria as stipulated in the maintenance contract.

Siemens implements a combination of vibration analyses and use based maintenance at Sere wind farm. Vibration data is continuously analysed by highly skilled Siemens staff from their remote location in Denmark. Specific maintenance instructions are then communicated to Siemens staff at the wind farm. Eskom is currently not involved in making these maintenance decisions. The utility has the opportunity to develop additional maintenance strategies in conjunction with the existing Siemens documents. This could increase the knowledge within the company and improve the life cycle management of their wind turbines.

The electrical generator is one of the main components in a wind turbine and its value is approximately 3.44 % of the total capital cost [13]. The generator also has the second highest replacement rate during a ten year period besides the rotor blades [14]. Failure of the generator can result in equipment damage, loss of power to the grid, long downtimes which amount to huge financial losses. Majority failures in wind turbine generators result from bearing and stator winding failures [15]. This study focuses on detecting and preventing stator winding failures in squirrel cage induction generators.

Induction generators dominate the generator market in wind turbines. There are two designs namely double fed induction generators (DFIGs) and squirrel cage induction generators (SCIGs). DFIG topologies are preferred by most wind turbine manufacturers and thus majority of research has been devoted to develop reliability and failure prediction models for this technology.

There is an opportunity to develop such models for SCIGs in variable speed wind turbines similar to Sere wind farm. These tools can assist Eskom to improve operating and maintenance (O&M) of their SCIG fleet. This study proposes the implementation of statistical and simulation models to develop condition monitoring techniques for stator windings in SCIGs.

Research objectives:

- Develop a statistical model with the aid of SCADA data. This model predicts stator winding temperatures over the entire operating range of the wind turbine.
- Perform a simulation study using MATLAB / Simulink software to evaluate the performance of the SCIG at rated steady state conditions. The model simulates stator winding degradation by varying the equivalent circuit parameters of a SCIG.
- Increase the knowledge of grid connected variable speed SCIGs.

Research questions:

- What factors cause stator winding degradation?
- Does SCADA data provide enough information to detect abnormal stator winding conditions?
- Can manipulation of the equivalent circuit parameters at steady state conditions simulate degradation in stator winding condition?

1.4   Thesis Layout

This section summarise the main objectives of each chapter and details the relevant contribution of the research. The research document is divided into 5 chapters.

- *Chapter 1* – Describes how the usage of fossil fuels mainly coal combustion for electricity generation has changed GHG in the atmosphere. It highlights that CO_2 levels post-industrial times have increased considerably because of coal related energy generation. It gives a brief overview of the South African energy mix and the policy mechanisms the country have implemented to develop a less carbon intensive energy system. The study statement and objectives are also discussed in this chapter.
- *Chapter 2* – This chapter gives an in-depth view of the associated literature studied on the main aspects of wind energy development. It presents an overview of the wind market, maintenance strategies, generator topologies and failure mechanisms of wind turbines.
- *Chapter 3* – Explains the methodology used to develop the statistical and simulation models for stator winding condition monitoring. The linear regression model in Microsoft Excel is discussed and all the variables that is important for stator winding temperature prediction. The mathematical derivation of the equivalent circuit parameters are also presented as well as the induction generator model in MATLAB.
- *Chapter 4* – Presents a detailed analysis of the results obtained from the statistical and simulation models. The accuracy of the models is validated in the section by applying it to real-time operating data of two wind turbines.
- *Chapter 5* – This chapter draws conclusions of the work and identifies areas for future research work. Recommendations are made on the outcome of the results.

CHAPTER TWO
LITERATURE REVIEW

In this section the literature review is presented. A global overview of the wind energy market is discussed, cost of wind energy, generator topologies, wind turbine failure rates and modes and maintenance strategies. A summary of variable speed wind turbines using SCIGs connected to the national grid is given.

2.1   Global wind energy resource and installed capacity overview

For centuries the wind has been used for pumping water, boat sailing, grinding food and its application for electricity generation only developed late in the 19th century when a 12 kW DC generator was built [16]. Advances in wind technology and turbine designs have improved performance and reduce costs. The sizes of wind turbines have increased for both onshore and offshore applications recently. The largest wind turbine is the V164 produced by the Danish wind company Vestas, rated at 8 MW and with blade lengths of 80 metres [17]. The estimated global onshore wind energy resource potential is listed in **Table 1** [18].

Table 1: Global onshore wind resource and future electricity demand

World Region	Electricity demand by 2025 (TWhy^{-1})	Installed capacity (GW)	Wind resource (TWhy^{-1}) [Class 4+ sites]	Wind resource (TWhy^{-1}) [Class 3+ sites]
North America	6700	18 700	62 400	93 500
Latin America	1800	6100	20 400	36 300
Europe	6200	15 200	50 500	92 500
Western Europe	3100	4400	14 700	21 000
Eastern Europe & Former Soviet Union	3100	10 800	35 800	71 300
Africa/ Middle East	2200	10 400	34 700	71 300
Asia	8700	1900	6400	21 500
India	1300			
China	4300			
Other Asia	3100			
Australia/ Oceania	400	3200	10 700	20 200
World Total	26 000	70 400	185 000	335 400

Note: Class 3+ and 4+ include both classes and above

Figure 3 [9] shows that wind power has a global installed capacity of 370 GW as of end 2014. During this time an estimated 51 GW of wind energy was grid connected worldwide according to [9]. The industry has achieved an average growth rate above 25% since the millennium [16] and future growth for wind energy looks promising.
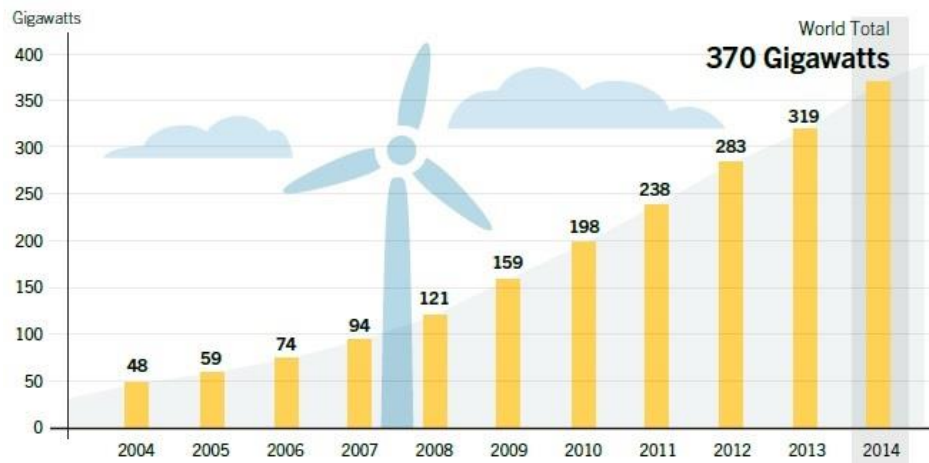
Figure 3: Estimated global installed wind power capacity between 2004 – 2014

According to the latest information on wind energy, 63 GW was added in 2015 bringing the global wind installed capacity to 432 GW [19]. Wind power in the European Union (EU) has the capacity to generate electricity consumption of 315 TWh during a calendar wind year [20]. Germany has the largest installed wind capacity of any EU country with 45 GW and during last year the country accounted for 47% of new wind energy installations [20]. In 2014 global wind energy investments made up 36.8% of the total investments in renewable energy [9].

Wind power in Denmark already provided 39% of electricity consumption in 2014 and by 2024 is expected to supply 23.3 TWh [21]. Currently the US produces less than 5% of their electricity from wind while other countries like Spain, Portugal and Ireland generate around 20% or more [9].

Figure 4 [19] illustrates the combined installed wind energy capacity of the leading ten countries worldwide as of 2015. Although China has the largest global installed wind capacity, wind energy produces less than 3% of their electricity which is small compared to other power generating systems.

Country	MW	% Share
PR China**	145,104	33.6
USA	74,471	17.2
Germany	44,947	10.4
India	25,088	5.8
Spain	23,025	5.3
United Kingdom	13,603	3.1
Canada	11,200	2.6
France	10,358	2.4
Italy	8,958	2.1
Brazil	8,715	2.0
Rest of the world	66,951	15.5
Total TOP 10	**365,468**	**84.5**
World Total	**432,419**	**100**
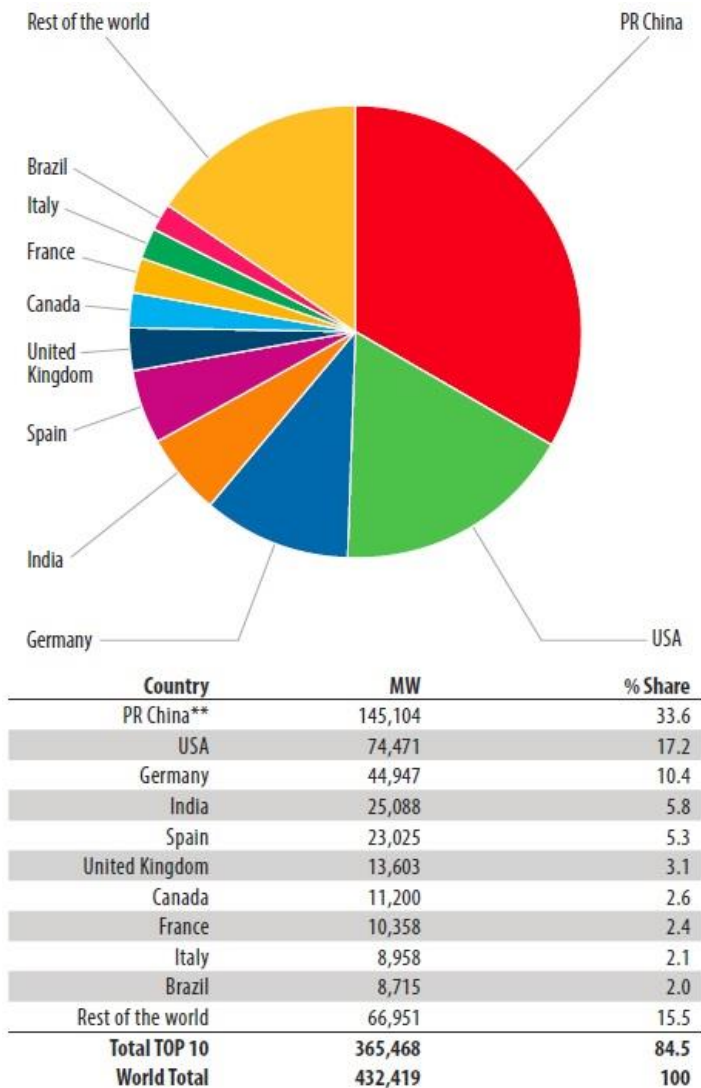
Figure 4: Combined wind power capacity of the ten leading countries by 2015

2.2 Africa and South African wind energy resource and installed capacity overview

South Africa is considered as the market leader in renewable energy attracting USD 5.5 billion out of USD 8 billion on the African continent in 2014 [22]. Wind energy in the country has seen rapid growth through the REIPPPP and is now the cheapest source of electricity through four competitive bidding rounds. The wind resources are the best around the coastal regions of the country and the major African regions have the following estimated technical potentials [23]:

- Eastern Africa (170 PWh/year);
- Northern Africa (130PWh/year);
- Southern Africa (110 Wh/year);
- Western Africa (40 PWh/year) and
- Central Africa (10 PWh/year).

South Africa has a realistic wind energy potential of 26 GW which can provide approximately 80.6 TWh towards electricity consumption [24]. The breakthrough for wind energy in South Africa came during 2014 when 560 MW was installed [23]. **Figure 5** [25] illustrates the development of wind power generation as a result of the REIPPPP.

Figure 5: Wind energy profile during REIPPPP bid windows as of June 2015

The largest wind farm on the African continent is the impressive 300 MW Tarfaya project in Morocco [22] whereas big wind farms in South Africa range between 130 MW – 150 MW. A summary of the installed wind power capacity of the leading African countries as of end 2015 is given in **Table 2** [16].

Table 2: Installed wind power capacity of leading countries in Africa

Country	End of 2014	End of 2015
South Africa	570	1053
Morocco	787	787
Egypt	610	610
Tunisia	245	245
Ethiopia	171	324
Total (MW)	2383	3019

There are still various political, economic, technical and social barriers preventing rapid uptake of wind energy on the African continent. The variable nature of wind energy also presents its own challenges and a lack of infrastructure, design and condition of existing power systems could delay integration. In most instances a local developed wind industry is absent in African countries which further prevents wind energy to make a significant contribution.

The REIPPPP has successfully implemented around 34 utility scale wind projects with a capacity of 3 357 MW as summarised by **Figure 6** [26]. Of these projects an estimated 15 wind farms are fully operational with an installed capacity of 1 147 MW [6].

	BW1		BW2		BW3		BW3.5		BW 4		ALL	
	Capacity MW	Number of Projects	Capacity MW	Number of Projects	Capacity MW	Number of Projects	Capacity MW	Number of Projects	Capacity MW	Number of Projects	Capacity MW	Number of Projects
Onshore Wind	649	8	559	7	787	7			1 362	12	3 357	34
Solar PV	627	18	417	9	435	6			813	12	2 292	45
Solar CSP	150	2	50	1	200	2	200	2			600	7
Landfill Gas					18	1					18	1
Biomass					17	1			25	1	42	2
Small Hydro			14	2					5	1	19	3
	1425	28	1040	19	1457	17	200	2	2 205	26	6 327	92

Figure 6: Renewable energy generation projects up to mid-2015

There are currently five utility scale wind generating facilities that use SCIGs in their design [27]:

- Jeffreys Bay Wind Farm (138 MW, fully operational);
- Sere Wind Farm (100 MW, fully operational);
- Khobab Wind Farm (140 MW, under construction);
- Loeriesfontein 2 Wind Farm (140 MW, under construction) and
- Noupoort Mainstream Wind (80 MW, under construction.

It is evident that SCIGs in variable speed wind turbines connected to the South African power network will have a major impact in the future. As the level of wind power integration on the national grid increases, more variability is introduced and stringent measures are required to balance supply and demand. Accurate modelling of these generator concepts is required to estimate their grid performance and implement optimum maintenance strategies.

2.3   The cost of wind energy

Wind energy has reached commercial maturity remarkably fast and has seen its cost dropped significantly to such levels that it's now cost competitive with coal power generation. This trend has also been observed in other renewable energy technologies like solar PV. The levelised cost of electricity (LCOE) of onshore wind projects worldwide is around USD 0.05/kWh on a regular basis without any subsidies [28].

The real cost of wind energy in the United States (US) has reduced by 58% over the last five years bringing it in the same price range as coal and natural gas [29]. **Figure 7**[28] shows the weighted average electricity costs of various utility scale renewable energy technologies in comparison to fossil fuels from 2013 to 2014.
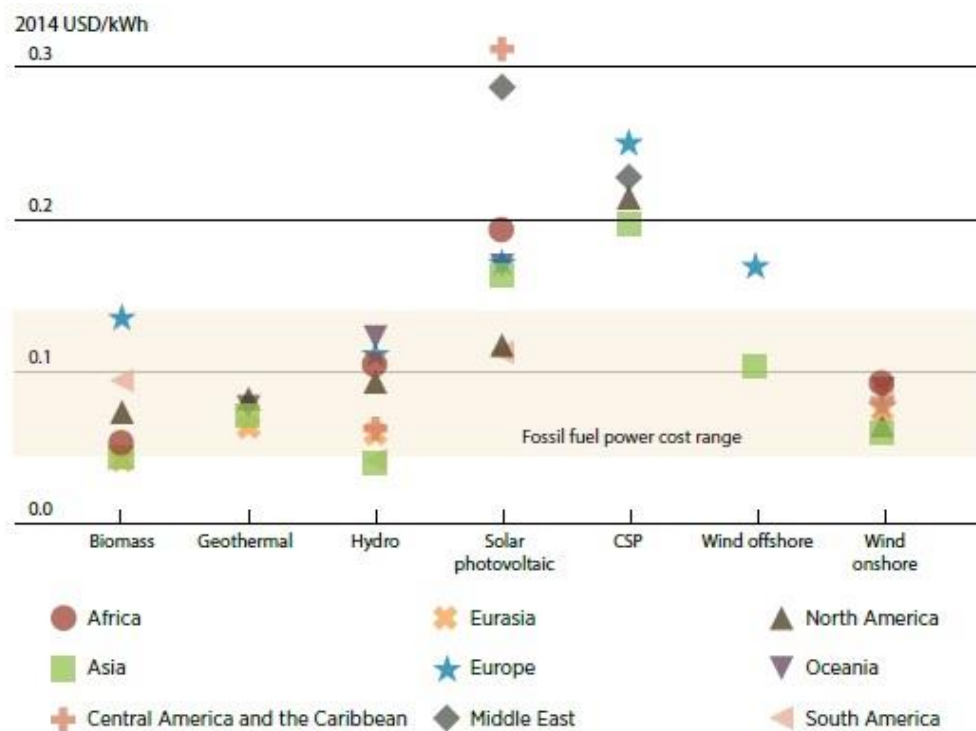
Figure 7: Weighted average cost of utility scale renewable energies versus fossil fuels

For any power generation technology, the cost of production is variable and influenced by technology maturity, operating conditions, location and the capacity rating of the plant [16]. The LCOE for wind energy is affected mainly by the following factors [28]:

- Operation and Maintenance (O&M) costs;
- Annual energy production (AEP);
- Capital costs;
- Financing costs.

Figure 8 [30] indicates the capital cost breakdown of all the major components of a typical onshore wind turbine and it is evident that the major costs are related to the turbine itself. Other costs such as manufacturing, delivery and erection are included in the overall cost of the wind turbine. LCOE can be reduced if wind turbine manufacturers enhance turbine technology so that a variety of designs are available for different wind resource conditions. This can be achieved through larger rotors, improved blade aerodynamics and taller towers.
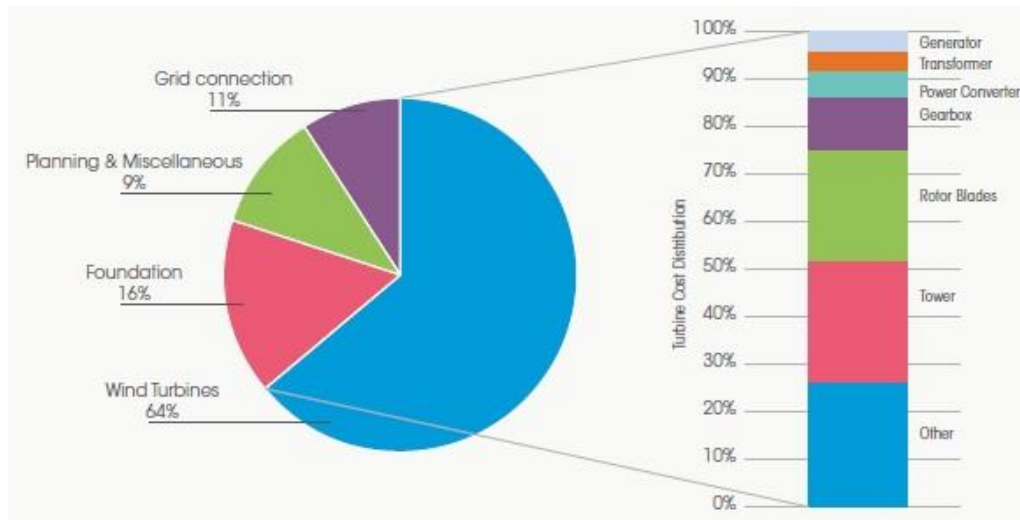
Figure 8: Typical onshore wind turbine capital cost breakdown

The capacity factor (CF) indicates how frequent the wind turbine was able to produce power at rated or name plate capacity over a given period which is normally a year. Capacity factors for onshore wind turbines are assumed to range between 30% - 35% [31]. This figure varies considerably depending on turbine design and the local wind resource. In conventional power generation technologies the AEP is generally proportional to the generator size. However in a wind turbine the rotor swept area can have a bigger influence than the generator size on the power generation capability [32].

Therefore the relationship between the rotor swept area and generator size can influence capacity factors of wind turbines. In other words a wind turbine with a specific rotor swept area connected to two different size generators will have different capacity factors. The smaller size generator will operate at a higher capacity factor compared to the bigger size generator with the same wind conditions. Wind turbine manufacturers should therefore optimize this relationship for specific site conditions and grid integration requirements to ensure the lowest possible costs.

O&M costs of wind turbines vary over the lifespan of the plant and escalate with age as the risks of failure of the equipment increase. The O&M costs of wind turbines have reduced considerable over the last 30 years and accounts between 20% - 30% of the total life cycle costs for onshore projects [33]. O&M costs for offshore wind projects are higher because of the severe operating conditions in the sea, access to site, complex maintenance tasks and transmission infrastructure costs. The costs for onshore wind projects are approximately USD 0.01/kWh versus USD 0.0.27/kWh to 0.054/kWh for offshore projects [28].

In South Africa the price for wind energy started at 1.36 R/kWh in bid window 1 and reduced to 0.62/ RkWh in bid window 4 [34]. This is a cost reduction of more than 50% between the four bid windows which are attributed to the competitiveness of the REIPPPP, increased local content and reduced capital cost of wind turbines [35]. The costs of wind energy in South Africa compare favourably with the weighted average LCOE of USD 0.06/kWh to 0.09/kWh [28].

2.4   Classification of wind turbines

The operating principle of all wind turbines make either use of aerodynamic lift or aerodynamic drag forces. Aerodynamic lift forces are perpendicular to the direction of the wind whereas drag forces are in the same direction [36]. Modern day wind turbines are mainly designed to use aerodynamic lift forces where the rotor blades are turned into the direction of the wind. The perpendicular lift force produce the required driving torque via the leverage of the rotor [37].

Only wind turbines operating on aerodynamic lift will be discussed and these are classified in accordance to the direction of the rotating axis i.e. horizontal axis wind turbines (HAWTs) and vertical axis wind turbines (VAWTs) [38]. In **Figure 9** a and b [39] the direction of the rotating axis in a HAWT is parallel to the ground whereas in a VAWT it's perpendicular to the ground.
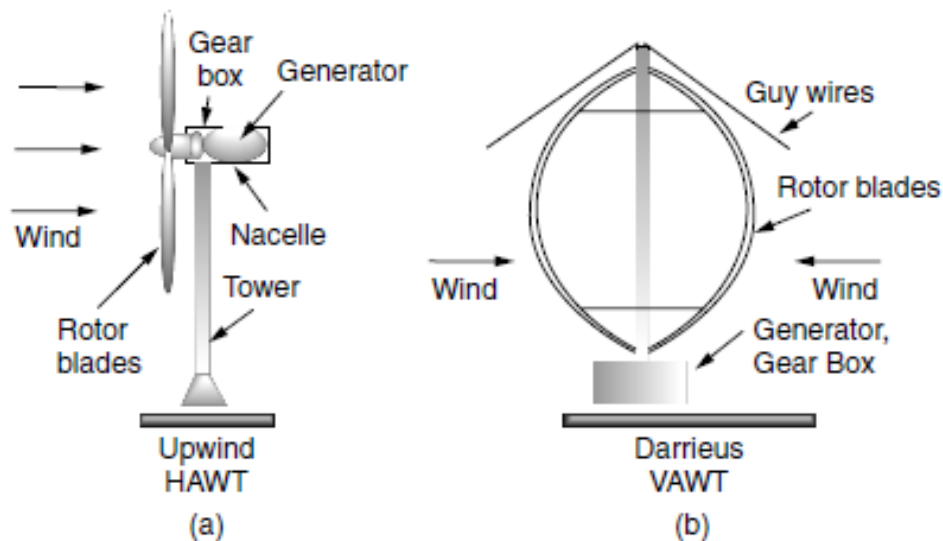
Figure 9: Wind turbine rotor designs

2.4.1   Horizontal axis wind turbines

Historically the design of HAWTs developed via three operating philosophies [40]:

- First philosophy designs concentrated on low tip speeds, enhance reliability and the capability to endure high wind loads;
- Second philosophy designs conformed to shed loads requirements and superior operation;
- The last and modern philosophy grid connected wind turbines are designed to handle electrical and or mechanical loads better even with a lower tip speed ratio than the second philosophy designs. It's visually more appealing, uses less material, is more cost effective and provides a smoother power output irrespective of temporary wind speed fluctuations.

Other factors influencing the design of HAWT are upwind or downwind rotor position, number of blades, rotor hub connection type, drivetrain or direct drive, fixed or variable speed, power control method and the rating of the wind turbine [41]. Wind turbines can also be installed in the sea, simply known as offshore wind turbines.

The majority of HAWTs are also known as axial flow equipment where the rotating axis is continuously moved by a "yaw drive system" in the direction of the wind [36]. The yaw drive system rotates the nacelle in the direction the wind blows and uses either an electrical or hydraulic system to perform this function. The nacelle is mounted on top of the tower, where the main components like the generator, gearbox and the rotor are located.

Wind turbine rotors suitable for electricity generation have predominantly three blades which deliver more stable output power, is more efficient, visually pleasing and experience less severe aerodynamic loading [42]. The rotor mass moment of inertia of three bladed rotors has polar symmetry which simplifies the structural dynamic equations, making them easier to solve and understand [40]. Two bladed wind turbines could be more suited for offshore wind power generation where wind resources are better, noise and aesthetic factors are less of a concern [36].

2.4.2 Vertical axis wind turbines

Designs of VAWTs were predominantly developed during 1970's and early 1980's but when it was concluded that HAWTs were more feasible, research in the technology slowed down [43]. Since then HAWTs has dominated the wind energy market and has provided excellent and reliable performance.

VAWTs can produce power irrespective of the wind direction and therefore its rotor doesn't require continuous alignment into the wind. The drive system and power generation units can be located at the base of wind turbine which reduces installation and maintenance costs [44]. The three main types of VAWT designs are the Savonius, Darrieus and the H-Rotor type [45].

Guide wires for some designs are installed for rotor shaft support and positioning as well as reducing mechanical vibrations [16]. For small power generation applications where other superior features of HAWTs are less essential, low noise operation and omni-directionally of VAWTs are preferred [46]. Because of blade design, the big angles of attack causes stalling [47] at low wind speeds which prevent self-starting of almost all types of VAWTs.

In grid connected applications this limitation can be resolved by starting the wind turbine via the grid as a motor [44]. It is recognized that VAWTs experience smaller fluctuating gravitational loads which could be beneficial if a machine of 10 MW with similar availability features as HAWTs is designed [48]. Gravitational loading is considered as the limiting factor for developing very large HAWT rotors as the blades would be exposed to very high mechanical stresses.

Torque ripple occurs in VAWTs because the angle of attack constantly changes between the blades and the wind and in HAWTs it is caused by wind shear and tower shadow [49]. These time dependent torque fluctuations are transmitted to the drivetrain components and eventually to the load side leading to power quality issues [50]. By increasing the number of rotor blades, the magnitude of the torque ripples can be reduced [51].

2.4.3   Energy conversion potential of WECs

It is impossible for the rotor to capture all the kinetic energy in the wind, meaning that the wind would have to stop after passing the rotor blades for 100% energy capture. The power coefficient of the wind turbine is defined as the ratio of the generated power in relation to the available wind power [46]. The power coefficient is affected by the tip speed ratio (TSR) and the rotor blade pitch [52].

For superior energy conversion the ideal angle of attack as the wind speed changes is achieved by varying the rotor speed in proportion to the wind speed [53]. The maximum energy capture from the wind known as the Betz limit, is 16/27th fraction of the kinetic energy capacity in the wind [37]. This equates to a power coefficient of approximately 0.59 (16/27) i.e. 59% of the available wind energy can be theoretically converted although practical experiences show much lower figures are achieved.

Figure 10 [54] shows how the power coefficient for a given TSR varies. When the TSR is between six and eight, the HAWT with three blades has the best aerodynamic efficiency compared to other wind turbine designs and rotor configurations. The TSR is an unitless number and represents the ratio of the rotor blade tip speed to the wind speed [55].
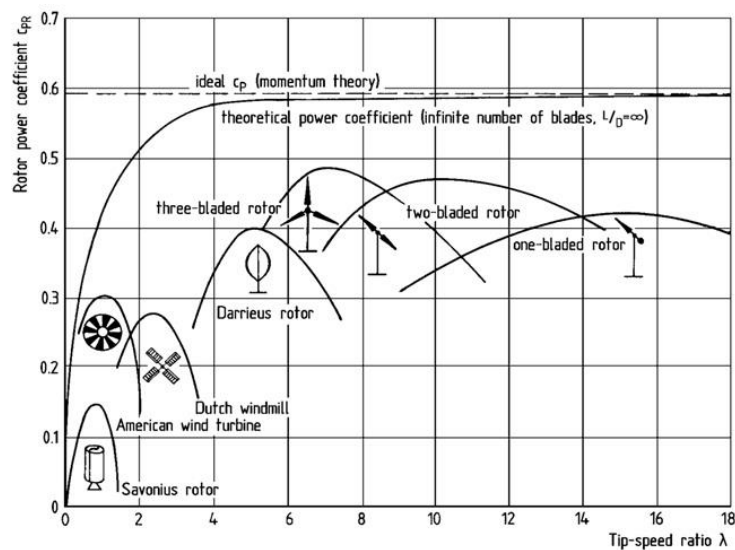
Figure 10: Power coefficients of different wind turbine designs

2.4.4   Speed characteristics of wind turbines

Wind turbines can rotate at a fixed speed where the optimum energy conversion takes place at a specific wind speed or at variable speed which has a more complicated electrical design [56] but is efficient over a wind speed range . The fixed speed of the wind turbine technology depends on the gearbox ratio, frequency of the grid and the electrical generator design characteristics [57]. From 1980 to early 1990's all wind turbines used for large scale power generation was fix speed and used gearboxes [58].

Fixed speed wind turbines are of a rugged design, cost effective to build but experience higher power fluctuations as a result of the constant generator speed against varying wind speeds [59]. These turbines unfortunately draw large reactive power from the grid [60] which are compensated for by installing power factor correction capacitors. The disadvantage of power factor correction capacitors is power quality problems like harmonic resonance on the grid [61].

Variable wind speed turbines are designed to reduce mechanical stresses, maximise wind energy capture and provide smoother output power which is more suited to the grid [62]. This technology became popular in the 1990's at the same time when advances in power electronics, reactive power control, variable speed induction generators and synchronous generator systems [60] happened.

By connecting the electrical generator via a power electronics system to the grid, the wind turbine speed can be adjusted [63]. Harmonic currents from the power electronics systems in variable speed wind turbines also cause power quality problems. Associated transient voltage peaks of 100 times more than the expected values between windings cause insulation damage of windings and ultimately failure of the machine [53].

For a certain wind resource with specific Weibull distribution parameters, it was shown that additional annual energy captured by a variable speed turbine was 2.3% more than a similar rated fixed speed turbine [46]. The additional costs of a variable speed wind turbine compared to a fixed speed wind turbine of the same rating at a given location are off-set by its ability to capture more energy in the wind.

The study in [46] revealed that a variable speed wind turbine produces more power than the fixed speed turbine of the same rating. Although the difference might appear small, the amount of power generated over the life cycle of the wind turbine which is typically 20 years can deliver substantial generation profit.

Power regulation is normally done by pitching the rotor blades, stall control or a combination of the two in order to avoid overloading the wind turbine [64]. The aerodynamic forces acting on the rotor and the output power of the turbine are reduced during high wind speeds [65].Variable speed wind turbines in conjunction with dynamic blade pitch for power and load control is considered as the accepted industry standard for most modern wind turbines [66].

2.4.5   Wind turbine classes

Factors such as the average yearly wind speed magnitude, wind turbulence and severe gusts speeds [67], determine if a wind turbine design is suited for safe operation at a particular site. The International Electrotechnical Commission (IEC) standard IEC 61400-1, stipulates the different wind turbine classes based on aerodynamic loading in **Table 3** [67]. As of late wind turbines classified as low wind "Class IV" i.e. S111 according to IEC 61400-1 are now becoming feasible to enter the power generation market [68].

Table 3: Wind turbine classes

Wind turbine class		I	II	III	S
V_{ref}	(ms^{-1})	50	42.5	37.5	Values specified by the designer
A	I_{ref} (-)	0.16			
B	I_{ref} (-)	0.14			
C	I_{ref} (-)	0.12			

Notes: V_{ref} is average wind speed reference per 10 min interval, A – C turbulence profile at hub height, I_{ref} represents expected value of turbulence intensity at 15 ms^{-1}.

Wind classes I, II and III can be equated to high, medium and low wind sites in general. Locations with low wind resources are suited for wind turbines designed with bigger rotors and higher towers to balance energy conversion and costs. These wind turbines types are largely coupled to smaller drivetrain and power generating units to increase their effectiveness in these less promising wind conditions. Medium and low wind turbines have become more popular than high wind turbines with Asia leading the international market [69].

2.5   Generator types in wind turbines

The electrical generator in the wind turbine converts the mechanical energy from the turbine rotor into electrical energy which is supplied to the grid as depicted in **Figure 11** [70]. In conventional power systems where synchronous generators are used, power is produced at constant speed. Applying these generating systems in wind energy is a challenge because of the variable nature of the resource.
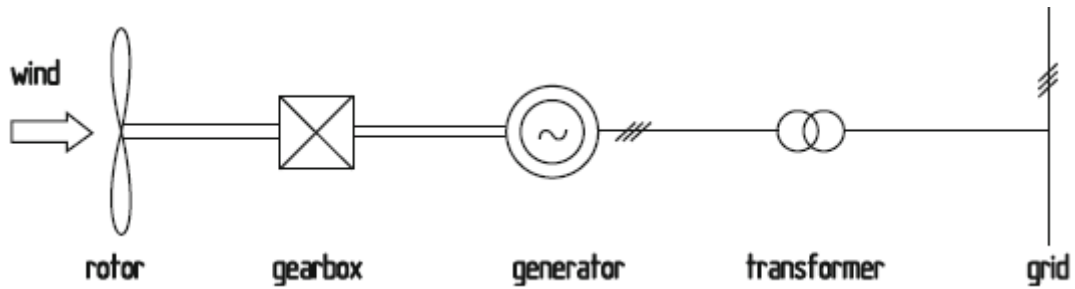
Figure 11: Electrical power conversion in WECs

A road map for wind energy conversion technologies based on variable speed and grid connected via power electronics systems is shown in **Figure 12** [71], [72].
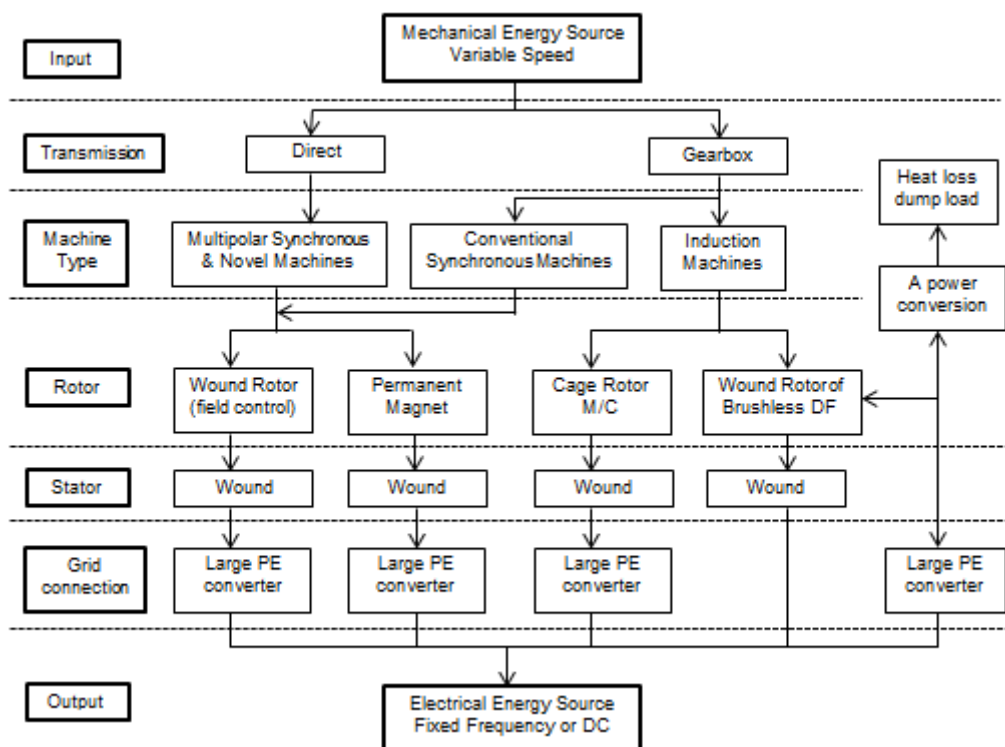
Figure 12: Road map: Power electronics converters for energy conversion in wind energy technologies

2.5.1 Induction Generators

Induction generators also known as asynchronous generators because they do not rotate at a fixed speed are the most commonly used electrical generator in WECs today [73]. The application of induction generators in the power industry is limited compared to induction motors which are seen as the workhorses in power systems consuming approximately 33% of global generated electricity [39]. There are several advantages that make induction generators suitable for wind energy technologies as mentioned by [73], [74], [75].

Induction generators are classified according to their rotor structure which is squirrel cage and wound rotor types [71]. The stator design of both induction machines are the same. The term power converter in the following paragraphs refers to all power electronic systems such as soft-starters, inverters, rectifiers or frequency converters.

2.5.1.1 Squirrel cage induction generators

SCIGs are used in fixed speed or variable speed wind turbine concepts as shown by **Figure 13** (a) and (b) [71].
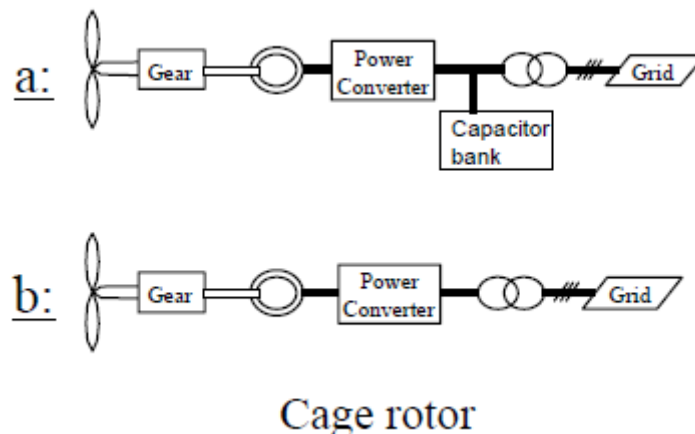
Figure 13: SCIGs used in WECs

In **Figure 13 (**a), the SCIG stator is connected to the grid via a power transformer and a power converter is used to reduce the inrush current. The function of the capacitor bank is to reduce the reactive power consumption and support the generator voltage. This configuration is also known as the Danish concept and the first generation was directly connected to the grid without any power converters.

Technology developments and subsequent reduction in power electronics costs have been main drivers for the use of SCIGs in variable speed wind turbines as in **Figure 13** (b). The generator is connected to the grid via a full rated converter which controls the stator current instead. This configuration has full control of real and reactive power and operates across the full speed range.

The size of the generator is more compact and lighter compared to other full converter designs. This type configuration is predominantly used by Siemens Wind Power which has a 4.1% global market share [69]. According to [69] North America has an installed capacity of 1.5 GW, the rest of the world 0.98 GW excluding European and Asian markets.

The power quality of SCIGs at low and high wind speeds are better compared to wound rotor induction generators (WRIGs) while the latter produce less harmonics near synchronous speed [76]. Other attributes which makes SCIGs desirable over WRIGs are [60]:

- Better grid stability because of the larger converter;
- No brushes or slip ring maintenance as well as reduced losses;
- Robust rotors which can provide better electrical and mechanical performance;
- It is cost effective and readily available.

The converter in this configuration needs to be sized to the full capacity of the generator which makes it very expensive. The harmonic filters are also rated at full converter capacity which is costly and difficult to design [77]. The performance of the converter has to be very good over the entire power range to ensure optimum efficiency and generation capacity [78].

2.5.1.2 Wound rotor induction generators

Wound rotor induction generators (WRIGs) have been mainly used in variable speed wind turbines using converters that are smaller to enhance performance and control as illustrated in **Figure 14** [71]. The reduced rated converter is also cheaper than the full capacity design.
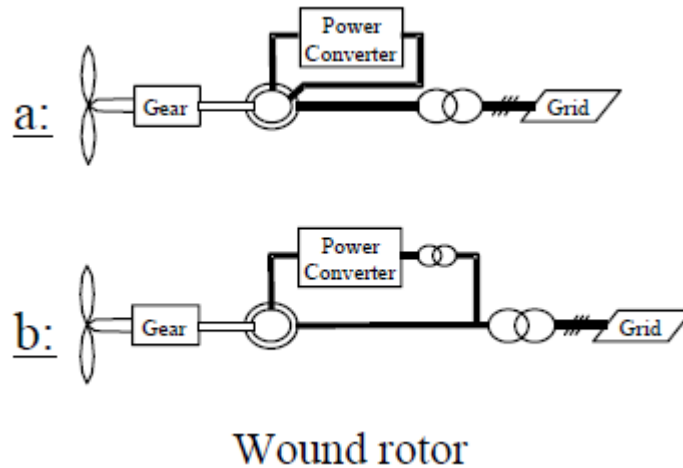
Figure 14: WRIGs used in WECs

In **Figure 14 (**a), the stator of the WRIG is directly connected to the grid and the rotor circuit connected to a converter. By varying the resistance of the rotor through the converter, the speed range can be improved between 2 – 5% [63]. This enable the generator to regulate the output power at higher wind speeds which is an improvement compared to the design in **Figure 13** (a).

The additional heat in the rotor is dissipated by an external resistor which should be adequately rated to handle optimum power generation in the rotor. This configuration is also known as the OptiSlip which is essentially a limited variable speed design where power is supplied to the grid above synchronous speed by the stator only [79].

This configuration can make use of slip rings or not and requires power factor correction and power converters that prevent high inrush currents when coupled to the grid [74]. According to [74] the Danish wind manufacturer Vestas employ designs with no slip rings where the power converter and external resistor are housed on the rotor.

The configuration in **Figure 14** (b) above is a DFIG where the stator is directly connected to the grid and the rotor is also connected to the grid through a power converter. This concept is currently the preferred wind generator topology with a market share of approximately 60% amongst wind manufactures as shown in **Figure 15** [69].
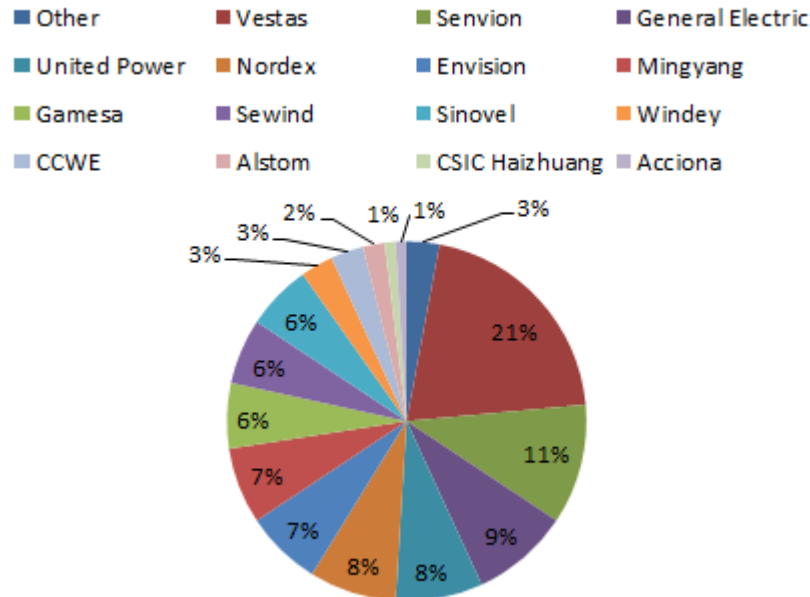
Figure 15: DFIG market base amongst wind turbine manufacturers in 2013

This design offers variable speed operation across a broader speed range from 60% to 110% and the capacity of the rotor converter is ~25% of the generator [80]. It clearly out performs the Optislip concept and has cost benefits because of the smaller rotor converter. The latest power converters are constructed as a double back to back converter with self-commutated voltage control pulse width modulation (PWM) [81].

The rotor side converter is linked to the grid side converter by an intermediate dc bus and these converters control the generator and dc bus respectively [82]. Harmonics distortion is less and therefore the filters are smaller and cheaper as well as lower losses in the power converter [77]. Control of both real and reactive power result in better grid interconnection and performance [63].

This design has higher losses and maintenance cost because of slip rings, brushes and the use of a gearbox contributes approximately 70% towards the overall losses annually [83]. The concept is susceptible to grid faults resulting in potentially high stator and rotor currents leading to severe mechanical stresses on the gearbox. It therefore requires complex control systems to provide adequate fault ride through performance [74].

2.5.2 Synchronous Generators

Synchronous generators are matured technologies in fossil fuels and nuclear power systems and produce grid power at constant speeds. Their robustness and ability to control grid voltage by adjusting the rotor excitation make them ideal for power systems. This is particularly important during grid problems like faults where the generator is to remain connected to the grid and support the grid voltage through reactive power control. Because of these attributes synchronous generators are now being used in WECs and their rotors can be separately excited or make use of permanent magnets [75].
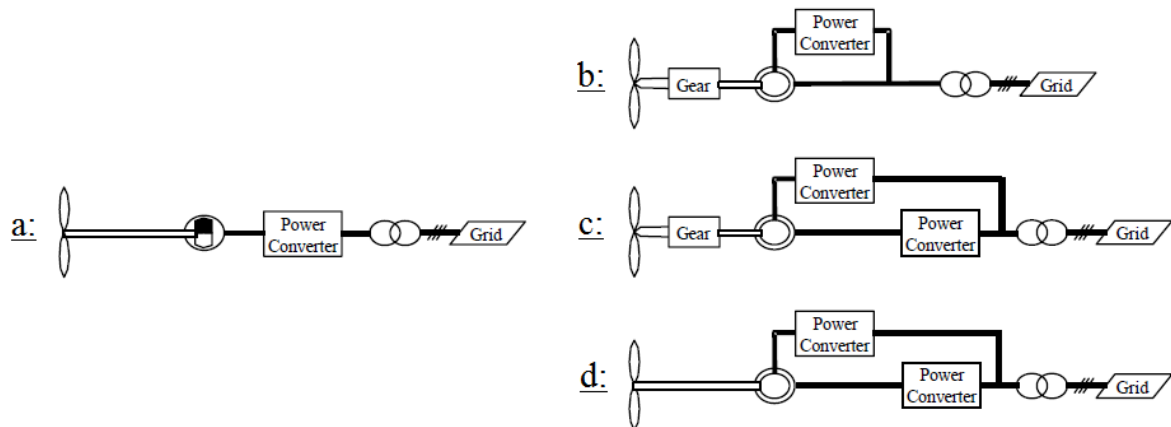
Figure 16: Variable speed wind turbines using synchronous generator concepts

Figure 16 (a) [71] shows a synchronous generator with a permanent magnet rotor without a gearbox connected to the grid through a full rated power converter. The absence of slip rings, gearbox and external excitation reduce the overall losses and its flexibility is maintained by the full rated power converter [83]. The full rated converter and magnetic material costs make this concept very expensive but energy efficiency is improved [74]. Different permanent magnet synchronous generators designs are described and analysed by [84], [85].

The concepts in **Figure 16** (b) and (c) were classified to be less suited for utility scale wind turbines because of their complex designs and additional maintenance requirements [71]. Rapid advances in wind turbine technology have made these concepts more suited for utility scale power generation especially in **Figure 16** (c). This concept can either use a permanent magnet rotor (not indicated) or externally excited rotor in combination with a gearbox and full rated converter.

Figure 16 (d) illustrates another direct drive concept where the synchronous generator is coupled straight to the turbine rotor which produces high torque at low speeds. The rotor is externally excited and has a salient geometry for low speed applications but cylindrical rotors are available for higher speed requirements. A full rated converter connects the generator to the grid. This concept is expensive despite having no gearbox because of the large multi-pole rotor diameter, cost of full rated converter, external excitation parts and maintenance requirements [79].

The output voltage amplitude and frequency can be regulated by controlling the field current in the rotor [86]. New wind turbine technologies including future generators, transmission systems, drivetrains and converters were proposed and discussed by [80]. **Figure 17** [69] illustrates some synchronous generator concepts that are popular amongst global wind manufacturers and refers to the configurations in **Figure 16**.

DDPMR - Direct Drive Permanent Magnet Rotor
DTPMR - Drivetrain Permanent Magnet Rotor
DDEER - Direct Drive Externally Excited Rotor
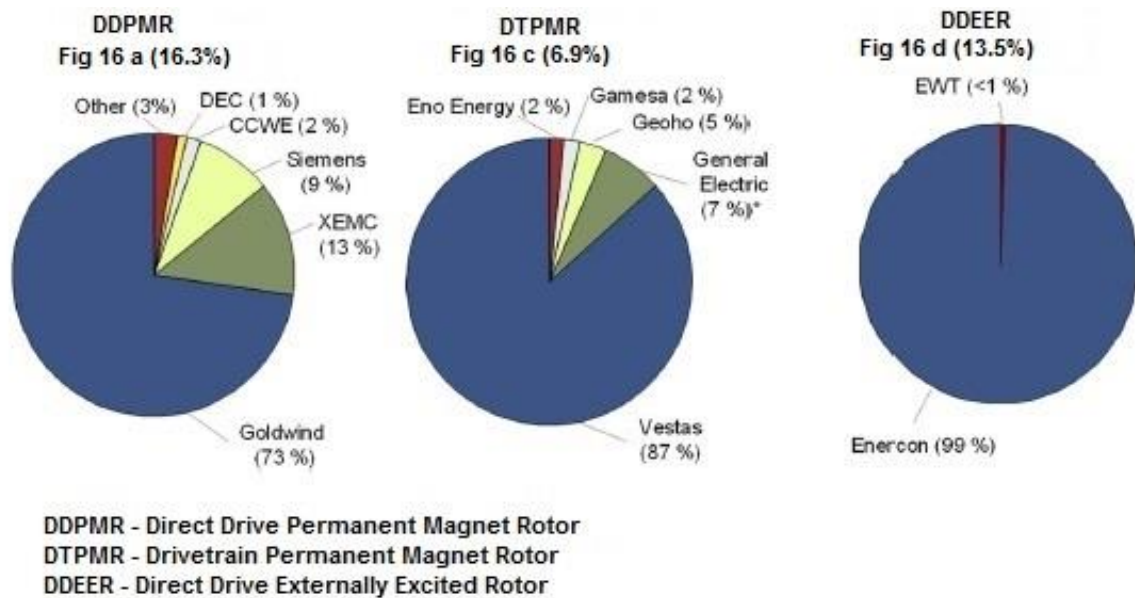
Figure 17: Market share of different synchronous generators concepts amongst wind turbine manufacturers in 2013

2.6   Wind turbine components and costs

A wind turbine is manufactured from ready available industrial material and comprises 8000 parts or more with the rotor, main bearing, drivetrain and power module its major components [87]. As a complex power system it is important to understand how breakdowns in wind turbines occur despite its current level of maturity.

High reliability and availability is thus expected over a typical 20 year design life. Costs related to wind turbines were previously discussed but a detailed breakdown of the main individual components or systems costs are shown in **Figure 18** [13].
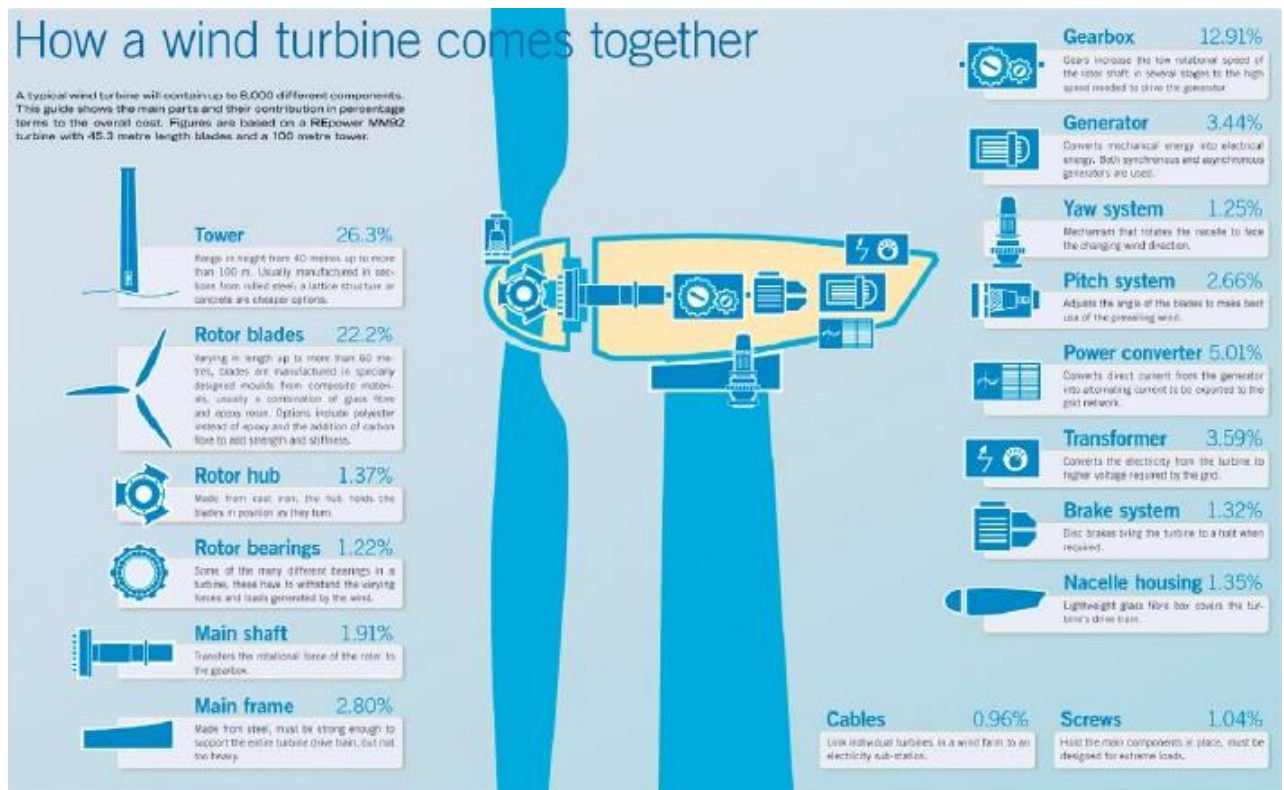
Figure 18: Cost contribution of main components and systems of a 5 MW wind turbine

2.7   Failures in wind turbines

Failures in wind turbines can result from various sources including poor quality, inferior design and manufacturing standards, construction and erection deficiencies, local operating conditions, transmission system design and general maintenance [88]. In a study conducted on more than 750 wind turbines in Sweden over a 16 year period it was concluded that 15% of failures contributed to a yearly downtime of 75% [33]. Mechanical failures occur the most, gearbox failures cause the longest downtimes and failure rates above one failure per turbine annually is still common [14].

In **Figure 19** [89] the failure rate of majority wind turbine components or systems increase as designs move away from well-established towards new concepts which are less matured. A similar observation was made when the wind turbine generator rating increases from small to large [90]. In a study of about 800 wind turbines it was established that the availability was over 90% for the majority of turbines irrespective of size [91]. This study also showed that the difference between availability figures amongst major wind turbine manufacturers were small. The primary course of failures is due to wear out as the hazard rate increases during the last phase of component design life [89].
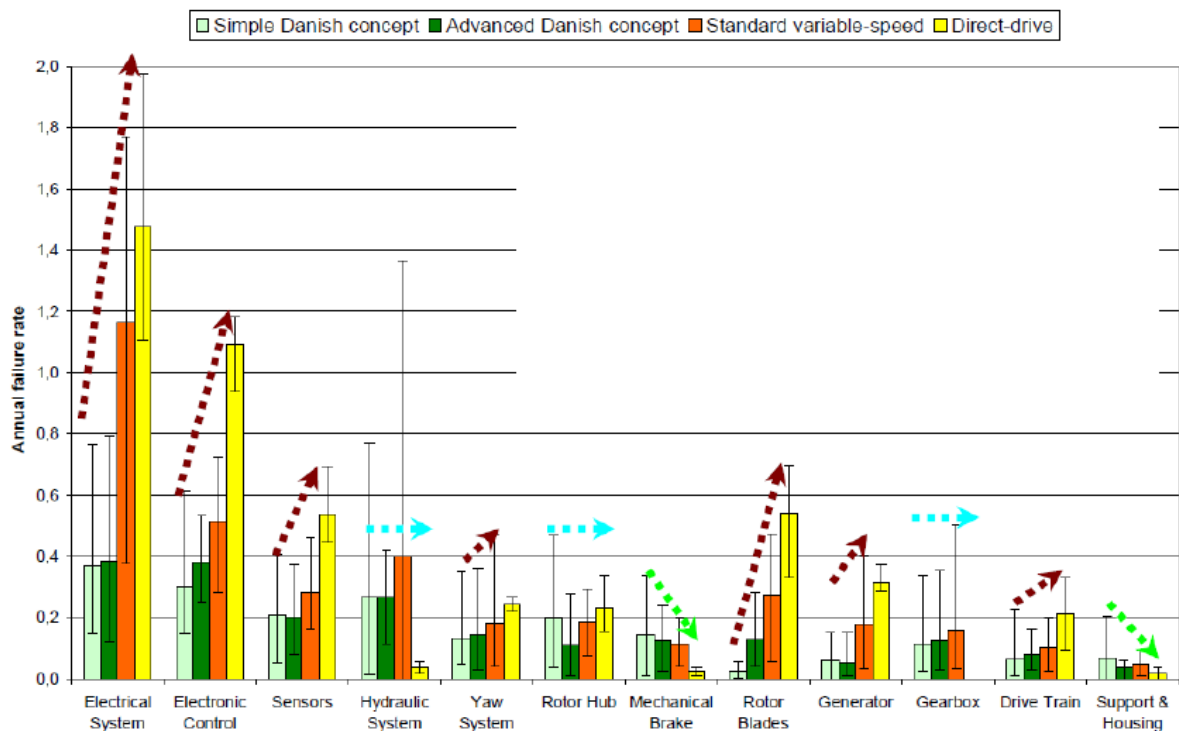
Figure 19: Different wind technology topologies and related failure

The authors in [89] concluded that gearbox failures cause the longest downtimes and that the average downtime reduced as technologies improved.

Figure 20 [92] indicates the failure rates and downtime of subsystems during a survey done on more than 1500 wind turbines in Germany over a 15 year period. Generator failures represent approximately 4% of the total number of failures in these wind turbines.
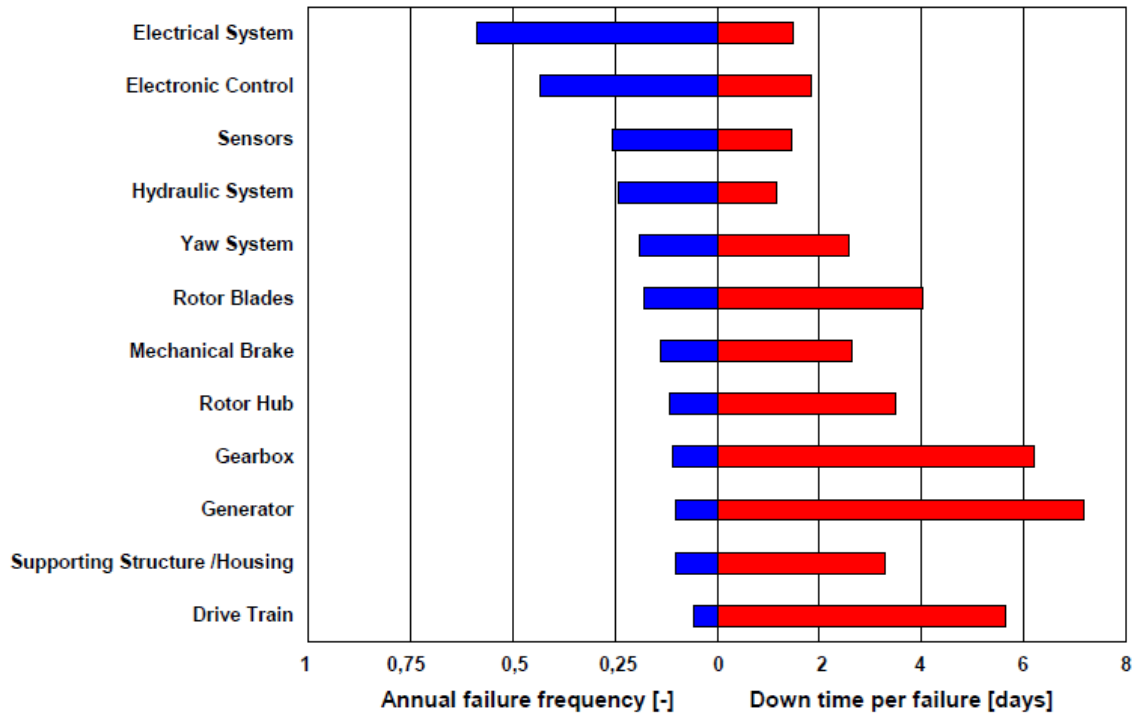
Figure 20: Downtime and failure frequency of wind turbine components

The failure rates of the four major components inside an indirect drive wind turbine is depicted in **Figure 21** [93].
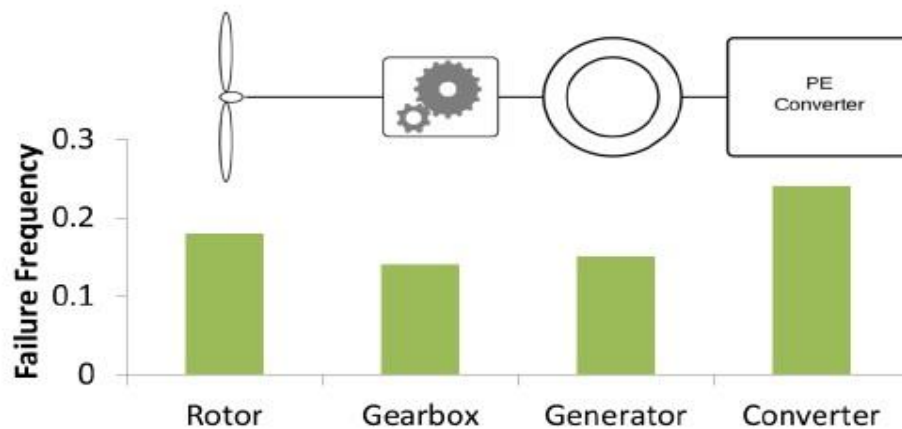
Figure 21: Drivetrain sub-assembly failure frequency

41

Figure 22 [14] illustrates that the rotor blades and generator are the two components most likely to be replaced during the life cycle of the wind turbine within a 10 year period.
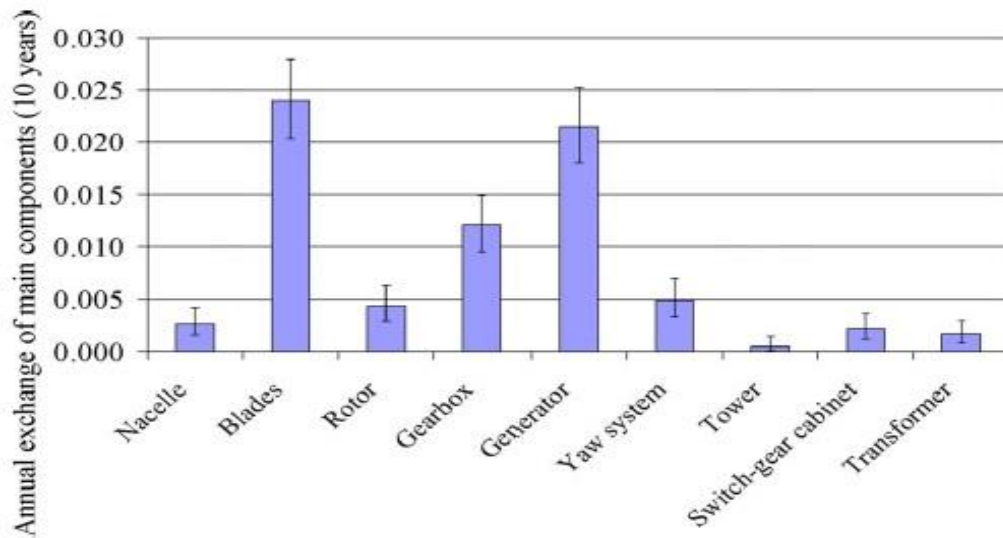
Figure 22: Yearly replacement rate of main components over a 10 year period

2.7.1   Generator failure causes

A failure chart for typical wind generators is presented in **Figure 23** [93].
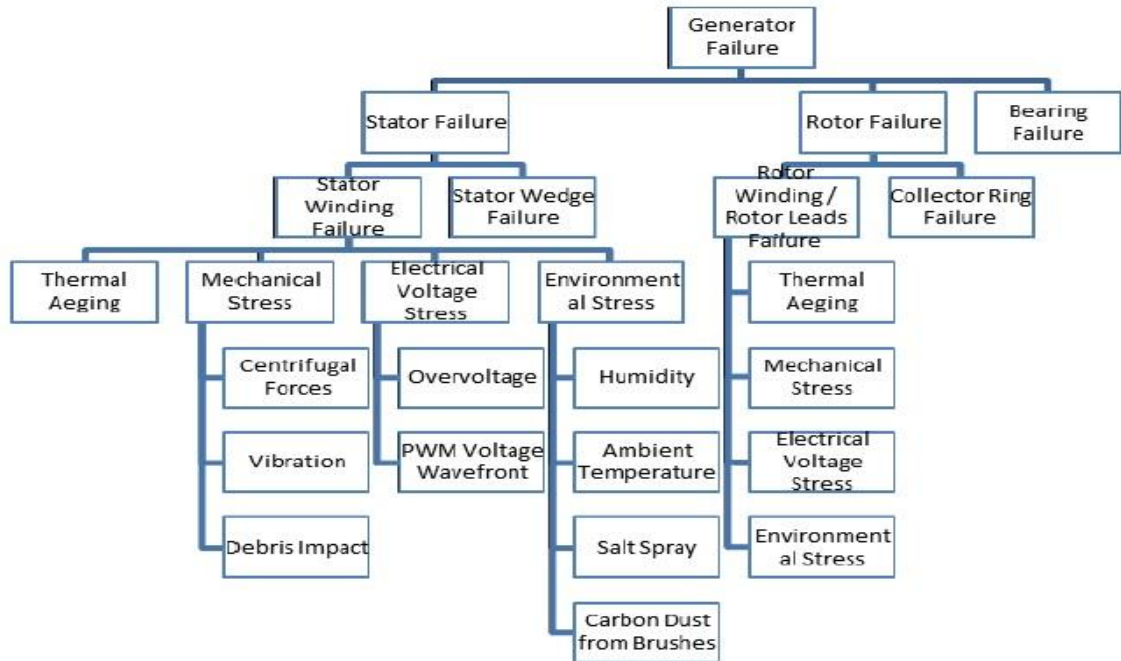
Figure 23: Typical wind turbine generator failure chart

From **Figure 24** [15] it is obvious that the major cause of failure in electrical machines irrespective of their applications is related to bearings and windings.
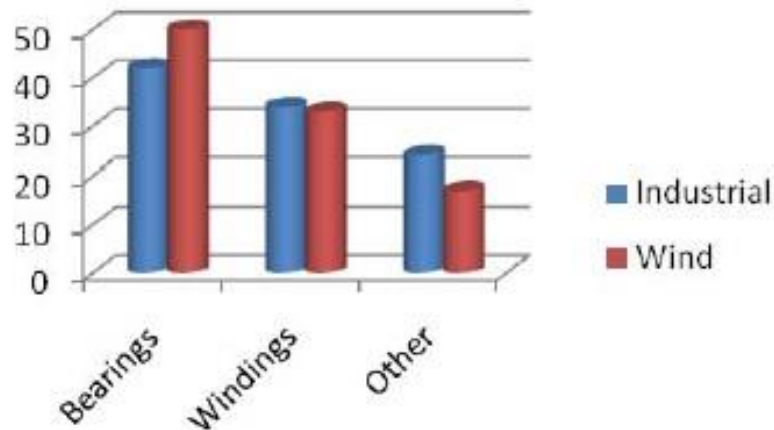
Figure 24: Electrical machine faults in wind turbines and industrial applications

From the failure chart in **Figure 23** the following components are responsible for the majority failures in wind generators using induction generators [15]:

- Bearings;
- Winding failures in both the stator and rotor;
- Rotor cages and leads;
- Slip rings;
- Magnetic wedges in the stator;
- Cooling plant.

The size of the generator also influences which components fail as manufacturers try to optimize designs for various power requirements and wind conditions. The three major faults identified across various generator ratings are summarised in **Table 4** [15]. Failure modes 1 – 3 represent the major faults ranging from most dominant to less dominant failure modes.

Table 4: Major failure modes across different wind generator sizes

Generator Size	Failure mode 1	Failure mode 2	Failure mode 3
Small < 1 MW	Rotor	Stator	Bearings
Medium 1 - 2 MW	Bearings	Collector Rings	Rotor
Large > 2 MW	Bearings	Stator	Stator Wedge

Rotor winding problems in small to medium generators are caused by conductor and banding failures while stator winding problems are related to contamination and maintenance issues. Failures of bearings, stator windings and rotor windings contribute more than 80% of the total failures in induction machines [94]. This translates to a failure distribution for bearings (41%), stator (37%), rotor (10%) and other faults (12%) [95], [96], [97].

2.7.2　Stator failures in wind generators

1) Stator windings

Main ageing mechanisms causing insulation failure of rotor and stator windings are thermal effects, vibration stresses, voltage spikes from the power converters and material degradation because of temperature changes [98]. Environmental conditions can accelerate insulation degradation and moist operating conditions should be avoided. Failure modes of windings irrespective of the cause are categorized as shown in **Figure 25** [99].
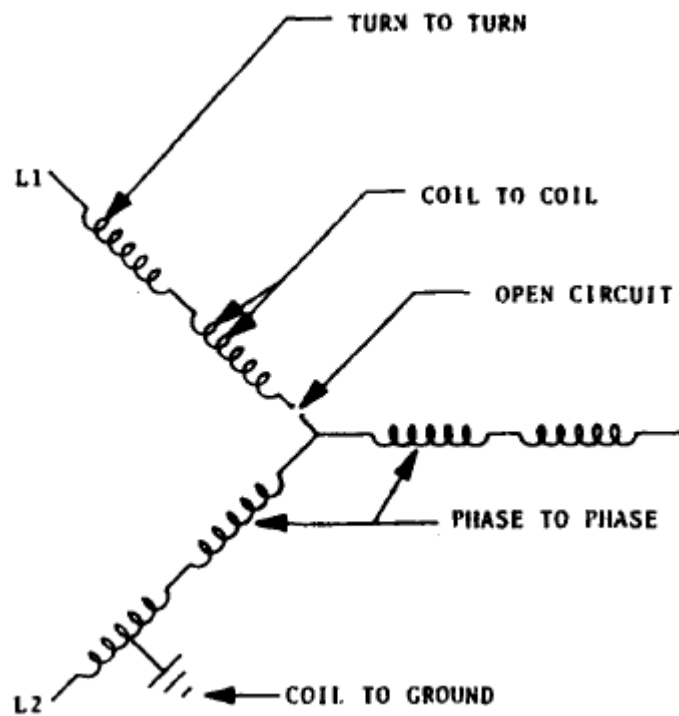
Figure 25: Stator winding failure modes

The occurrences of short circuits escalate with time and are caused by overheating, ageing and vibrations while open circuits result from termination problems or damaged windings [33]. Voltage spikes caused by power converters in variable speed induction machines are also responsible for winding insulation failures. Because of very fast switching times in the PWM circuit, multiple reflected waves travel between the converter and the machine as illustrated in **Figure 26** [98].
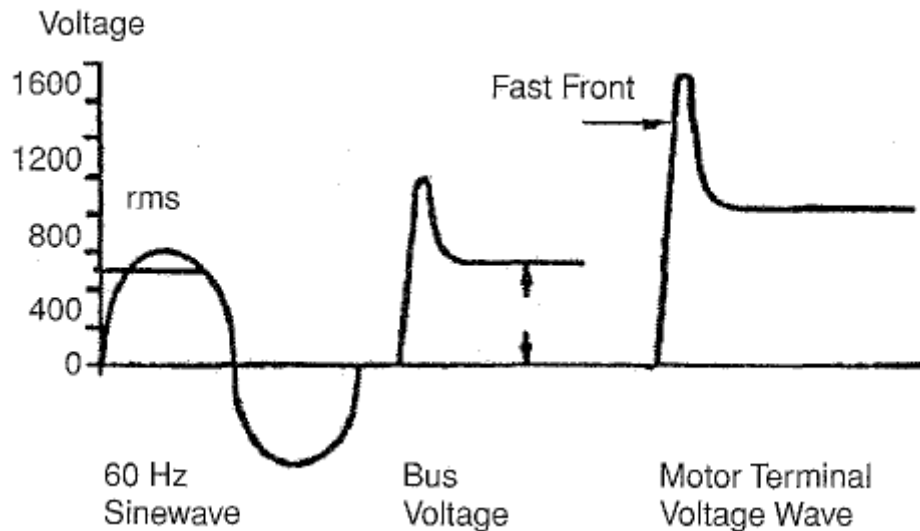
Figure 26: Voltage spikes generated by PWM circuits

Impedance differences between the output cable and the generator create these reflected waves which become more severe as the cable length increases and the switching frequency of the semiconductors increases [98]. The reflected waves occur at the front of the voltage wave and can reach magnitudes up to 2.5kV for a generator rated at 690V [93].

Winding insulation design requirements should comply with the following conditions as a minimum [100]:

- Design life and mean time between failure (MTBF) of 20 000 hours under accelerated ageing tests conditions;
- Rated voltage capacity test plus 10% - 15% and then 2.5kV peak – peak "withstand" voltage after the ageing test;
- Initial partial discharge voltage test higher than the maximum peak – peak voltage after ageing test.

2) Stator wedge failures

Conductive wedges are used to keep the stator windings in the core and secure it against mechanical forces and vibrations. It also improves efficiency, limits magnetic flux distortion, inrush currents and increases the thermal properties of the machine [101]. An example of exposed stator coils where the wedges came loose and fell out of the stator slots are shown in **Figure 27** [15]. The rotating magnetic field is the main cause that stator wedges become loose and this can result in grounds faults and or damage to stator coils [15].

Figure 27: Missing stator slot wedges

The composition of the wedge material should be correctly selected to optimize mechanical strength and magnetic properties [102]. Moisture ingress into the machine can also affect the material properties of the wedges and bonding failures may result due to oxidation and corrosive elements [101]. The use of non-magnetic wedges in future generator designs could be an alternative solution to reduce wedge failures.

Non-magnetic wedges do not experience the same amount of forces exerted by the rotating magnetic field, are more flexible and manufactured from high tensile materials. The semi-closed slot design for non-magnetic wedges compared to the open slot design for magnetic wedges also provides better support and exerts less stress on the wedge [102]. Better cooling should be considered if non-magnetic wedges are used to maintain overall efficiency and additional focus on design improvements in wedge and insulation systems are recommended [103].

3) Bearing Failures

Bearing failures contribute a significant amount towards wind generator failures and common causes are incorrect installation or misalignment [104] as well as poor lubrication, overheating and mechanical breakage [105]. Bearing wear through normal ageing together with "indentation, smearing, surface distress, corrosion" [33], electric current flow and overloading can also lead to bearing failure.

It is recommended that maintenance practises comply with bearing lubrication schedules to reduce bearing failure rates. Damaged bearings cause excessive vibrations of the rotor which disturbs the uniform shape of the airgap between the stator and rotor. If not picked up these vibrations can cause contact between the stator and rotor which will lead to catastrophic damage of both components.

2.8   Maintenance

2.8.1   Maintenance Strategies

Maintenance is the activity that assist production operations with optimum levels of availability, reliability and operability at the lowest cost [106]. Maintenance strategies can be broadly classified into three main strategies namely breakdown maintenance, preventive maintenance and corrective maintenance [107].

Currently all three maintenance strategies or a combination of them are used in the wind industry depending on the age of the wind turbine. Breakdown maintenance is the typical "run to failure" approach, preventive maintenance is done before a problem leads to a failure and corrective maintenance is scheduled to rectify existing plant specific problems [107]. Preventive maintenance is further classified as use-based or predictive maintenance and the former is performed at predetermined instances which is related to the age of the equipment or at certain expired calendar times [106]. Use-based maintenance can lead to over or under maintenance as resources are not optimally used [108].

Condition based maintenance has the capability to estimate the remaining useful life of equipment [109] in order to implement the best maintenance strategy before failure occurs. It can be done by doing inspections or monitoring certain variables using sensors like temperature, voltage, current, noise or vibrations to determine the condition of the equipment. The process of condition monitoring can be online or offline and is made up of three primary steps [110]:

- Data acquisition – gathering data that is pertinent to equipment health;
- Data processing – analytical verification, comprehension and refinement of collected data;
- Decision making – deciding which maintenance strategy is ideal to ensure long term plant health at the lowest cost.

2.8.2 Condition monitoring techniques in wind turbines

The application of condition monitoring in WEC systems is ideal as concluded by [111]. Several condition monitoring techniques like oil analyses, vibration analysis, electrical effects, acoustic emissions, ultrasonic methods, radiographic inspections, strain measurements, thermography, temperature measurements, shock pulse method and equipment performance are used as discussed by [112], [106], [113], [114], [109], [115], [116]. Current wind turbine condition monitoring focus on critical equipment like the gearbox, generator and main bearing [88] which are high cost components and cause long downtimes.

Vibration analysis is the most common condition monitoring method used in wind turbines although its ability to detect electrical faults could be limited. Its effectiveness in direct driven or other modern wind turbine concepts is also questionable [113]. Probabilistic measures in addition to data received from sensors are required for a more precise determination of the equipment condition as the operating nature of wind turbines is stochastic [117]. A breakdown of condition-based maintenances applicable to wind power systems is given in **Figure 28** [115].
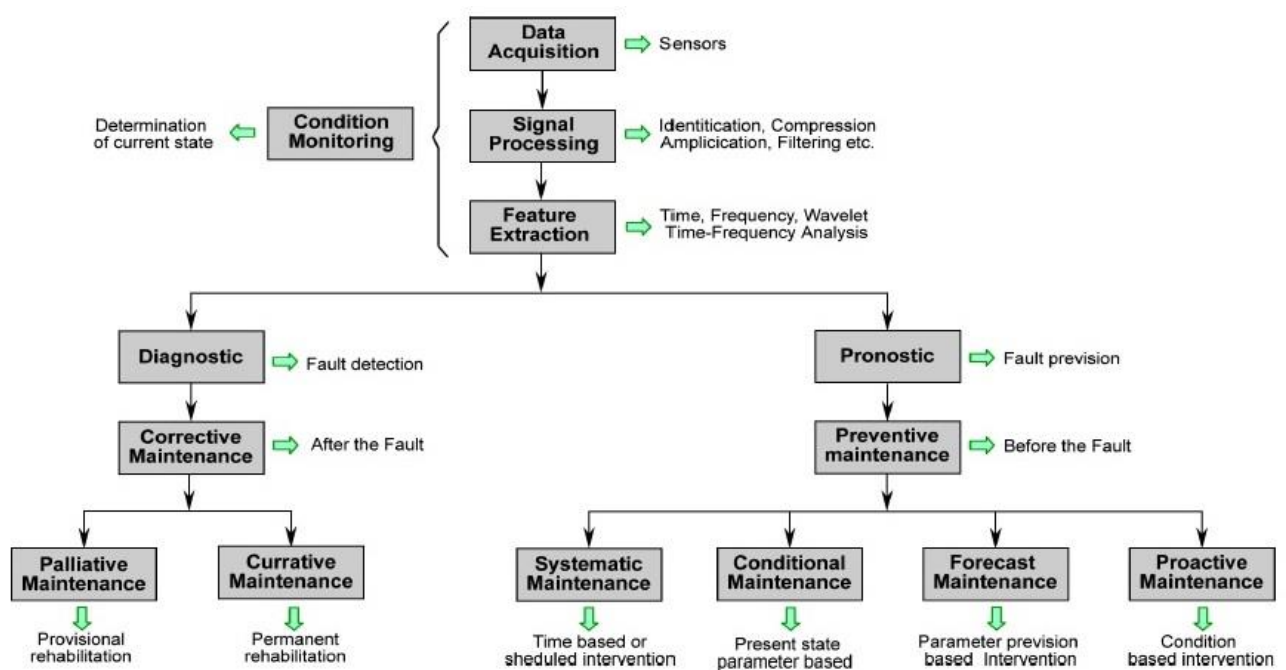
Figure 28: A breakdown of the condition based maintenance in wind turbines

2.8.3   Generator stator windings condition monitoring

Accurate condition monitoring techniques of stator winding faults are required as it is the second largest failure mechanism in generators. Shorted windings cause the most damage in the machine as it produces additional heat in the windings which further reduce the design life of winding insulation material. These faults originate as undetected inter turn faults that gradually isolate multiple turns or when an arc exist between two points on a winding [118].

Detection of inter turn winding faults is complex because the machine can still operate without any obvious fault signatures. These faults can rapidly evolve and cause complete failure of the winding and damage to the machine.

Temperature monitoring is considered as one of the oldest conditioning monitoring techniques [119] and is commonly used in wind turbines to detect abnormalities in bearings and generator windings [120], [115]. High stator winding temperatures under normal operating conditions is generally a sign of possible winding damage. Other factors such as high ambient temperatures or problems with the generator cooling have a similar effect. Insulation life is reduced by 50% for every 10 °C increase in temperature as oxidation rates increase above certain temperature limits [121]. Oxidation makes the insulation material fragile and some parts of the winding might experience delamination.

Majority of modern wind turbines are designed with condition monitoring systems which incorporates a Supervisory Control and Data Acquisition (SCADA) system. One of the functions of the SCADA system is to capture operating parameters from the wind turbine. Various mechanical and electrical sensors measure operating and performance data which are recorded on a computer system for analysis. The SCADA data is recorded and stored as 10 minute average values by the computer system. Analysis of SCADA data for fault prognosis is seen as cost effective maintenance strategy although its data content doesn't reveal abnormalities in a clear and explicit manner [122], [123].

Proper data analysis and modelling techniques are required to identify and understand component degradation. This will enhance component health predictions and guarantee the implementation of optimum maintenance strategies. According to [111] physical models depend on detailed understanding of failure modes whereas data driven models involve extensive data requirements to validate continuous degradation processes.

The application of SCADA data as a condition monitoring technique in the wind industry has become a prevalent research topic as found in many studies [124], [125], [122], [126], [127], [123]. These methods usually consist of various physical and statistical models of a particular system. In [128] multiple linear regression (MLR) was applied to determine generator stator winding condition.

Generator winding temperature represented stator winding condition and its relationship with other SCADA data was investigated. The result from the MLR model in this study showed that active power had the biggest impact on generator winding temperature at all operating conditions.

Harmonics in line currents and magnetic flux, torque pulsations, reduced mean torque, high losses, abnormal winding temperatures and reduced efficiency are all indicators which highlight problems in induction machines [129]. A review of recent literature reveals that inter turn faults and asymmetries [130] in the rotor or stator are the main focus of most condition monitoring techniques. Electrical signature analyses of the stator parameters such as current, voltage and power under steady state operating conditions prove to be successful in sensing winding faults as well as other failure mechanisms [131].

These methods have been found to be susceptible to machine loading [129] and that other effects that produce similar fault signatures like design defects and voltage unbalance were not properly quantified [132]. Steady state fault diagnostics and monitoring are techniques that are questionable as the wind turbine operates under transient conditions which may require more stochastic analysis for improved accuracy.

The application of motor current signal analysis (MCSA) is predominantly used to establish the condition of an induction machine as investigated by [133], [116].Stator winding fault detection in DFIGs was performed by [118], [134]. It was observed that instantaneous power spectrum analysis out performs current analysis as it reveals more fault data and that wavelet transforms could provide improved accuracy under stochastic operating conditions [134].

In [130] it was established that monitoring the mechanical torque-speed relationship in direct driven synchronous wind generators, detection of winding and mechanical faults in the drive train is possible. In this study it was concluded that through power signal analysis drive train faults can be easily detected instead of using more complex methods like torque or vibration signals.

Developing a magnetic equivalent circuit to represent winding failures has also been investigated. The accuracy of these models remains questionable as saturation and magnetic non-linearity is normally neglected. Winding function theory was used to detect the input impedance of the winding which according to the authors was a simple and effective method [135]. Another popular technique to determine winding condition is symmetrical component analysis which concentrates on negative sequence components [136].

2.10 Induction machine construction and operating principle

The squirrel cage induction machine can be used as a motor or a generator without making changes to the physical properties of the machine. The stator consists of laminated silicon steel which reduces losses and contains slots where the three phase windings are located. The rotor also contains a laminated core where rotor bars are housed which are shorted at both sides by end rings [16]. The construction and the main components of a squirrel cage induction machine are shown in **Figure 29** [16].
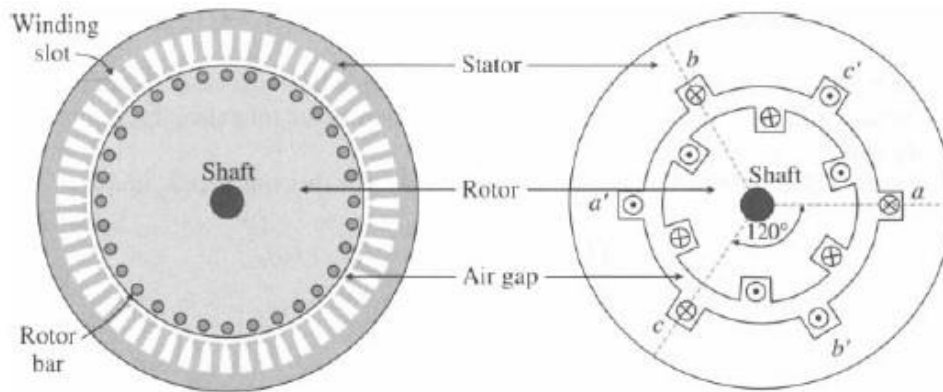
Figure 29: SCIG cross-sectional view

A rotating magnetic field is created in the air gap between the stator and the rotor when the stator is coupled to a three phase source. This magnetic field rotates at synchronous speed which is calculated using the equation:

$$N_S = \frac{60f}{p} \qquad (1)$$

where Ns denotes the synchronous speed in rpm, f denotes the source frequency in Hertz and p denotes the number of pole pairs of the machine.

The interaction of the rotating magnetic field and the induced currents in the rotor circuit produces an electromagnetic torque which speeds up the rotor. The induction machine operates as a motor if the rotor speed is less than the synchronous speed where the torque produced by the machine equals that required by the load.

When the rotor is driven by a wind turbine above the synchronous speed, the machine operates as a generator and delivers power when connected to a load or grid. Generator mode is only possible when the rotor turns above synchronous speed and this is also known as the supersynchronous operation [137]. The direction of the power flow in the stator is reversed by the induced currents and electromagnetic torque in the rotor circuit during this operation.

The difference between the synchronous speed of the rotating magnetic field and the speed of the rotor is called the slip and is calculated as follows:

$$S = \frac{N_S - N_r}{N_S} \tag{2}$$

where s is the slip in per unit or percentage, N_S denotes the synchronous speed in rpm and N_r denotes the rotor speed in rpm

Figure 30 [16] summarises the operating modes of the induction machine as generator and motor. The machine parameters are negative in generating mode which is based on the assumption that in motoring mode the direction of currents are into the stator and considered positive.

Connection		
Phasor diagram		

Operating mode	Generating mode		Motoring mode	
Stator power	$P_s = 3V_s I_s \cos \varphi_s < 0$		$P_s = 3V_s I_s \cos \varphi_s > 0$	
Slip and torque (normal operation)	$s < 0$	$T_m < 0, T_e < 0$	$s > 0$	$T_m > 0, T_e > 0$
Power factor angle and power factor	$90° \leq \varphi_s < 180°$	$-1 \leq PF_s \leq 0$	$0 \leq \varphi_s < 90°$	$0 \leq PF_s \leq 1$

Figure 30: Induction machine operating modes

The parameters in **Figure 30** are defined as follows:

Ps	-	Stator Power (MW)	Vs	-	Stator Voltage (V)
Is	-	Stator current (A)	s	-	Slip
Tm	-	Mechanical Torque (Nm)	Te	-	Electromagnetic Torque (Nm)
PF	-	Power Factor	φs	-	Power Factor Angle (°)
ωm	-	Mechanical Speed (rpm)			

2.11 Operation of induction generators in variable speed wind turbines

The basic characteristics and design parameters of a variable speed wind turbine using a SCIG was discussed in the previous chapter. **Figure 31** [16] shows this wind turbine topology where variable speed is achieved through changing of the generator frequency in relation to the wind speed while the grid frequency remains constant [138]. Which means the dynamic operating characteristic of the generator is separated from the grid [139].
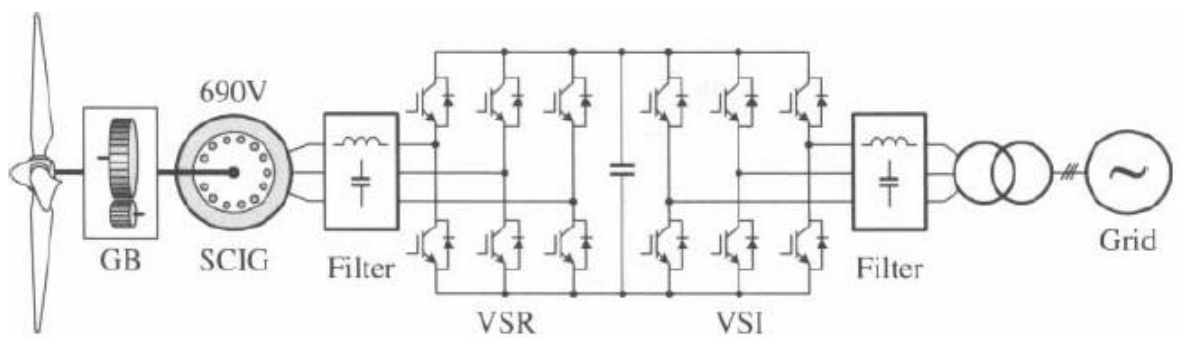
Figure 31: SCIG variable speed wind turbine configuration

The power converter consists normally out of two back-to-back PWM voltage source converters (VSCs) which allows for bi-directional power flow that is dependent on the converter design [138]. The machine converter known as the voltage source rectifier (VSR) rectifies the three phase AC output voltage of the generator to a DC voltage.

The network converter known as the voltage source inverter (VSI) inverts the DC link voltage into three phase AC voltage which matches the grid voltage.

The back-to-back VSCs have the following benefits [138]:

- It's a mature technology in machine drive-based industry;
- Components are tailor made for its purpose;
- The ability to control both converters individually because of the DC link capacitor.

The converters have individual active and reactive power control. The machine VSR controls generator torque or speed whereas the network VSI maintains a steady DC link voltage [16]. Both converters are designed to operate in reverse functionality where the machine VSR operates as a VSI and the network VSI operates as a VSR. It is possible to control active and reactive power flows through varying the load angle and the magnitude of the output voltage of the network converter [138].

Figure 32 [138] illustrates the steady state operation of the variable speed SCIG wind turbine at different operating frequencies. To ensure optimum power extraction under varying wind speeds, the generator speed is adjusted accordingly by changing the frequency of the machine through the converters. **Figure 32** b shows a significant change in the generator power while the reactive power remains relatively constant.

The slip is adjusted in accordance with the wind speed to achieve this. The generator operates in a very narrow speed band to ensure the required torque is maintained which provides stable operating conditions.
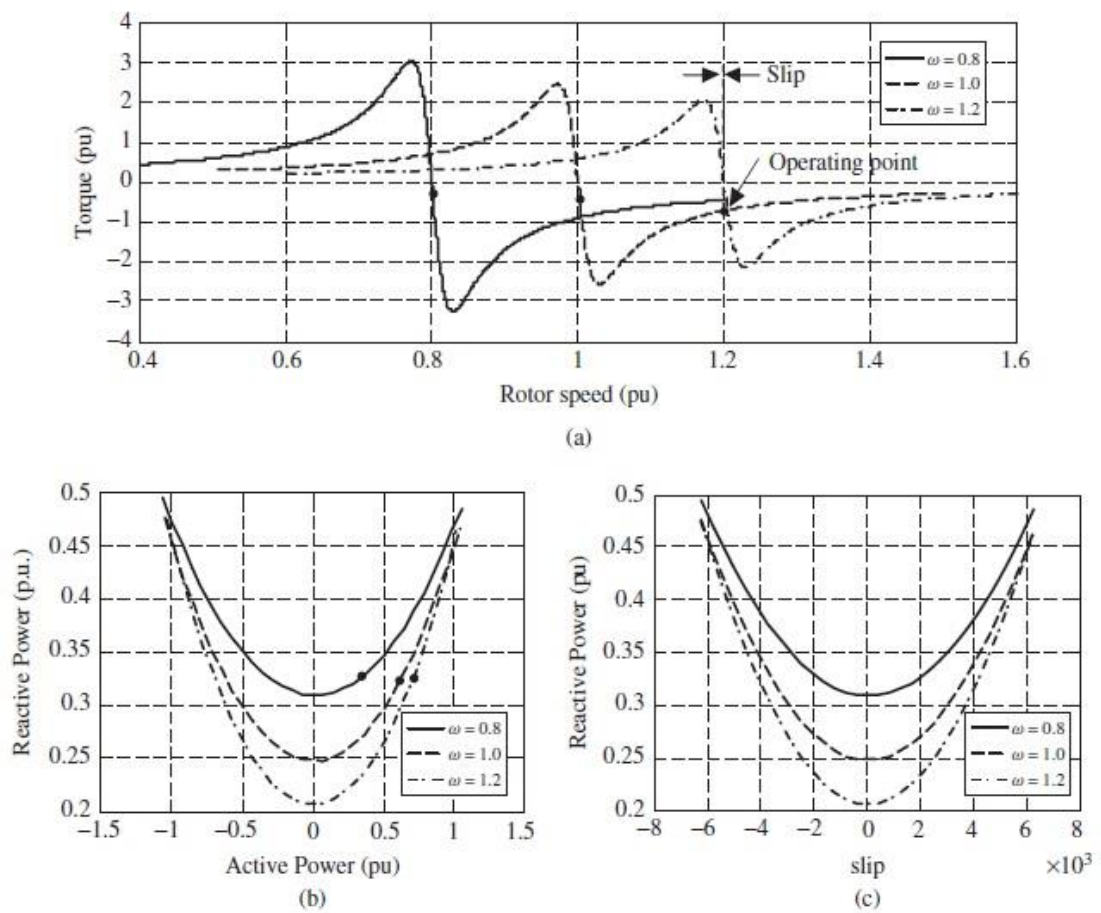
Figure 32: Steady state operating characteristics of a variable speed SCIG wind turbine

CHAPTER THREE
SYSTEM MODELLING AND DESIGN

In this section the derivation of mathematical equations to obtain the equivalent circuit for a SCIG is presented. These equations are applied to determine the performance of the SCIG at rated operating conditions. A statistical model predicting generator stator winding temperature between minimum and rated output power of two different wind turbines is also discussed. The model illustrates the relationship of various operating parameters with stator winding temperature.

3.1   SCIG steady state equivalent circuit

The equivalent circuit of the induction generator provides for analysis during steady sate conditions. It is derived from the space-vector model [16] described by the following equation:

$$\begin{cases} \vec{v}_s = R_s\vec{\imath}_s + p\vec{\lambda}_s + j\omega\vec{\lambda}_s \\[2mm] \vec{v}_r = R_r\vec{\imath}_r + p\vec{\lambda}_r + j(\omega - \omega_r)\vec{\lambda}_r \end{cases} \tag{3}$$

where

$\vec{v}_s, \vec{v}_r$ -   Stator and rotor voltage vectors (V)

$\vec{\imath}_s, \vec{\imath}_r$ -   Stator and rotor current vectors (A)

$\vec{\lambda}_s, \vec{\lambda}_r$ -   Stator and rotor flux-linkage vectors (Wb)

R_s, R_r -   Stator and rotor winding resistances (Ω)

ω -   Rotating speed of the arbitrary reference frame (rad/s)

ω_s -   Rotor electrical angular speed (rad/s)

p -   Derivative operator ($p = d/dt$).

The terms $j\omega\vec{\lambda}_x$ and $j(\omega - \omega_r)\vec{\lambda}_r$ in Equation 3 are referred to as speed voltages induced by the rotation of the reference frame at the arbitrary speed of ω [16]. The equivalent circuit is determined using the space-vector model in the synchronous frame which leads to:

$$\bar{V}_s = R_s\bar{I}_s + j\omega\bar{\Lambda}_s \tag{4}$$

$$\bar{V}_r = -R_r\bar{I}_r + j(\omega_s - \omega_r)\bar{\Lambda}_r$$

where phasor quantities are shown in upper case letters and $\vec{v}_s = v_{ds} + v_{qs}$, $\bar{V}_s = Re(\bar{V}_s) + jIm(\bar{V}_s)$ with $V_s = \frac{v_s}{\sqrt{2}}$

Equation 4 can be rewritten as:

$$\bar{V}_s = R_s\bar{I}_s + j\omega_s(L_{ls}\bar{I}_s + L_m\bar{I}_m) \tag{5}$$

$$\bar{V}_r = -R_r\bar{I}_r + j\omega_{sl}(-L_{lr}\bar{I}_r + L_m\bar{I}_m)$$

where ω_{ls} is the angular slip frequency calculated by $\omega_{ls} = \omega_s - \omega_r$ and through division of the rotor voltage equation through the slip

$$s = \frac{\omega_{ls}}{\omega_s} \tag{6}$$

Rearranging Equation 5 we obtain

$$\bar{V}_s = R_s\bar{I}_s + jX_{ls}I_s + jX_m\bar{I}_m \tag{7}$$

$$\frac{\bar{V}_r}{s} = -\frac{R_r}{s}\bar{I}_r - jX_{lr}\bar{I}_r + jX_m\bar{I}_m$$

The stator leakage reactance, rotor leakage reactance and the magnetizing reactance, X_{ls}, X_{lr} and X_m respectively are calculated using the following:

$$X_{ls} = \omega_s L_{ls} \tag{8}$$

$$X_{lr} = \omega_s L_{lr}$$

$$X_m = \omega_s L_m$$

Thus Equation 7 represents the steady-state equivalent circuit for and induction generator. The SCIG with the short-circuit rotor, meaning the rotor voltage V_r is zero, is shown in **Figure 33** [16].
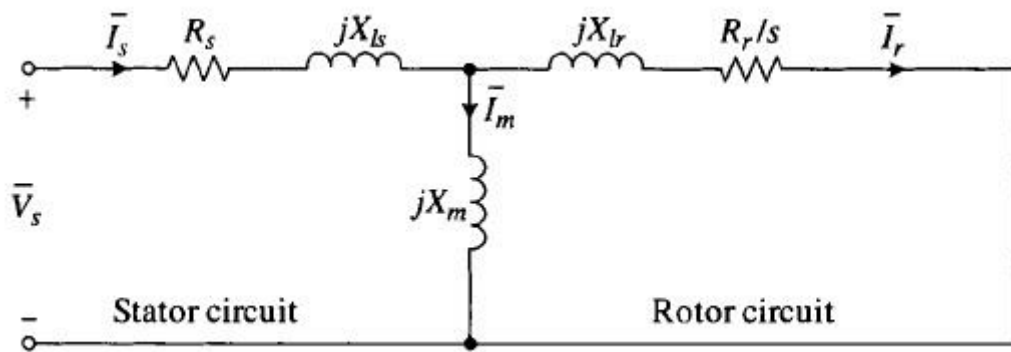
Figure 33: SCIG steady-state equivalent circuit

Figure 34 [16] highlights the power flow and machine losses in the induction generator.
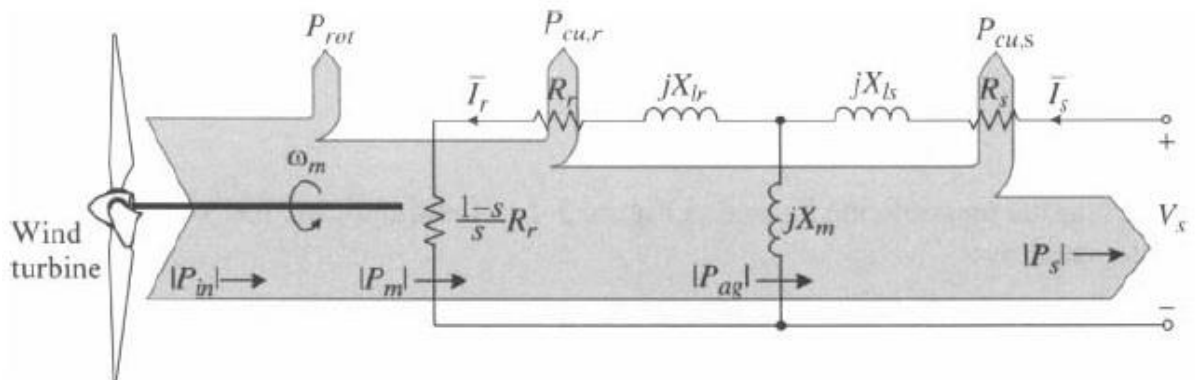
Figure 34: Induction generator power flow and machine losses

The copper losses in the stator and rotor windings $P_{cu,s}$ and $P_{cu,r}$ respectively can be determined using:

$$P_{cu,s} = 3I^2{}_s R_s \qquad (9)$$

$$P_{cu,r} = 3I^2{}_s R_r$$

3.1.1 Using the equivalent circuit to detect stator winding degradation

The electromagnetic energy conversion in an induction machine is due to the magnetizing or main flux crossing the air gap which links both the stator and rotor [140]. Magnetic flux that only links the stator or rotor is called the leakage flux. Leakage flux consists of various leakage components as shown in **Figure 35** [141]. These leakage fluxes are represented as equivalent inductances in the stator and rotor and forms part of the overall flux linking the winding.
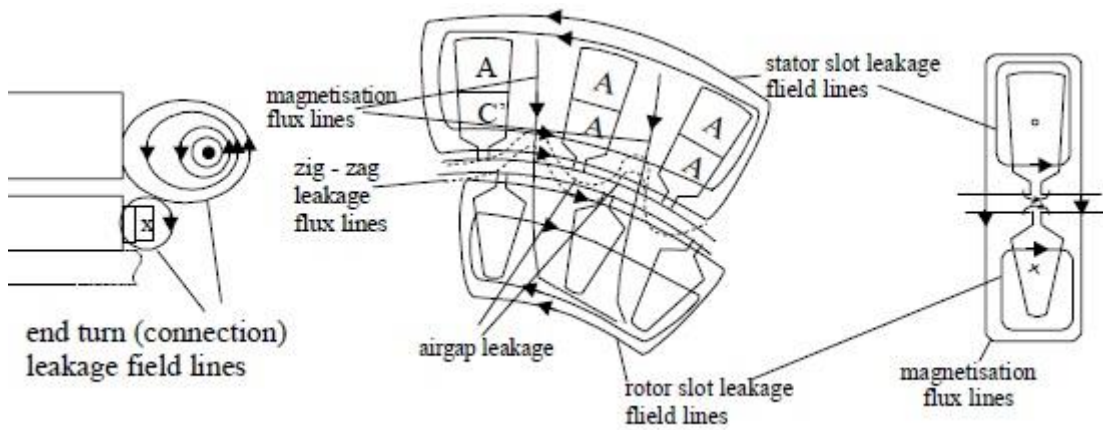
Figure 35: Different leakage flux flow

Leakage fluxes are responsible for additional losses in the machine and therefore affect the design of the machine. More leakage flux leads to a bigger magnetic structure, higher magnetizing current and stator winding copper losses because of increased skin effect caused by slot leakage flux [140]. The leakage inductance is the sum of all the different flux leakages which produces stator and rotor leakage inductances L_{ls} and L_{lr} respectively.

The stator and rotor self-inductances also called total stator or rotor inductances comprise of the leakage inductance and the magnetizing inductance. The formulae for per phase inductances and reactances are:

$$L_s = L_{ls} + L_m \tag{10}$$

$$X_1 = X_{ls} + X_m$$

$$L_r = L_{lr} + L_m \tag{11}$$

$$X_2' = X_{lr} + X_m$$

The induction generator parameters of the equivalent circuit are usually determined in accordance with IEEE 112 – Standard Test Procedure for Polyphase Induction Motors and Generators. The values of stator and rotor winding resistances, reactances and magnetizing reactance are determined with the No-load test and the Locked rotor test. Once the equivalent circuit parameters are obtained the performance characteristics of the machine including current, power factor, torque, efficiency etc. can be determined at steady state conditions [142].

Changes in the condition of the stator windings affect R_s, L_m and L_{ls}. These parameters in turn determine how the machine performs at various operating conditions. Since the stator leakage inductance represents only flux that overlaps the stator winding, degradation affects its value and the overall stator inductance. By varying the stator equivalent circuit parameters and keeping the rotor equivalent circuit parameters constant, the performance of the SCIG can be analysed.

MATLAB is a very popular software modelling tool for wind generating systems and the package is constantly revised to include the latest control and mathematical models [143]. Included in MATLAB is Simulink which offers a graphical user interface (GUI) for creating power system component models in the form of block diagrams. Simulink software has the capacity to model, simulate and study linear and nonlinear systems such as SCIGs.

This study assumes that stator winding degradation occurs in a linear manner. Skin effect and saturation are ignored in all simulation calculations. The simulation focuses on the overall condition of the stator winding by evaluating generator performance at rated conditions. The hypothesis is that stator winding degradation leads to a reduction in the values of R_s, L_m and L_{ls}. The SCIG model is then simulated in MATLAB / Simulink with reduced values of the stator and mutual inductance equivalent circuit parameters. The severity of the stator winding degradation is calculated as percentage values from 1% to 15% of the original stator and mutual inductance equivalent circuit parameters.

3.1.2 SCIG design parameters

The SCIG in this study has the following design parameters as shown in **Table 5**.

Table 5: SCIG design parameters

SCIG 2.3 MW, 690 V, 50 Hz	
Rated Output Power	2.3 MW
Rated Line to Line Voltage	690 V
Rated Phase Voltage	398.4 V
Rated Stator Current	2100 A
Rated Stator Frequency	50 Hz
Rated Power Factor	0.88
Rated Rotor Speed	1510 rpm
Synchronous Speed	1500 rpm
Rated Slip	-0.0069
Number of poles	4
Stator Winding Resistance, R_s	1.01 mΩ
Rotor Winding Resistance, R_r	1.3 mΩ
Stator Leakage Inductance, L_{ls}	0.093 mH
Rotor Leakage Inductance, L_{lr}	0.054 mH
Magnetizing Inductance, L_m	2.78 mH
Rated Mechanical Torque	16.313 kNm
Moment of Inertia	63 kgm³

3.1.3   Asynchronous model in MATLAB/Simulink

The SCIG is simulated using the asynchronous machine model in Simulink which can be operated as a motor or a generator depending on the sign of the input torque value. The machine block diagram is illustrated in **Figure 36** and has two inputs for torque (Tm) and stator voltages (Terminals A, B and C). Output parameters are available via terminal m which provides various mechanical and electrical signals for display and analysis.
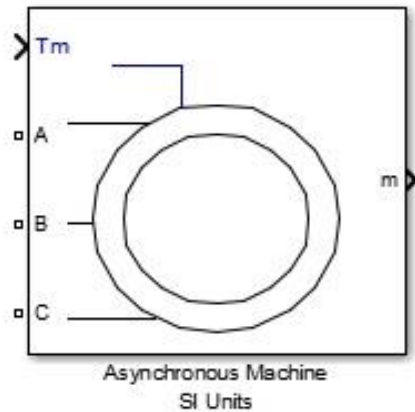
Figure 36: Asynchronous machine block diagram

The asynchronous machine block model parameters can be accessed by double clicking on it and values can be entered as per unit or SI. Four tabs are displayed which allow customization of the model as shown in **Figure 37** and **Figure 38.**
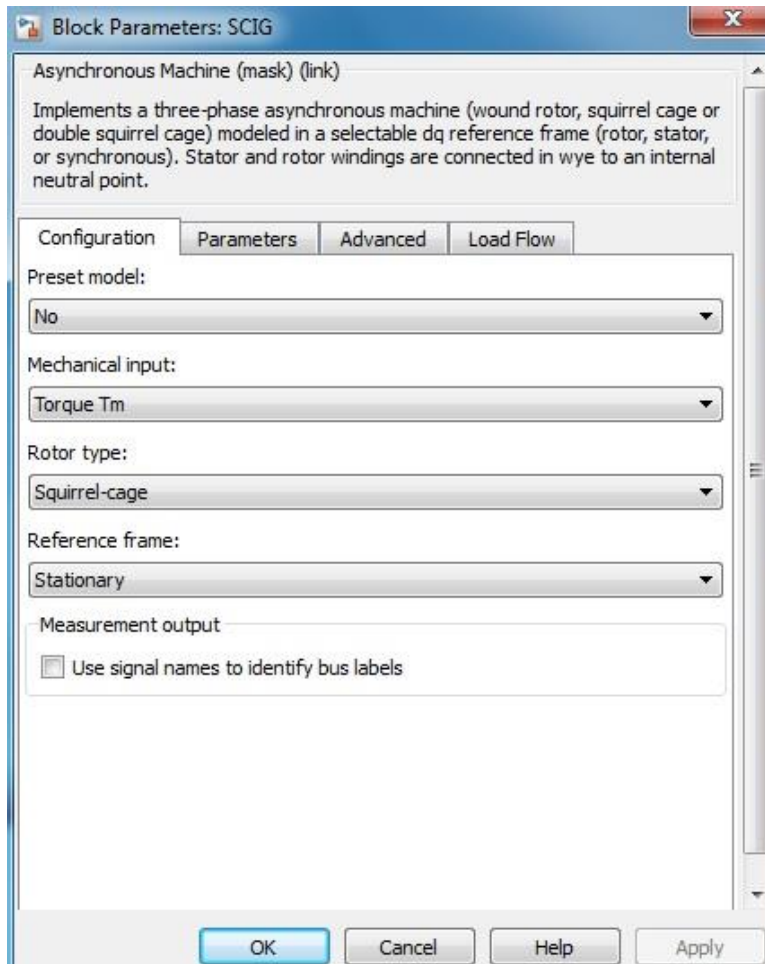
Figure 37: SCIG block configuration

Mechanical input tab is selected to decide whether rotor speed or shaft torque is used to drive the generator. Torque is used as a Simulink input to the asynchronous machine block in this simulation.
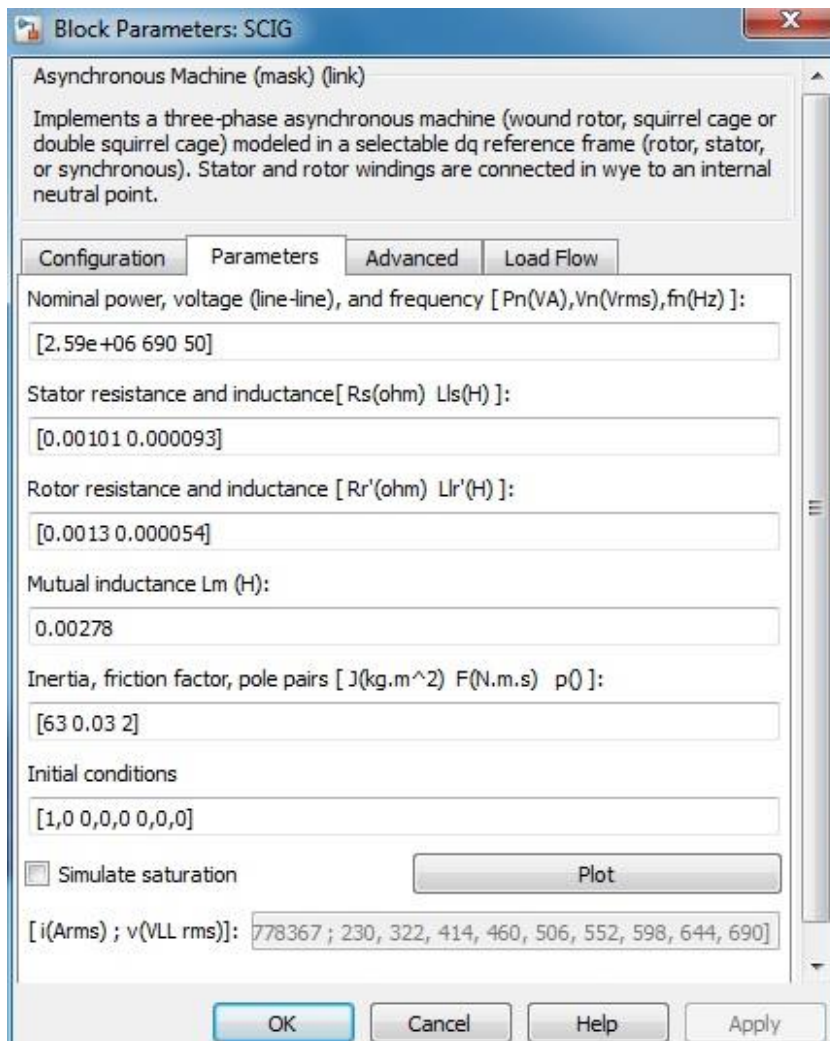
Figure 38: SCIG block parameters

It is not required to change the Advanced and Load Flow tab settings for this simulation. The stator and mutual inductance parameters values will be changed while the rotor parameters are kept constant. The initial conditions of the machine remain as is and will be activated under the Machine Initialization tab in the Powergui block which is shown in **Figure 39**. For each new value of stator parameters, the Initial conditions have to be manually reset to calculate the performance of the machine at the new values.
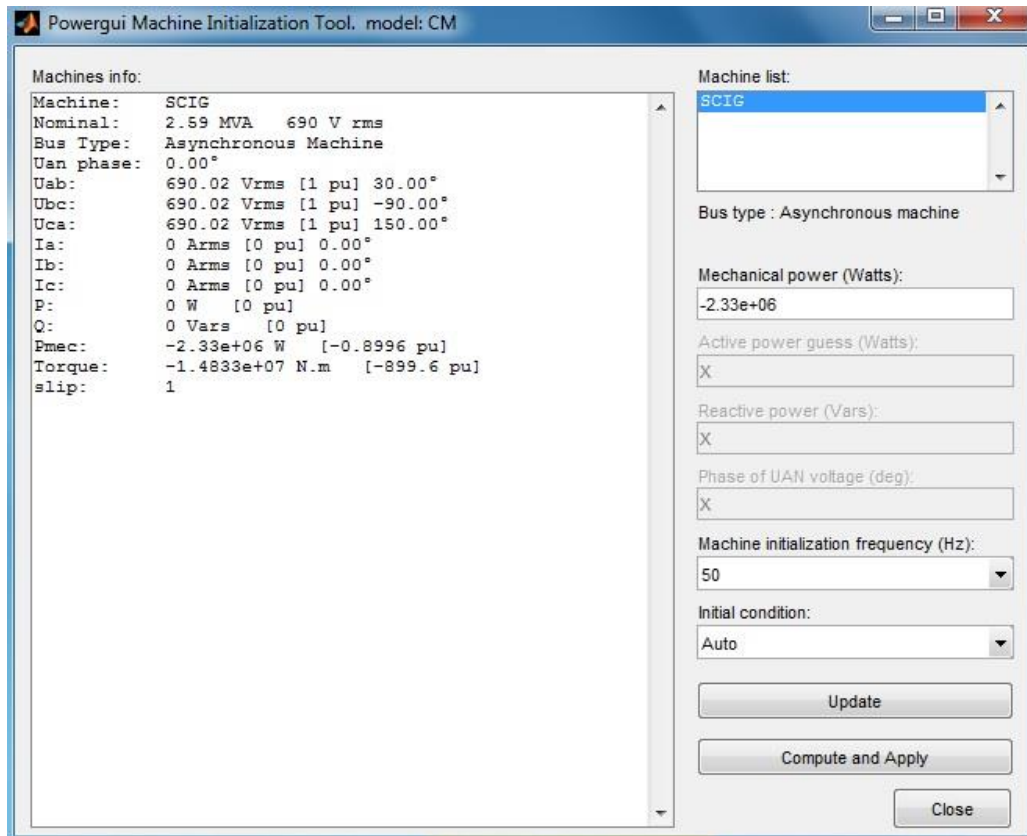
Figure 39: Machine initialization tool

Mechanical power or Tm is reduced to ±90% of the rated value to compensate for the absence of the control system which regulates the output power. This ensures that the output power and phase currents are kept close to rated values which are comparable to actual operational data of the wind turbine.

3.1.4 Torque input (Tm) model

The asynchronous machine model can either be used as a motor or generator depending on the value of Tm. If the value of Tm is negative the model is used as a generator and vice versa. A Constant Simulink block is used for Tm which produces either a real or complex constant output value. **Figure 40** (a) and (b) show the source and parameter blocks for Tm.

Constant

(a)

(b)
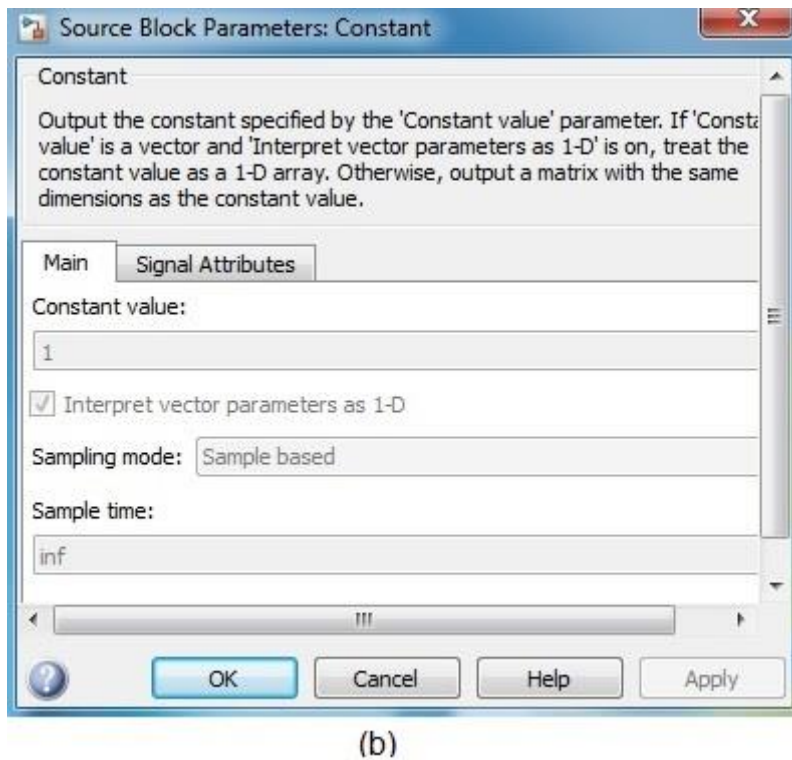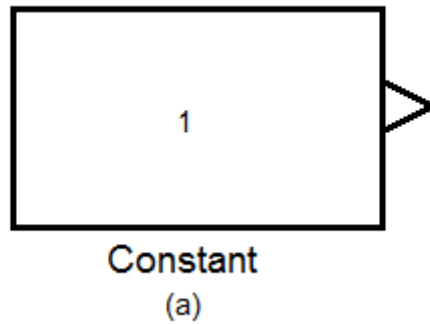
Figure 40: Torque block diagram

3.1.5 Stator voltage block

The stator of the SCIG is normally connected to the grid via two back-to-back PWM voltage source power converters. Because the focus of the simulation is on steady state conditions, each of the generator stator phases is connected an ideal AC voltage source. The stator voltage source and parameter blocks are illustrated in **Figure 41** (a) and (b).

(a)
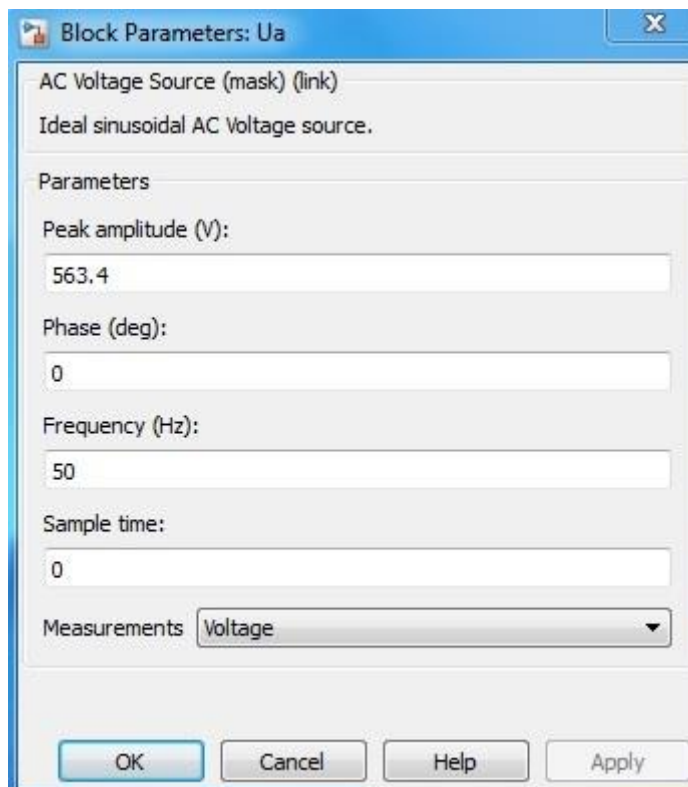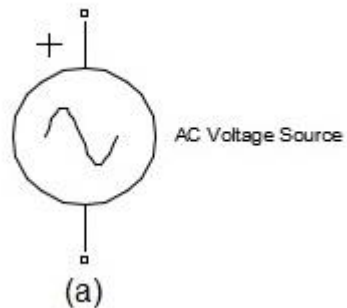
(b)

Figure 41: AC voltage block

The complete SCIG wind turbine model operating at steady state conditions is shown in **Figure 42**.
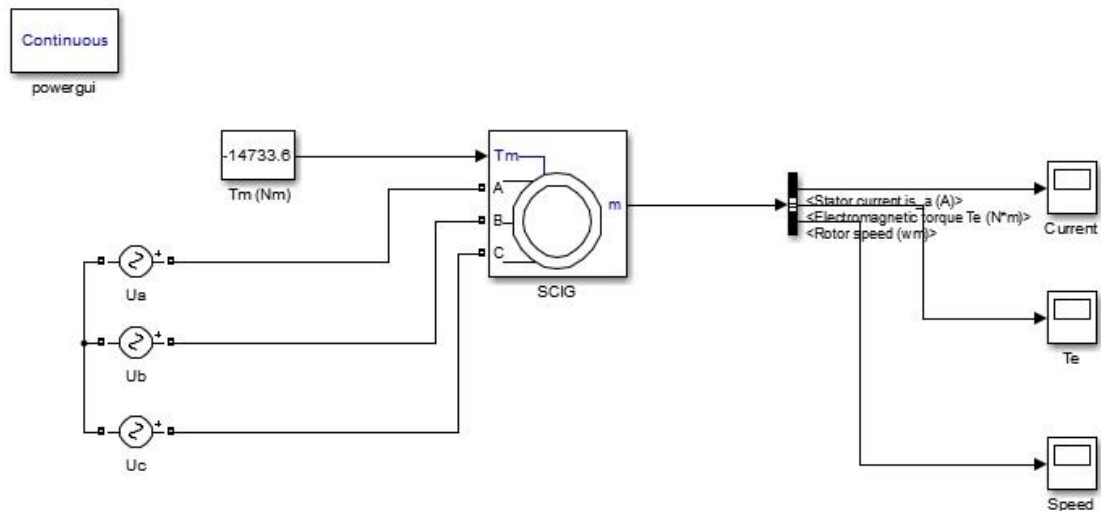
Figure 42: The complete SCIG Simulink model

When the machine initialization tool is activated, the simulation calculates the parameters at rated steady state conditions as shown in **Figure 43**. The information can be then analysed to establish how the machine performance is affected by varying the stator and mutual inductance equivalent circuit parameters.
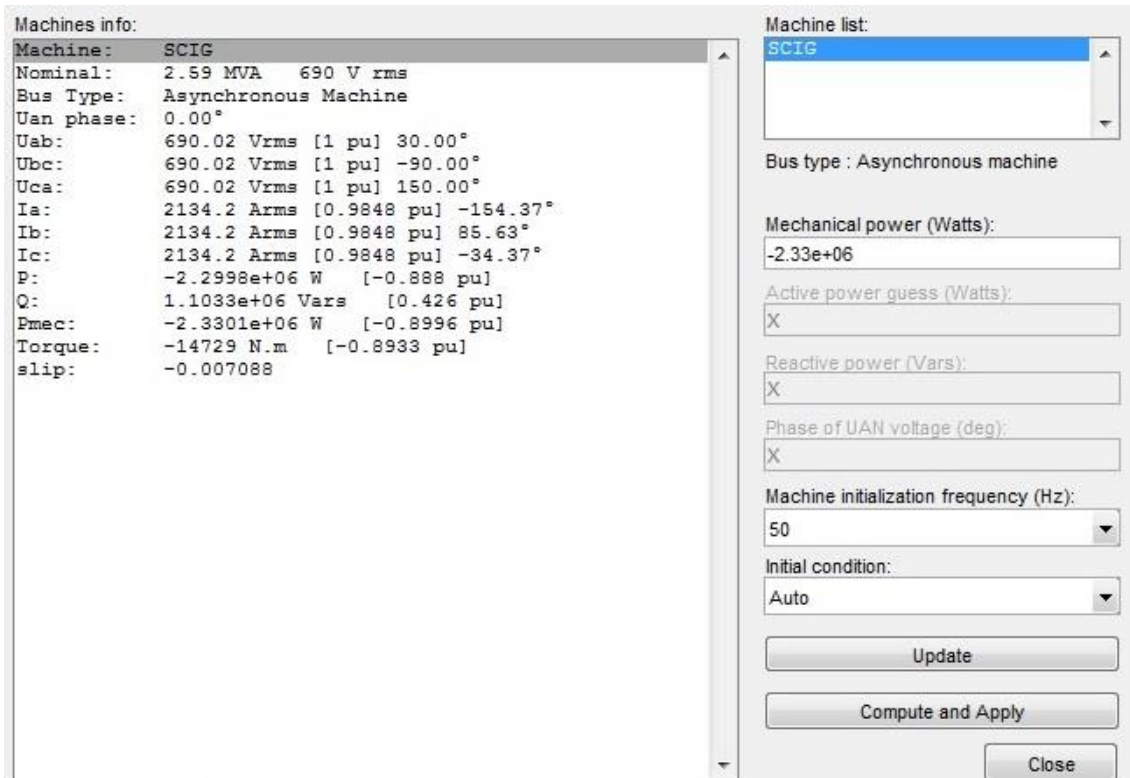
Figure 43: SCIG machine initialization calculations

3.2   Prediction model of stator winding temperatures

SCADA data from 2 wind turbines is used to model generator winding temperature between minimum and maximum output power which corresponds to 0 MW – 2.4 MW. Data for wind turbines (WTs) 4 and 38 was collected from June 2015 until October 2015. The maximum designed generator stator winding insulation temperature for the wind turbines is 155 ⁰C which corresponds to a Class F rated insulation material.

Multiple linear regression analysis is a statistical method that estimates or model relationships between different variables that are linked in a nondeterministic way [144]. It uses more than one independent variable compared to linear regression which has only one independent variable. The stator winding temperature prediction model is designed using Stepwise Regression (SR) in Microsoft Excel. The model output also highlights which variables have the biggest influence on stator winding temperature. Modelling of stator winding temperature in this study equates to the generator temperature.

SR perform multiple regressions that add or remove independent variables at each step based on performing a partial F-test [144] on the new independent variable. The F-test calculates if different variables are mutually important and that their output has a significant effect on the dependent variable. It selects the independent variable with the highest correlation with the dependent variable initially, then adds or removes independent variables in the model based on calculating its F-test value which should be higher or at least equal to the previous value.

When you have two independent variables, the F-test value is calculated using [144]:

$$F_1 = \frac{SS_R(\beta_1|\beta_2,\beta_0)}{MS_E(x_1,x_2)}$$ (14)

where:

F_1 -   F-statistic of independent variable x_1

SS_R -   Sum of squared residuals due to regression

MS_E -   Mean square error for the model containing x_1 and x_2

β_0,β_1,β_2 -   Slope coefficients

The following assumptions are made to establish how a linear regression model fits the data [144]:

- The residuals should be uncorrelated random variables with a zero average and constant variance.
- The residuals should be normally distributed.
- The order of the model is correct and that the data being investigated has linear characteristics.

A linear regression model where the dependent variable Y is related to k regressor (independent) variables has the form [144]:

$$Y = \beta_0 + \beta_1 x_1 + \beta_2 x_2 + \cdots + \beta_k x_k + \in \qquad (15)$$

where:

Y   -   Dependent variable

β_0 -   Intercept

β_j, j = 0,1,…,k -   Regression coefficients

x   -   Regressor variables

$\in$ -   Random error term

The model therefore provides an acceptable estimation of the dependent variable across certain ranges of the independent variables because the real relationship between them cannot be determined [144]. Regression coefficients represent the rate at which the dependent variable changes in relation to individual independent variables.

They are calculated in SR using the least squares method represented by the following matrix notations [144], [145]:

$$
y = \begin{pmatrix} y_1 \\ y_2 \\ .. \\ y_n \end{pmatrix}, \quad \beta = \begin{pmatrix} \beta_1 \\ \beta_2 \\ .. \\ \beta_n \end{pmatrix}, \quad \in = \begin{pmatrix} \in_1 \\ \in_2 \\ .. \\ \in_n \end{pmatrix}, \quad \beta = (X'X)^{-1}X'y \tag{16}
$$

$$
x = \begin{pmatrix} 1 & x_{11} & x_{12} & .. & x_{1k} \\ 1 & x_{21} & x_{22} & .. & x_{2k} \\ .. & .. & .. & .. & .. \\ 1 & x_{n1} & x_{n2} & .. & x_{nk} \end{pmatrix}
$$

The calculation of the predicted value of y is obtained by [144]:

$$
\hat{y} = \beta_0 + \beta_1 x_1 + \beta_2 x_2 + \ldots \ldots + \beta_k x_k \tag{17}
$$

3.2.1 Evaluating the adequacy of the model

The SR model needs to satisfy certain criteria to justify whether its linear function is sufficient to predict generator stator winding temperature over the proposed output power range of the wind turbines.

The following parameters are selected as variables in the SR model:

- **Ambient Temperature (AT)**

  The AT refers to the outside temperature conditions. The outside air is used to cool the generator as well as the inside of the nacelle. This independent variable is labelled as "Mean Ambient Tmp" in the SR model.

- **Nacelle Temperature (NT)**

  The temperature in the nacelle affects the generator operating conditions directly as well as other components. High nacelle temperatures cause the generator to run hotter which affects its performance. The nacelle temperature is not regulated. This independent variable is labelled as "Mean Nacelle Tmp" in the SR model.

- **Generator Output Power (GOP)**

  The stator winding temperature is related to the square of the phase current flowing in the windings. Therefore the higher the generated output power, the hotter the windings become. This independent variable is labelled as "Active Power" in the SR model.

- **Stator Winding Temperature (SWT)**

  The stator winding temperature is the dependent variable which the model regresses. Having knowledge which independent variable has the highest influence on stator winding temperature is important to optimize the generator operation. The SWT is predicted by the model based on the values of the independent variables AT, NT and GOP. The dependent variable is labelled as "Mean Winding Tmp U1" in the SR model.

3.2.1.1 Significance of regression model

The first check if the SR model is acceptable is to evaluate the value of the Coefficient of Determination R^2 ($0 \leq R^2 \leq 1$) which also means the goodness of fit test. It shows the proportion of the variation of the dependent variable explained by the independent variables. A value of R^2 close to 1 is ideal but it doesn't always imply that the model fits the data best or that future predictions by the model are perfect. It is affected by the number of independent variables, scatter or distribution of the independent variable(s) as well as adding higher polynomial values of the independent variable(s) in the model [144]. R^2 can be calculated using:

$$R^2 = \frac{SS_R}{SS_T} \qquad (18)$$

where:

SS_R -   Regression sum of squares.

SS_T -   Total sum of squares.

The F-test based on an F- distribution confirms the significance of the regression model. The following hypothesis is valid:

H_0: $\beta_1, \beta_2 \ldots \beta_k = 0$.

H_1: $\beta_j \neq 0 \ldots$ for at least one j

The F- critical value of the F- distribution is calculated in Microsoft Excel using the function:

$$\text{F.INV(probability, DoF 1, DoF 2)} \qquad (19)$$

F.INV   -   Calculates the inverse of the F-distribution

Probability   -   95% confidence level.

DoF 1   -   Degrees of freedom. Number of independent variables.

DoF 2   -   Degrees of freedom. Number of residuals.

If F- critical >value needs to be larger than F – model value for the Null Hypothesis H_0 to be rejected which confirms that the model fits the data adequately with a 95% confidence level. Additionally the regression coefficients ($\beta_0 - \beta_3$) in this model should all have p-value less than 0.05 which also confirms that H_0 can be rejected.

3.2.1.2 Analysis of residuals

The residuals also called the errors are defined as the difference between the actual observation and the predicted observation from the model [144]:

$$e_i = y_i - \hat{y}_i, i = 1,2, \ldots \ldots n \tag{20}$$

where:

e_i -   Residual or error.

y_i -   Actual observation.

$\hat{y}_i$ -   Predicted observation from the model.

By plotting the residuals it can illustrate how the model best fit the data and show up any deviations from the previous assumptions made on applying linear regression. To check for normality in the residuals of the model, a normal probability plot of the residuals can be obtained in Microsoft Excel. A plot of the residuals versus the predicted observation $\hat{y}_i$ can also be retrieved in the same manner. This plot has to show the residuals outlined in a horizontal distribution about the zero average without any distinctive pattern for the model to be adequate [128]. Residual plots can have one of the four general outlines as shown in **Figure 44** [144]. **Figure 44** (a) shows that the model is ideal, whereas the other plots (b – d) contain anomalies which show that the model could be inadequate for the data sample.
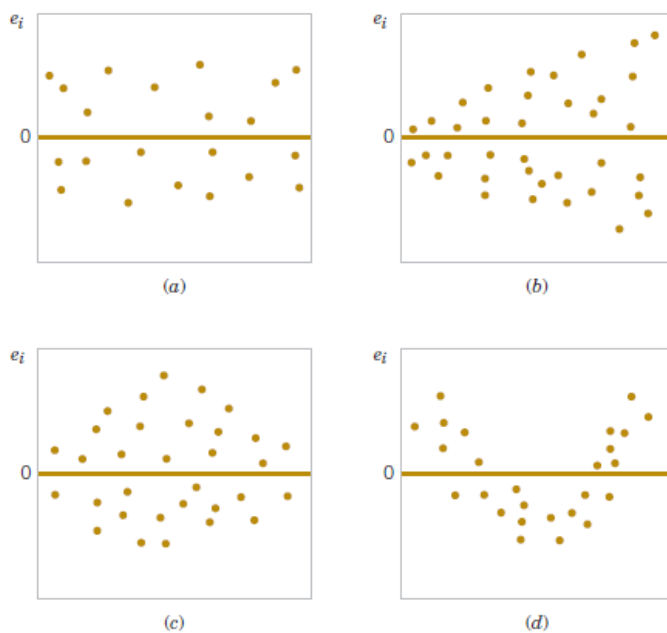
Figure 44: General residual plot patterns

In this study a normal probability plot of residuals versus their standardized Z-scores is given. The procedure to construct the normal probability plot is as follows:

- Obtain the normal residuals from Microsoft Excel (SR);
- Rank each of the residuals;
- Calculate the percentile or proportion of the residuals that is smaller than a particular residual using [146]:

$$P_i = \frac{Rank\ value - 0.375}{n + 0.25} \tag{21}$$

where n is the number of observations;

- Calculate the Z-score using Microsoft Excel Normal Distribution function:
$$= norm.s.inv(P_i) \tag{22}$$
- Print a scatter plot residuals vs Z-scores.

This method is considered an improvement of the normal probability plot of the residuals in Microsoft Excel. If the residuals are normally distributed, 99.72% of the data will fall within 3 standard deviations of the mean. Therefore we can conclude that Z-score values outside these ranges do not have the same characteristics as the rest of the data and are possible outliers.

3.2.1.3 Intrinsically linear models

Linear regression can also be applied to investigate nonlinear characteristics between variables. Instead of using a straight line, linear regression has the functionality to fit curves to data which could be more appropriate for nonlinear conditions [147]. In this case transformation of the dependent and or independent variables are required [144].

Intrinsically linear models or curve fitting the data can be done through polynomial regression where the independent variables are transformed in consecutive powers i.e. X, X^2, X^3 etc. [147]. Polynomial regression is used to detect any nonlinearity between the independent and dependent variables. Therefore the 2nd and 3rd powers of all three dependent variables AT, NT and GOP together with the linear values are used in the SR model.

A cubic polynomial with one independent variable [147] has the following form:

$$Y = b_0 + b_1 X + b_2 X^2 + b_3 X^3 \tag{23}$$

If we set $x_1 = X$, $x_2 = X^2$, $x_3 = X^3$ then Equation 21 can be rewritten as:

$$y = \beta_0 + \beta_1 x_1 + \beta_2 x_2 + \beta_3 x_3 + \epsilon \tag{24}$$

which is a multiple linear regression model similar to Equation 15.

CHAPTER FOUR
RESULTS AND ANALYSIS OF CONDITION MONITORING MODELS

In this section the simulation results of the wind turbine generator model is discussed and its ability to simulate stator winding degradation. The results from the statistical model are also presented. It examines how well the SR model can predict future stator winding temperatures based on actual operating conditions.

4.1   SCIG MATLAB / Simulink Model analysis

A MATLAB / Simulink model for stator winding degradation is simulated by varying the machine's stator and mutual inductance equivalent circuit parameter values. The model results are shown in **Table 6**. The table displays the percentage degradation, stator current, apparent power, active power and the reactive power.

Table 6: SCIG MATLAB / Simulink model results

Degradation (%)	Stator Current (A)	S (MVA)	P (MW)	Q (MVArs)
0	2134.2	2.59	-2.3	1.1033
1	2134.9	2.59	-2.3	1.1048
2	2135.5	2.59	-2.3	1.106
3	2136.1	2.59	-2.3	1.107
4	2136.9	2.59	-2.3	1.1095
5	2137.8	2.59	-2.3	1.1116
6	2138.5	2.59	-2.3	1.1133
7	2139.5	2.59	-2.3	1.1156
8	2140.4	2.59	-2.3	1.1178
9	2141.3	2.59	-2.3	1.12
10	2142.4	2.59	-2.3	1.1227
11	2143.5	2.59	-2.3	1.1256
12	2144.6	2.59	-2.3	1.1282
13	2145.8	2.59	-2.3	1.1312
14	2147.2	2.59	-2.3	1.1346
15	2148.6	2.59	-2.3	1.11381

The simulated phase current value is larger than the actual rated current of 2100A even with no degradation present. The absence of a control system in the model and the fact that skin effect and magnetic saturation was ignored could result in some model deficiencies. There is also no provision for reactive power consumption in the model. As the values of the equivalent circuit parameters become smaller, the phase current and reactive power consumption of the generator increases.

The difference in stator current with zero and 15% degradation are shown in **Figure 45** and **Figure 46** respectively.
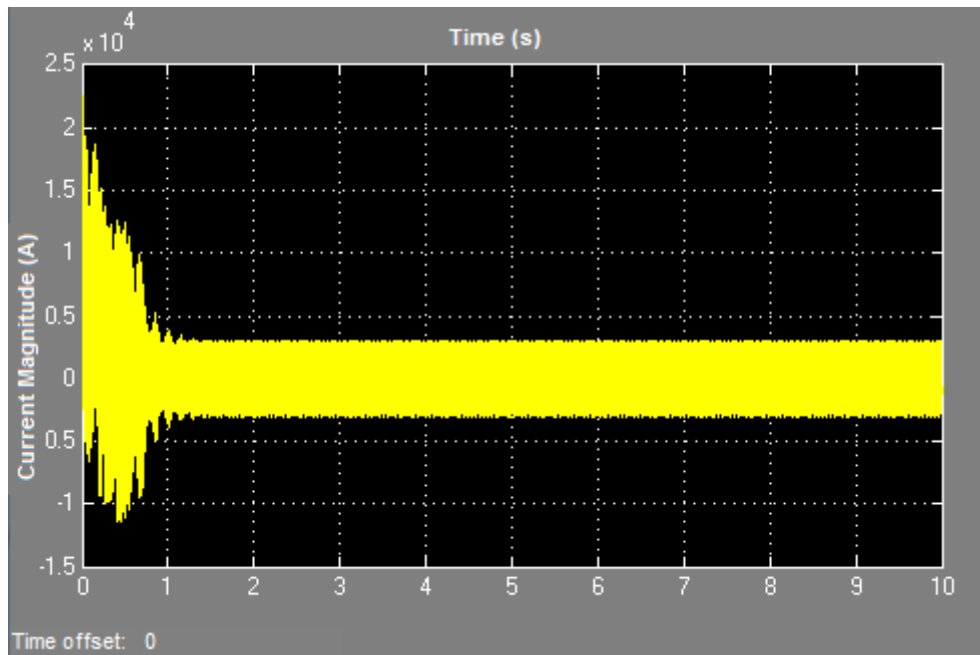
Figure 45: Stator phase current with zero degradation
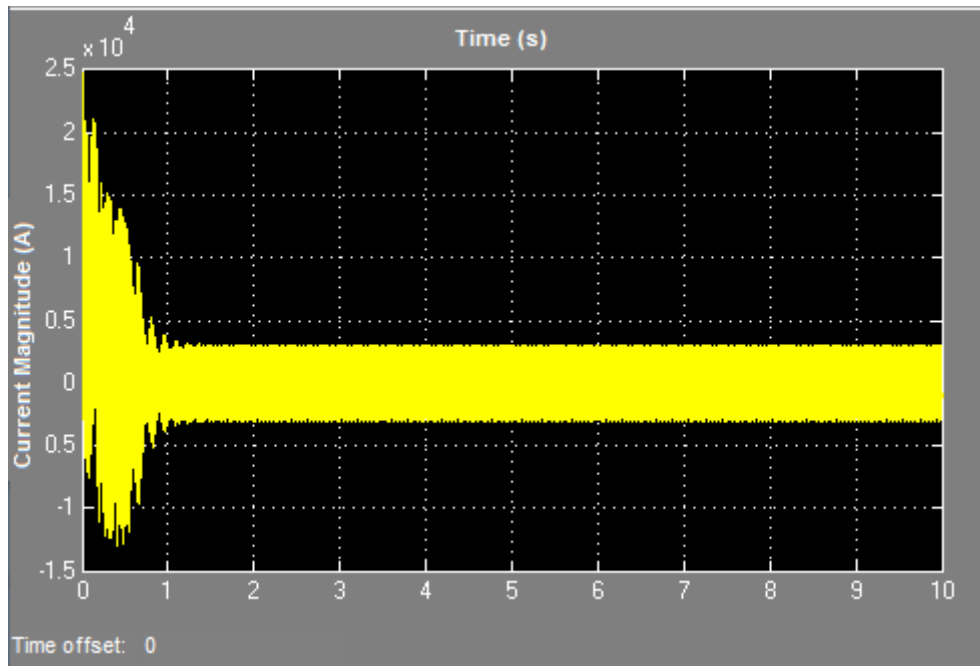
Figure 46: Stator phase current with 15% degradation

The lower values of the equivalent circuit parameters cause larger inrush currents before the generator reaches steady state operation. Since the focus of the simulation is on steady state operations, the value and quality of the current at these conditions are thus of importance.

Because the overall impedance of the phase circuit reduces, the stator current has to increase. The presence of winding degradation also means that less airgap flux is produced and therefore the machine draws more magnetizing current to meet the rated power supplied to the grid.

Motor current signal analysis has been extensively applied as condition monitoring technique in the stator windings. Stator winding degradation will definitely cause distortion of the airgap flux which can be reflected in the stator currents. This technique is very sensitive to machine loading and other limitations makes it very challenging to implement [148].

The time to frequency domain analysis of the stator phase current is performed by the Fast Fourier Transform Analysis tool as shown in figures below. **Figure 47** represents the healthy condition with zero damage and Figure 48 indicates winding degradation with 15% damage. In both figures the fundamental frequency of 50Hz has a magnitude of 100% which cannot be read from the figures.
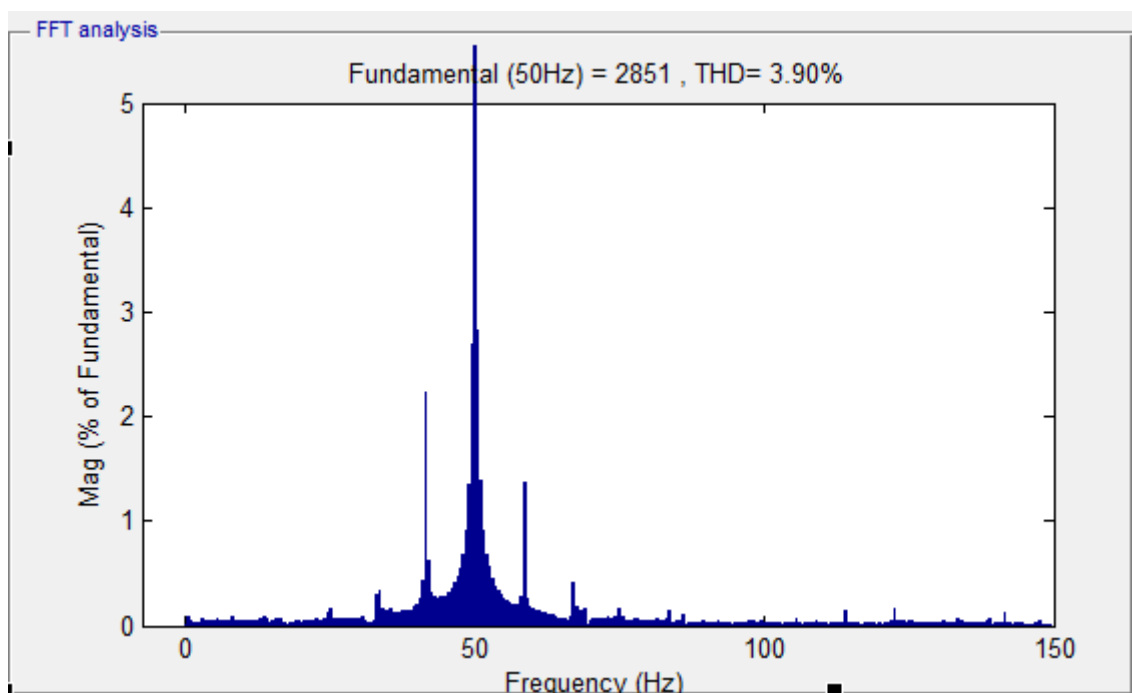
Figure 47: FFT analysis of stator phase current with zero degradation
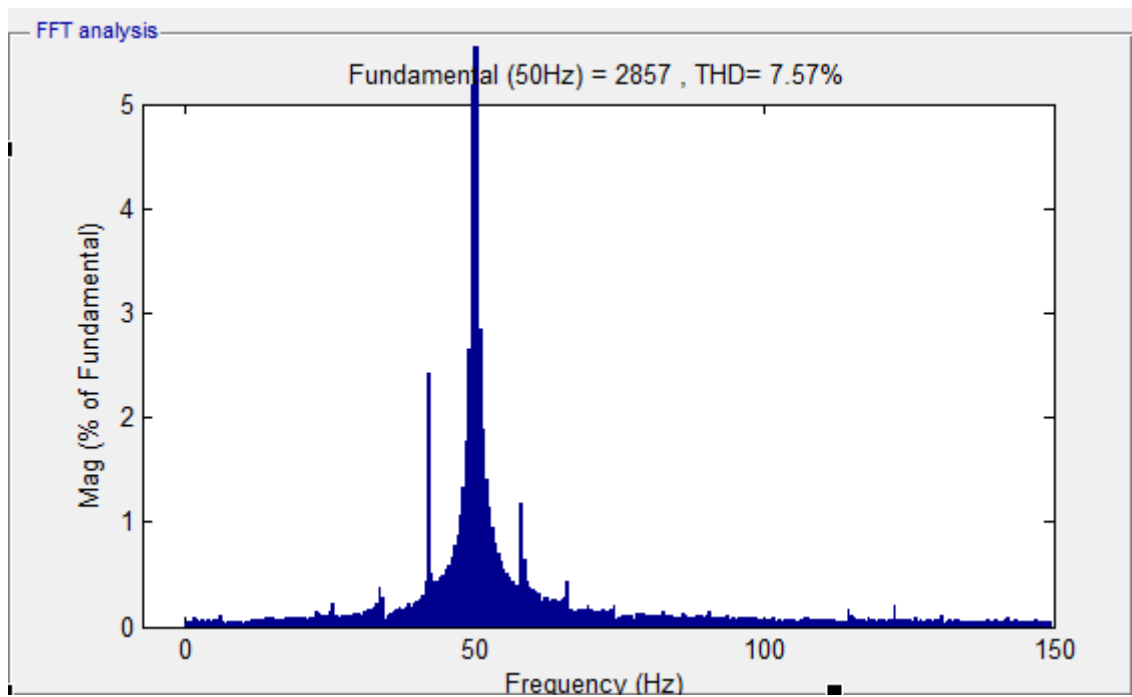
Figure 48: FFT analysis of stator phase current with 15% degradation

Based on the increase in the total harmonic distortion which almost doubled, the conclusion can be drawn that damage could be present. However considering the complexity of the simulation model and the fact that the generator is not loaded, further analysis is required to verify the accuracy of these results.

The electromagnetic torque and rotor speed of the SCIG are shown in **Figure 49** and **Figure 50.**
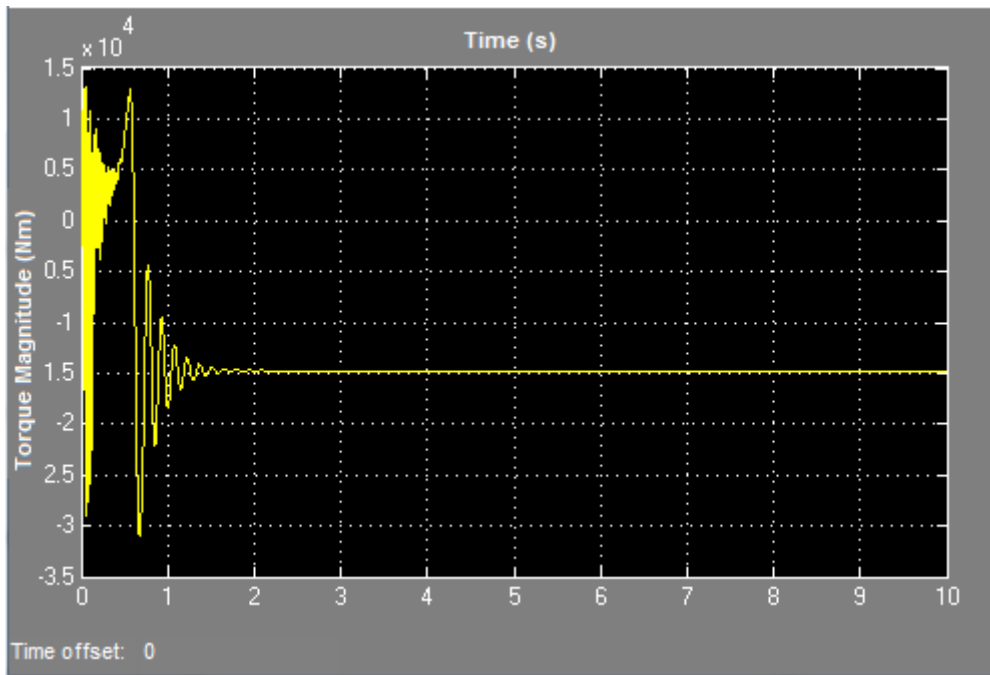
Figure 49: SCIG electromagnetic torque output
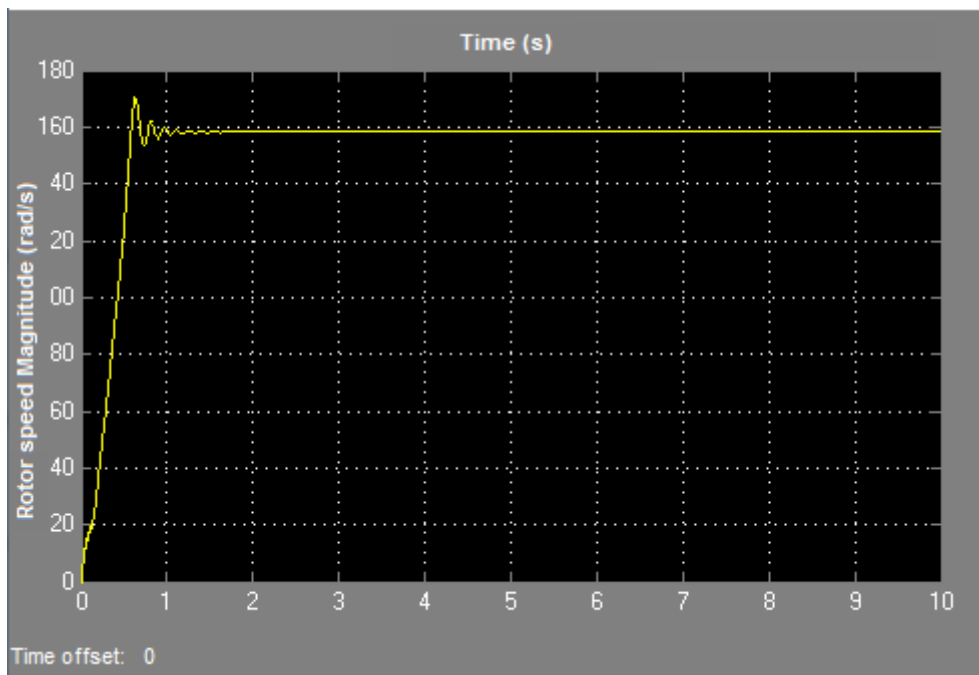
Figure 50: SCIG rotor speed waveform

4.2 Statistical model analysis

Generator output power followed by nacelle temperature affects stator winding temperature the most as shown in **Table 7**. Full details of the SR models can be found in Appendices A and Appendix B for WT4 and WT38 respectively.

Table 7: Independent variables coefficients

WT4 SR Coefficients				
	Coefficient	Std Err	t-value	p-value
Constant	-15.9430	0.5025	-31.7252	0.0000
Active_Power	0.0192	0.0001	175.4487	0.0000
Mean_Nacelle_Tmp	2.3350	0.0328	71.2527	0.0000
Mean_Ambient_Tmp	-0.6295	0.0290	-21.6973	0.0000
WT38 SR Coefficients				
	Coefficient	Std Err	t-value	p-value
Constant	-25.3452	0.5051	-50.1823	0.0000
Active_Power	0.0168	0.0001	175.2132	0.0000
Mean_Nacelle_Tmp	2.7916	0.0304	91.9546	0.0000
Mean_Ambient_Tmp	-0.8144	0.0254	-32.0913	0.0000

This is expected as higher generated output power, cause more current flow through the windings and more heat is generated which is proportional to the square of the current. The nacelle temperature represents the ambient temperature of the generator and therefore also has a big impact. Insulation material of electrical machines is generally designed for an ambient temperature of 40 ºC [149] and higher temperatures degrades the winding insulation material.

Temperatures higher than 40 ºC in the nacelle can therefore cause the generator to shutdown to maintain the temperature rise limit of the insulation which is 105 ºC for Class F. The temperature rise limit is calculated by subtracting the ambient temperature from the hot temperature of the insulation which is 155 ºC – 40 ºC.

The outside temperature referred to as ambient temperature in the SR model is used for cooling of the stator windings. The outside air temperature has a limit of 45 ⁰C before the controller shuts down the machine to prevent overheating of the stator. Effective cooling can also be affected by dirty or blocked air filters. These can be checked during routine maintenance activities and replaced as required.

According to the SR model its ability to predict stator winding temperature for WT4 and WT38 can be obtained using:

$$SWT = 0.0192AP + 2.335NT - 0.6295AT - 15.943 \text{ (WT4)} \qquad (25)$$

$$SWT = 0.0168AP + 2.7916NT - 0.8144AT - 25.3452 \text{ (WT38)} \qquad (26)$$

where,

AP   -   Active Power (Generator Output Power)

NT   -   Nacelle Temperature

AT   -   Ambient Temperature

It can be concluded that the location and wind resource of the two turbines have a significant impact on the stator winding temperature. Environmental conditions could be less ideal for one turbine which effects the cooling of the nacelle and generator. Access to optimum wind conditions means a higher capacity factor and also higher average stator winding temperatures. The level of maintenance also needs consideration as one turbine can be exposed to severe dusty or moist conditions.

4.3 Adequacy of the SR model

Linear regression models such as SR need to meet certain criteria for accurate modelling of relationship between variables. It is generally assumed that these relationships between the variables are linear for the modelling to be successful.

4.3.1 Significance of the model

The coefficient of determination or R^2 indicates how well the independent variables explain the variability in the depended variable. The SR model calculated $R^2 = 0.911$ for WT4 and $R^2 = 0.9234$ for WT38. Although the value of R^2 in both models is high, the ability of the models to predict stator winding temperature accurately is not guaranteed. It does however indicate that GOP, NT and AT has a huge impact on the stator winding temperature.

The F-test (value) confirms if the regression is significant. If the F-test falls to the left of the F-critical value in the F Distribution, the Null Hypothesis is accepted which means the regressors have no influence on the depended variable. If F-test > F-critical, the Null Hypothesis is rejected. The ANOVA Tables of both SR models in **Table 8** shows that the regression is significant which means the models for both wind turbines are adequate. In **Table 7** the p-values of the regressors are all less than 0.05 which also confirms the significance of the model.

Table 8: ANOVA statistics of SR

ANOVA Table	WT4						
	Source	df	SS	MS	F	p-value	$F_{critcial}$
	Explained	3	6718214	2239405	50097.77	0	2.606
	Unexplained	14644	654596.8	44.70068			
ANOVA Table	WT38						
	Source	df	SS	MS	F	p-value	$F_{critcial}$
	Explained	3	7320599	2440200	62981.03	0	2.605
	Unexplained	15683	607637.7	38.74499			

4.3.2 Residual analysis

A normal probability plot of the residuals is another check whether the SR is adequate to predict stator winding temperature accurately. If the residuals are normally distributed as assumed initially their probability plots represent a straight line. The residuals normal probability plots as shown in **Figure 51**(a) and (b) resemble that of a straight line which implies that the SR model is adequate.

However there are potential errors in the model's prediction at both extreme ends of the data distribution. These terms fall outside the 3 standard deviations from the mean which is indicative of a data set with heavier tails compared to the normal distribution. Nonlinearity is the likely explanation for these deviations which means the presence of outliers in the data set. The results confirm the nonlinear operation of a wind turbine over its power range which is pronounced at the start and when rated power is produced. Between these regions the wind turbine has a very linear operating characteristic which justifies the application of the SR model.
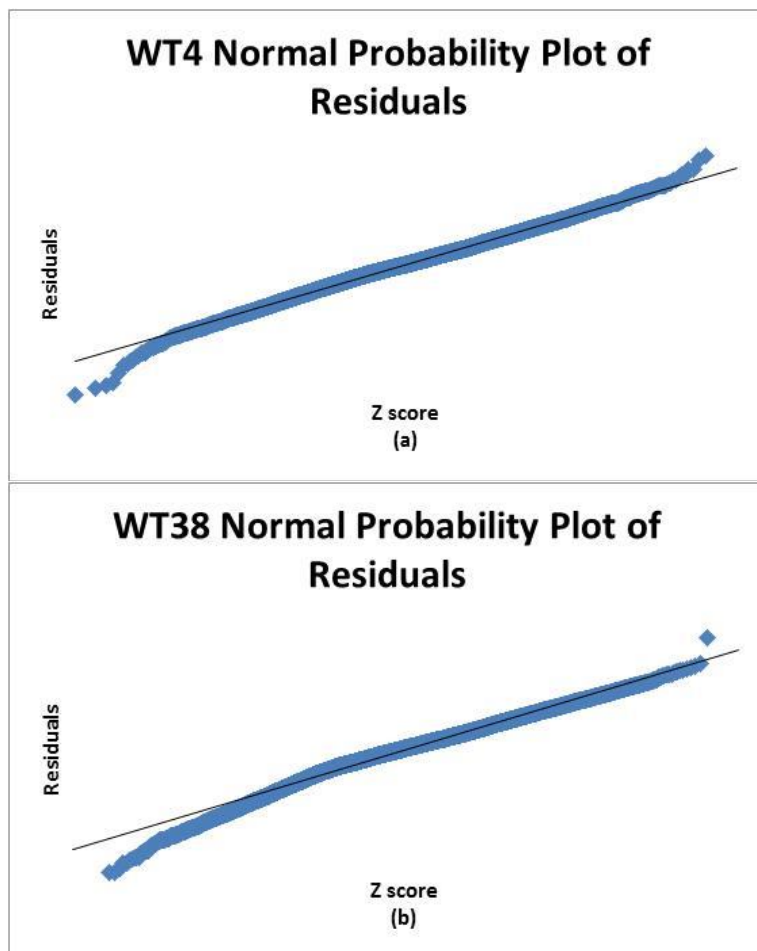
Figure 51: Normal probability plots of residuals

4.3.3 Using intrinsically linear models

The use of intrinsically linear models allows linear regression to model nonlinear relationships through the transformation of the variables. In this study a 3rd degree polynomial regression model was applied to establish if it predicts stator winding temperature more accurately than the straight line model. The results of the polynomial regression models of WT4 and WT38 are shown in **Figure 52**.

				Change	% Change		
Polynomial regression model WT4							
Summary measures				Change	% Change		
	Multiple R	0.964441347	6.46E-05	6.7E-05			
	R-Square	0.930147111	0.000125	0.000134			
	Adj R-Square	0.930104196	0.00012	0.000129			
	StErr of Est	5.931544781	-0.00509	-0.00086			
ANOVA Table							
	Source	df	SS	MS	F	p-value	
	Explained	9	6857799	761977.7	21657.42	0	
	Unexplained	14638	515012	35.18322			
Regression coefficients							
		Coefficient	Std Err	t-value	p-value		
	Constant	66.28877258	6.471363	10.2434	1.53E-24		
	AP	0.052948587	0.000618	85.73081	0		
	NT	-5.181650639	0.712859	-7.26883	3.81E-13		
	APP	-3.25668E-05	6.86E-07	-47.4844	0		
	APPP	8.10425E-09	2E-10	40.43946	0		
	AT	-2.567992449	0.285145	-9.0059	2.4E-19		
	NTT	0.239891365	0.023366	10.26647	1.21E-24		
	NTTT	-0.002414912	0.000251	-9.63068	6.89E-22		
	ATT	0.08771053	0.015003	5.846328	5.13E-09		
	ATTT	-0.00130075	0.000254	-5.11248	3.22E-07		
Polynomial regression model WT38							
Summary measures				Change	% Change		
	Multiple R	0.96881697	8.58E-06	8.86E-06			
	R-Square	0.938606322	1.66E-05	1.77E-05			
	Adj R-Square	0.938575029	1.28E-05	1.36E-05			
	StErr of Est	5.571918011	-0.00058	-0.0001			
ANOVA Table							
	Source	df	SS	MS	F	p-value	
	Explained	8	7441493	930186.6	29961.3	0	
	Unexplained	15678	486743.4	31.04627			
Regression coefficients							
		Coefficient	Std Err	t-value	p-value		
	Constant	104.6125031	6.801321	15.3812	0		
	AP	0.04850667	0.000597	81.27563	0		
	NT	-10.14899158	0.672786	-15.085	0		
	APP	-2.87167E-05	6.24E-07	-45.9856	0		
	APPP	6.92473E-09	1.76E-10	39.29534	0		
	AT	-1.03334105	0.043768	-23.6096	0		
	NTT	0.403902978	0.022257	18.14721	0		
	NTTT	-0.004041215	0.000242	-16.7315	0		
	ATTT	8.7034E-05	4.22E-05	2.062563	0.039171		

Figure 52: Polynomial regression model

where

X   -   AT, NT and AP

X²   -   ATT, NTT and APP

X³   -   ATTT, NTTT and APPP

The value of R^2 in the polynomial regression models show an improvement of less than 0.1 % compared to the SR models. Therefore both models explain the variation in stator winding temperature by the independent variables with the same accuracy. The F-test of the SR model is much higher than the polynomial regression model, which means the SR model is more significant.

The significance of the independent variables as determined by SR indicates that the linear independent variables are more important than the transformed independent variables. The SR model is simple, easy to implement and performs better than the polynomial regression model according to the various tests that were done. Considering the complexity and timeous development of the polynomial regression model, its application in this study is not justified.

4.3.4   Performance of the SR models

The regression model in this study is applied to identify abnormal high stator winding temperatures in the induction generator. Stator temperature SCADA logs of 10 minute intervals during November 2015 will be used as input to both wind turbine models. High stator winding temperatures outside the normal operating range of the generator can possibly be attributed to:

- Physical damage of the stator winding;
- Inadequate maintenance or cooling;
- Incorrect measurements,
- Equipment failure or
- Adverse operating conditions.

In WT4 where stator winding temperatures are below 40 °C, the predicted temperatures by the SR model are higher than the actual temperatures. This over estimation can also be observed at the higher temperature ranges although the prediction errors are smaller. The SR model for WT38 has similar performances when the stator winding temperatures are below 40 °C but has frequent under estimations at higher temperatures.

The performances of the SR models for WT4 and WT38 are shown in **Figure 53** and **Figure 54** respectively. Both models are able to predict the temperature trends in an acceptable manner and show very good accuracy when the stator winding temperatures are between 50 °C and 90 °C.
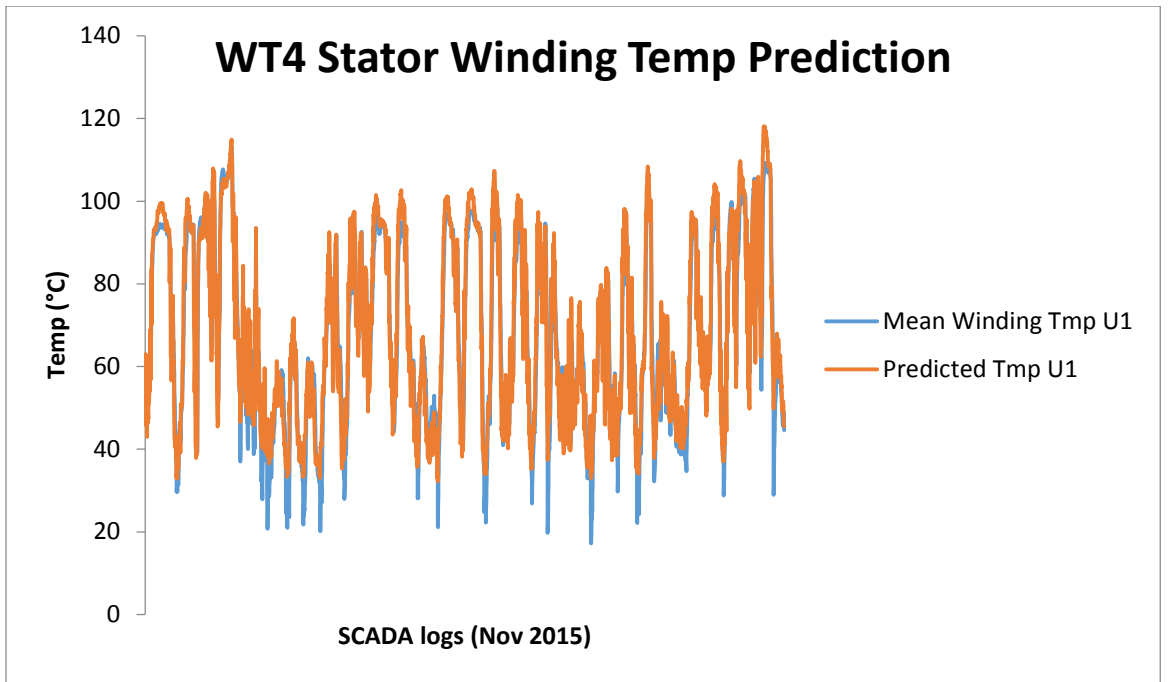
Figure 53: WT4 SR model performance
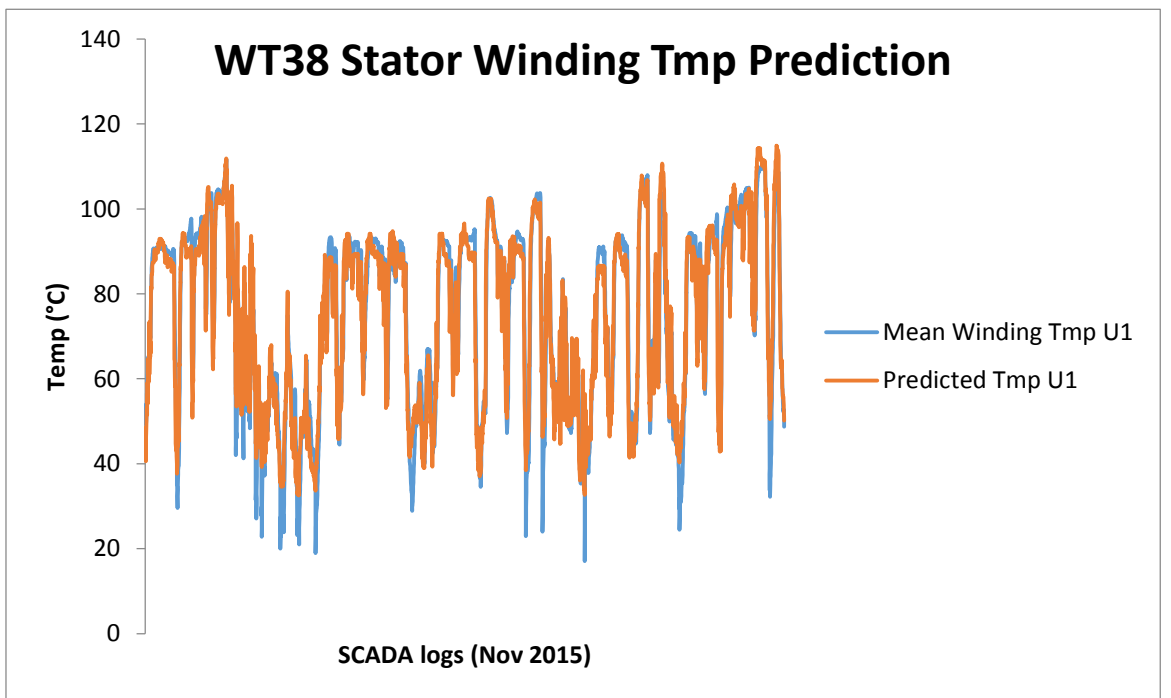
Figure 54: WT38 SR model performance

The SR model deficiencies at the two extreme ends of the data distribution are possibly caused by nonlinear behaviour. These data points fall outside the three standard deviations of the normal distribution of temperature ranges as shown by Error! Reference source not found.. There is a clear deviation by these data points away from the straight line function used in SR model.

Because wind turbines produces power below rated capacity the majority of the time, very low power regions just above the Cut-in wind speed can result in different stator winding temperatures even if the environmental conditions are the same. These represent the stator winding temperatures below 40 °C where the SR model performances are inadequate.

Above rated speeds the wind turbine control system regulates its output power which requires predominantly nonlinear control strategies. The rotor blade aerodynamics are changed rapidly to prevent excess power generation and loading on the wind turbine.

CHAPTER FIVE
CONCLUSIONS AND RECOMMENDATIONS

This chapter reviews the results and discuss the conclusions. Recommendations are made for further research and investigations.

5.1   Conclusions

The use of predominantly coal for power generation is causing harmful effects on the Earth's climate. High concentrations of CO_2 in the atmosphere are contributing to the phenomena called global warming. Because South Africa enjoys rich coal reserves, generating electricity from it seems a logical approach for the foreseeable future. As resources become depleted and expensive, these strategies might change driven by uncertain financial markets and degrading environmental conditions.

Cheaper cost of renewable energy technologies like wind energy has led to the diversification of Eskom power generating fleet. The construction of Sere wind farm by Eskom and the implementation of other renewable energy projects by the REIPPPP are examples that the South African government is building energy networks that are less carbon intensive. There is currently only 12% of the proposed 8.4 GW wind power connected to the national grid. With major changes in the energy policies recently, it is uncertain whether the renewable energy targets in the IRP of 2010 will be reached by 2030.

The lack of wind energy skills within Eskom has created the need to understand the technical impacts of wind turbines on the national grid. This knowledge will aid the production of cost effective electricity and ensure that supply and demand is met. High maintenance cost of wind turbines means that more predictive strategies like condition monitoring techniques are necessary to manage life cycle costs of critical components. Without this knowledge Eskom is forced to rely on O&M contracts provided by Siemens and other maintenance companies.

5.1.1 Condition monitoring methods

The main aim of this study was to develop new condition monitoring techniques for stators in SCIGs. A software simulation modelling stator winding degradation at steady state conditions using equivalent circuit parameters was proposed. Additional to this a statistical model was developed using SCADA data to estimate the relationships between winding temperatures and other variables. Predicting faults in stator windings are challenging because the unhealthy condition rapidly evolves into a functional failure.

The results from the simulation model showed that stator current and reactive power consumption increase when there is damage present in the winding. The magnitude of the increased current depends on the severity of the fault. The harmonic analysis of the stator phase current showed that the total harmonic distortion almost doubled between zero and 15% winding degradation. However the validity of these results is questionable and should only be used as initiation to implement proven condition monitoring techniques for stator winding. The implementation of the proposed simulation model can therefore not be used as a condition monitoring tool for stator windings in SCIGs.

The analysis of SCADA data as condition monitoring tool for stator windings has been proven to be adequate. Active power, ambient and nacelle temperatures showed that the effects on stator winding temperature are significant as calculated by the statistical model. The capability of the model is proven in the analysis of the normal probability plots of the residuals, F-test and the value of R^2. The statistical model performs very well when the wind turbine produces power at a constant rate below rated capacity.

This operating region of the wind turbine has a more linear characteristic. Since a wind turbine spends the majority of the time in this operating region, the model can definitely be used as a conditioning monitoring tool for the SCIGs at Sere wind farm.

5.1.2   Wind Technology

The literature review clearly shows that wind energy has evolved into a mature, cost effective and sustainable power technology. The size of wind turbines are growing on a continuous basis and new topologies allow for better integration into electricity grids. Power electronics development has provided the functionality of variable speed operation which is more energy efficient. SCIGs are more robust and cheaper to manufacturer compared to other generator types used in the wind turbines. The maintenance costs of SCIGs are therefore less.

As wind energy continues the upward growth in technology, the application of synchronous generators could become more competitive in future. Currently the size and material costs makes these generators expensive for wind power generation. Because of their proven history and superior grid operation in conventional power plants, wind energy systems can only benefit by incorporating them more in future designs.

Condition monitoring techniques for wind turbine generators are still at an infant stage compared to matured strategies used for generators in conventional power plants. The cost of wind energy can be further reduced if failures are predicted in advance which leads to less unplanned maintenance.

5.2   Recommendations

Further research is required to improve the MATLAB / Simulink model by addressing the following:

- A complete dynamical model is required as a wind turbine rarely operates at steady state conditions.
- Adding the aerodynamic, transmission, power converter and control system blocks to the model.
- Provision for reactive power compensation.
- Loading of the generator should be considered and advanced grid connection.
- Development of a customized SCIG model which allows manipulation of different machine parameters for realistic fault simulation.

The inadequacies of the statistical model can be solved by:

- Using SCADA data of at least one year to incorporate the environmental changes of all four seasons.
- Modelling only the operating region below rated output capacity.
- Separate temperature modelling at rated output capacity is recommended.

Eskom can improve the operating and maintenance strategies at Sere wind farm through:

- Implementing the proposed condition monitoring techniques on the SCIGs at Sere Wind Farm as a separate maintenance strategy to familiarize themselves with the different concepts required for optimum life cycle management.
- Assigning highly skilled engineering staff to study, develop and manage all conditioning monitoring techniques in conjunction with Siemens.
- Performing analysis of wind turbine SCADA data every three months and creating performance trends of the wind farm.
- Discussing their technical findings with Siemens and partnering to achieve continuous improvement in maintenance quality and cost.
- Ensuring that all safety, quality, engineering and financial aspects of operating the wind farm are in accordance with Eskom policies and standards.

APPENDIX A – Stepwise Regression Analysis WT4

Results of stepwise regression WT4						
Step 1 - Entering variable: Active_Power						
Summary measures						
	Multiple R	0.911				
	R-Square	0.830				
	Adj R-Square	0.830				
	StErr of Est	9.246				
ANOVA Table						
	Source	df	SS	MS	F	p-value
	Explained	1	6120828.088	6120828.088	71602.928	0.0000
	Unexplained	14646	1251983.000	85.483		
Regression coefficients						
		Coefficient	Std Err	t-value	p-value	
	Constant	33.7139	0.1118	301.4540	0.0000	
	Active_Power	0.0263	0.0001	267.5872	0.0000	
Step 2 - Entering variable: Mean_Nacelle_Tmp						
Summary measures			Change	% Change		
	Multiple R	0.9531	0.0419	%4.6		
	R-Square	0.9084	0.0782	%9.4		
	Adj R-Square	0.9083	0.0782	%9.4		
	StErr of Est	6.7922	-2.4535	-%26.5		
ANOVA Table						
	Source	df	SS	MS	F	p-value
	Explained	2	6697170.4007	3348585.2003	72583.0033	0.0000
	Unexplained	14645	675640.6875	46.1346		
Regression coefficients						
		Coefficient	Std Err	t-value	p-value	
	Constant	-8.9090	0.3901	-22.8381	0.0000	
	Active_Power	0.0206	0.0001	233.5036	0.0000	
	Mean_Nacelle_Tmp	1.7028	0.0152	111.7705	0.0000	
Step 3 - Entering variable: Mean_Ambient_Tmp						
Summary measures			Change	% Change		
	Multiple R	0.9546	0.0015	%0.2		
	R-Square	0.9112	0.0029	%0.3		
	Adj R-Square	0.9112	0.0028	%0.3		
	StErr of Est	6.6859	-0.1064	-%1.6		
ANOVA Table						
	Source	df	SS	MS	F	p-value
	Explained	3	6718214.276	2239404.759	50097.774	0.0000
	Unexplained	14644	654596.813	44.701		
Regression coefficients						
		Coefficient	Std Err	t-value	p-value	
	Constant	-15.9430	0.5025	-31.7252	0.0000	
	Active_Power	0.0192	0.0001	175.4487	0.0000	
	Mean_Nacelle_Tmp	2.3350	0.0328	71.2527	0.0000	
	Mean_Ambient_Tmp	-0.6295	0.0290	-21.6973	0.0000	

APPENDIX B – Stepwise Regression Analysis WT38

Results of stepwise regression WT38						
Step 1 - Entering variable: Active_Power						
Summary measures						
	Multiple R	0.9146				
	R-Square	0.8365				
	Adj R-Square	0.8365				
	StErr of Est	9.0915				
ANOVA Table						
	Source	df	SS	MS	F	p-value
	Explained	1	6631788.3280	6631788.3280	80234.3094	0.0000
	Unexplained	15685	1296447.8750	82.6553		
Regression coefficients						
		Coefficient	Std Err	t-value	p-value	
	Constant	34.4713	0.1190	289.7214	0.0000	
	Active_Power	0.0242	0.0001	283.2566	0.0000	
Step 2 - Entering variable: Mean_Nacelle_Tmp						
Summary measures			Change	% Change		
	Multiple R	0.9583	0.0437	%4.8		
	R-Square	0.9183	0.0818	%9.8		
	Adj R-Square	0.9183	0.0818	%9.8		
	StErr of Est	6.4255	-2.6660	-%29.3		
ANOVA Table						
	Source	df	SS	MS	F	p-value
	Explained	2	7280696.8280	3640348.4140	88172.5911	0.0000
	Unexplained	15684	647539.3750	41.2866		
Regression coefficients						
		Coefficient	Std Err	t-value	p-value	
	Constant	-15.1136	0.4044	-37.3771	0.0000	
	Active_Power	0.0189	0.0001	254.2693	0.0000	
	Mean_Nacelle_Tmp	1.9451	0.0155	125.3681	0.0000	
Step 3 - Entering variable: Mean_Ambient_Tmp						
Summary measures			Change	% Change		
	Multiple R	0.9609	0.0026	%0.3		
	R-Square	0.9234	0.0050	%0.5		
	Adj R-Square	0.9233	0.0050	%0.5		
	StErr of Est	6.2245	-0.2009	-%3.1		
ANOVA Table						
	Source	df	SS	MS	F	p-value
	Explained	3	7320598.5155	2440199.5052	62981.0323	0.0000
	Unexplained	15683	607637.6875	38.7450		
Regression coefficients						
		Coefficient	Std Err	t-value	p-value	
	Constant	-25.3452	0.5051	-50.1823	0.0000	
	Active_Power	0.0168	0.0001	175.2132	0.0000	
	Mean_Nacelle_Tmp	2.7916	0.0304	91.9546	0.0000	
	Mean_Ambient_Tmp	-0.8144	0.0254	-32.0913	0.0000	

REFERENCES

[1]   IRENA, "Renewable energy in the water, energy and food nexus," *International Renewable Energy Agency*, 2015. [Online]. Available: http://www.irena.org/documentdownloads/publications/irena_water_energy_food_nexus_2015.pdf. [Accessed: 15-Feb-2016].

[2]   IRENA, "AFRICA 2030: Roadmap For A Renewable Energy Future," 2015. [Online]. Available: http://www.irena.org/DocumentDownloads/Publications/IRENA_Africa_2030_REmap_2015_low-res.pdf. [Accessed: 03-Apr-2016].

[3]   IEA, "Africa Energy Outlook," 2014. [Online]. Available: www.iea.org. [Accessed: 18-Mar-2015].

[4]   M. Swilling and E. Annecke, *Just Transitions Explorations of sustainability in an unfair world*. UCT Press, 2012.

[5]   DoE, "Integrated Resource Plan," 2013.

[6]   Energyblog, "Energy Project Database," 2016. [Online]. Available: energgy.org.za/knowledge-tools/project-database. [Accessed: 25-May-2016].

[7]   IPCC, "Renewable energy sources and climate change mitigation: special report of the Intergovernmental Panel on Climate Change," *Choice Reviews Online*, 2012. [Online]. Available: http://www.cro3.org/cgi/doi/10.5860/CHOICE.49-6309. [Accessed: 12-Apr-2016].

[8]   IEA, "CO2 Emissions From Fuel Combustion," 2014. [Online]. Available: ww.iea.org. [Accessed: 19-Mar-2015].

[9]   REN21, "Renewables 2015 Global Status Report," 2015. [Online]. Available: www.ren21.net. [Accessed: 22-Jun-2015].

[10]   T. Bischof-niemz, "Financial Benefits of Renewables in South Africa in 2014," 2015. [Online]. Available: www.csir.co.za.

[11]   Eskom, "Eskom ' s generation plant mix," 2011. [Online]. Available: http://www.eskom.co.za/OurCompany/SustainableDevelopment/ClimateChangeCOP17/Documents/GenerationMix.pdf. [Accessed: 27-Aug-2015].

[12]   DoE, "REQUEST FOR PUBLIC PARTICPATION IN THE REVIEW OF THE REIPPPP," 2016. [Online]. Available: www.ipp-projects.co.za/Home/GetPressRelease? [Accessed: 19-Feb-2016].

[13]   C. Aubrey, "Supply Chain: The race to meet demand," *Wind Directions*, no. January/February, pp. 27–34, 2007.

[14]   E. Echavarria, B. Hahn, G. J. W. van Bussel, and T. Tomiyama, "Reliability of Wind Turbine Technology Through Time," *J. Sol. Energy Eng.*, vol. 130, no. 3, p. 31005, 2008.

[15]   K. Alewine and W. Chen, "A review of electrical winding failures in wind turbine generators," *IEEE Electr. Insul. Mag.*, vol. 28, no. 4, pp. 8–13, 2012.

[16]   B. Wu, Y. Lang, N. Zargari, and S. Kouro, *Power Conversion and Control of Wind Energy Systems*, IEEE Press. John Wiley & Sons, 2011.

[17]   Windpowermonthly, "10 biggest turbines," 2014. [Online]. Available: www.windpowermonthly.com/10-biggest-turbines. [Accessed: 22-Feb-2016].

[18]   J. . Greenblatt, "Wind as a source of energy, now and in the future," Amsterdam, 2005.

[19]   GWEC, "Global Wind Statistics 2015," 2015. [Online]. Available: www.gwec.net. [Accessed: 29-Feb-2016].

[20]   EWEA, "Wind in power," *2015 European statistics.*, 2016. [Online]. Available: http://www.ewea.org/fileadmin/files/library/publications/statistics/EWEA-Annual-Statistics-2015.pdf. [Accessed: 29-Feb-2016].

[21]   A. Nelsen, "Wind power generates 140% of Denmark's electricity demand," *The Guardian*, 2015. [Online]. Available: http://www.theguardian.com/environment/2015/jul/10/denmark-wind-windfarm-power-exceed-electricity-demand. [Accessed: 22-Oct-2015].

[22]   REN21, "SADC Renewable Energy and Energy Efficiency Status Report," 2015. [Online]. Available: http://www.ren21.net/wp-content/uploads/2015/10/REN21_webfile.pdf. [Accessed: 29-Feb-2016].

[23]   GWEC, "Global Wind Report," *Wind energy technology*, 2014. [Online]. Available: http://www.gwec.net/wp-content/uploads/2015/03/GWEC_Global_Wind_2014_Report_LR.pdf. [Accessed: 29-Feb-2016].

[24]   K. Hagemann, "SANEA Lecture Series South Africa â€™ s Wind Power Potential." 2013.

[25]   DoE, "State of Renewable Energy in South Africa," 2015. [Online]. Available: http://www.gov.za/sites/www.gov.za/files/State of Renewable Energy in South Africa_s.pdf. [Accessed: 29-Feb-2016].

[26]   DoE, "REIPPPP focus on wind," 2015.

[27]   Engineering News, "Siemens signs contracts for three new SA Wind Farms," 2016. [Online]. Available: http://www.engineeringnews.co.za/print-version/siemens-signs-contracts-for-three-new-sa-wind-farms-2015-02-18. [Accessed: 03-May-2016].

[28]   IRENA, "RENEWABLE POWER GENERATION COSTS IN 2014," 2015. [Online]. Available: www.irena.org/publications. [Accessed: 14-Aug-2015].

[29]   M. Dyrholm, "Vestas 55 000 wind turbines," *Climateaction*, 2015. [Online]. Available: www.climateactionprogramme.org. [Accessed: 23-Feb-2016].

[30]   M. I. Blanco, "The economics of wind energy," *Renew. Sustain. Energy Rev.*, vol. 13, no. 6–7, pp. 1372–1382, 2009.

[31]   N. Boccard, "Capacity factor of wind power realized values vs. estimates," *Energy Policy*, vol. 37, no. 7, pp. 2679–2688, 2009.

[32]   EWEA, "The economics of wind energy," *Renewable and Sustainable Energy Reviews*, 2009. [Online]. Available: www.ewea.org. [Accessed: 08-Mar-2016].

[33]   K. Fischer, F. Besnard, and L. Bertling, "Reliability-Centred Maintenance for Wind Turbines Based on Statistical Analysis and Practical Experience," in *IEEE Transactions on Energy Conversion*, 2011, vol. 27, no. 99, pp. 1–12.

[34]   D. Milazi and T. Bischof-Niemz, "UPDATE ON THE REIPPPP, CLEAN COAL, NUCLEAR, NATURAL GAS," in *The Sustainable Energy Resource Handbook*, 6th ed., Cape Town: alive2green, 2016.

[35]   D. L. Hoffman and T. S. Molinski, "How New Technology Developments Will Lower Wind Energy Costs," in *2009 Cigre/IEEE Pes Joint Symposium Integration of Wide-Scale Renewable Resources into the Power Delivery System*, 2009, pp. 524–530.

[36]   G. Boyle, B. Everett, and G. Alexander, *Renewable Energy - Power for a Sustainable Future*, Third. Milton Keynes: Oxford University Press, 2012.

[37]   H. Snel, "Review of the present status of rotor aerodynamics," *Wind Energy*, vol. 1, no. October, pp. 46–69, 1998.

[38]   T. Ackermann, Ed., *Wind Power in Power Systems*, Second. John Wiley & Sons, Ltd, 2012.

[39]   G. Masters, *Renewable and Efficient Electric Power Systems*. John Wiley & Sons, Inc, 2004.

[40]   R. Thresher and D. Dodge, "Trends in the evolution of wind turbine generator configurations and systems," *Wind Energy*, vol. 85, pp. 70–85, 1998.

[41]   IRENA, "Renewable Energy Technologies Cost Analysis Series : Wind Power," 2012. [Online]. Available: https://www.irena.org/documentdownloads/publications/re_technologies_cost_analysis-wind_power.pdf. [Accessed: 23-Oct-2015].

[42]   K. Y. Maalawi and M. A. Badr, "A practical approach for selecting optimum wind rotors," *Renew. Energy*, vol. 28, no. 5, pp. 803–822, 2003.

[43]   R. Howell, N. Qin, J. Edwards, and N. Durrani, "Wind tunnel and numerical study of a small vertical axis wind turbine," 2010.

[44]   S. Eriksson, H. Bernhoff, and M. Leijon, "Evaluation of different turbine concepts for wind power," *Renew. Sustain. Energy Rev.*, vol. 12, no. 5, pp. 1419–1434, 2008.

[45]   M. Islam, D. S. K. Ting, and A. Fartaj, "Aerodynamic models for Darrieus-type straight-bladed vertical axis wind turbines," *Renew. Sustain. Energy Rev.*, vol. 12, no. 4, pp. 1087–1109, 2008.

[46]   L. Y. Pao and K. E. Johnson, "A tutorial on the dynamics and control of wind turbines and wind farms," in *American Control Conference, 2009. ACC '09.*, 2009, pp. 2076–2089.

[47]   P. . Shankar, "Development of vertical axis wind turbines," in *Rural Technol Indian Academy of Science*, 1980, pp. 145–162.

[48]   M. Ragheb, "Vertical axis wind turbines," 2013. [Online]. Available: http://mragheb.com/NPRE 475 Wind Power Systems/Vertical Axis Wind Turbines.pdf. [Accessed: 14-Mar-2016].

[49]   B. F. Blackwell and L. V Feltz, "Wind Energy - A Revitalized Pursuit," 1975.

[50]   R. C. Reuter and M. H. Worstell, "Torque ripple in a vertical axis wind turbine," 1978.

[51] O. Ågren, M. Berg, and M. Leijon, "A time-dependent potential flow theory for the aerodynamics of vertical axis wind turbines," *J. Appl. Phys.*, vol. 97, no. 10, 2005.

[52] J. Aho, A. Buckspan, and J. H. Laks, "A tutorial of wind turbine control for supporting grid frequency through active power control," in *Proc. of the American Control Conference*, 2012, no. March, pp. 3120–3131.

[53] P. W. Carlin, A. S. Laxson, and E. B. Muljadi, "The history and state of the art of variable-speed wind turbine technology," *Wind Energy*, vol. 6, no. 2, pp. 129–159, 2003.

[54] R. Gasch and J. Twele, *Wind Power: Fundamentals, Design, Construction and Operation.* Springer-Verlag Berlin Heidelberg, 2011.

[55] J. D. M. De Kooning, L. Gevaert, J. Van De Vyver, T. L. Vandoorn, and L. Vandevelde, "Online estimation of the power coefficient versus tip-speed ratio curve of wind turbines," in *IECON Proceedings (Industrial Electronics Conference)*, 2013, pp. 1792–1797.

[56] D. Saheb-Koussa, M. Haddadi, M. Belhamel, M. Koussa, and S. Noureddine, "Modeling and simulation of windgenerator with fixed speed wind turbine under matlab-simulink," *Energy Procedia*, vol. 18, pp. 701–708, 2012.

[57] G. Bustos, L. S. Vargas, F. Milla, D. Sáez, H. Zareipour, and A. Nuñez, "Comparison of Fixed Speed Wind Turbines Models : A Case Study," 2012.

[58] H. Polinder, D. Bang, H. Li, Z. Chen, and M. Mueller, "Concept report on generator topologies, mechanical and electromagnetic optimization," *Proj. Upwind*, 2007.

[59] P. Chirapongsananurak and S. Santoso, "Harmonic analysis for fixed-speed wind turbines," 2013.

[60] S. S. Murthy, B. Singh, P. K. Goel, and S. K. Tiwari, "A Comparative Study of Fixed Speed and Variable Speed Wind Energy Conversion Systems Feeding the Grid," in *2007 7th International Conference on Power Electronics and Drive Systems*, 2007, pp. 736–743.

[61] M. Bradt, B. Badrzadeh, E. Camm, D. Mueller, J. Schoene, T. Siebert, T. Smith, M. Starke, and R. Walling, "Harmonics and resonance issues in wind power plants," 2012.

[62] M. F. Mimouni, M. N. Mansouri, and M. Mansour, "A Comparative Study of Fixed Speed and Variable Wind Generator with Pitch Angle Control."

[63] F. Blaabjerg, Z. Chen, R. Teodorescu, and F. Iov, "Power electronics in wind turbine systems," 2006.

[64] T. Burton, D. Sharpe, N. Jenkins, and E. Bossanyi, *Wind Energy Handbook*, vol. 53, no. 9. Chichester, England: John Wiley & Sons, Ltd, 2001.

[65] A. D. Hansen and L. H. Hansen, "Wind turbine concept market penetration over 10 years (1995-2004)," *Wind Energy*, vol. 10, no. 1, pp. 81–97, 2007.

[66] S. J. Johnson, C. P. C. Van Dam, and D. E. Berg, "Active Load Control Techniques for Wind Turbines," 2008. [Online]. Available: http://windpower.sandia.gov/other/084809.pdf. [Accessed: 13-Apr-2016].

[67] Vestas, "Turbine wind class." [Online]. Available: http://cvi.se/uploads/pdf/Master Literature/Wind Turbine Technology/Turbine_wind_class.pdf. [Accessed: 04-Apr-2016].

[68] A. Luipion-Romero, "Wind Power Technology Part 2. Unpublished class notes (Wind Energy 844 Module). Stellenbosch: Sustainability Institute." 2015.

[69] J. Serrano-Gonzalez and R. Lacal-Arantegui, "Technological evolution of onshore wind turbines—a market-based analysis," *Wind Energy*, 2016.

[70] E. Hau, *Wind turbines: Fundamentals, technologies, application, economics*, Second., vol. 9783642271. Springer, 2013.

[71] L. Hansen, L. Helle, F. Blaabjerg, E. Ritchie, S. Munk-Nielsen, H. Bindner, P. Sorensen, and B. Bak-Jensen, "Conceptual survey of Generators and Power Electronics for Wind Turbines," *Electrical Design and Control*, 2001. [Online]. Available: http://calvin.edu/~pribeiro/courses/Power Systems Interim/wind-generator-types.pdf. [Accessed: 17-Apr-2016].

[72] A. Wallace and J. Oliver, "Variable Speed Generation Controlled by Passive Elements," in *International Conference on Electrical Machines Volume 2*, 1998, pp. 240–245.

[73] T. Ackermann, *Wind Power in Power Systems*, vol. 8. Stockholm: John Wiley & Sons, Ltd, 2005.

[74] H. Li and Z. Chen, "Overview of different wind generator systems and their comparisons," 2007.

[75] S. Mohammad, N. Das, and S. Roy, "A Review of the State of the Art of Generators and Power Electronics Converter Topologies for Wind," vol. 3, no. 3, pp. 283–291, 2013.

[76] A. Manaullah and A. Hemant Ahuja, "Performance comparison of standalone SCIG and PMSG-based wind energy conversion systems," in *International Conference on Innovative Applications of Computational Intelligence on Power, Energy and Controls with their Impact on Humanity*, 2014, no. November, pp. 285–290.

[77] S. Muller, M. Deicke, and R. De Doncker, "Doubly Fed Induction Generator Systems for Wind Turbines," *IEEE Industrial Applications Magazine*, pp. 26–33, 2002.

[78] S. Soter and R. Wegener, "Development of Induction Machines in Wind Power Technology," 2007.

[79] H. Polinder, D. Bang, H. Li, and Z. Chen, "CONCEPT REPORT on GENERATOR TOPOLOGIES , MECHANICAL & ELECTROMAGNETIC OPTIMIZATION," 2007.

[80] H. Polinder, J. A. Ferreira, B. B. Jensen, A. B. Abrahamsen, K. Atallah, and R. a. McMahon, "Trends in Wind Turbine Generator Systems," *IEEE J. Emerg. Sel. Top. Power Electron.*, vol. 1, no. 3, pp. 174–185, 2013.

[81] N. Mohan, T. Undeland, and W. Robbins, *Power Electronics: Converters, Applications and Design*, 3rd ed. John Wiley & Sons, Inc, 2002.

[82] T. Haskew and R. Challoo, "Characteristic study for integration of fixed and variable speed wind turbines into transmission grid," in *2008 IEEE/PES Transmission and Distribution Conference and Exposition*, 2008, pp. 1–9.

[83] H. Polinder, F. F. A. Van Der Pijl, G. J. De Vilder, and P. J. Tavner, "Comparison of direct-drive and geared generator concepts for wind turbines," in *IEEE Transactions on Energy Conversion*, 2006, vol. 21, no. 3, pp. 725–733.

[84] Y. Chen, P. Pillay, A. Khan, and S. Member, "PM Wind Generator Topologies," *IEEE Trans. Ind. Appl.*, vol. 41, no. 6, pp. 1619–1626, 2005.

[85] N. Bianchi and A. Lorenzoni, "Permanent Magnet Generators for Wind Power Industry: An Overall Comparison with Traditional Generators," in *Opportunities and Advances in International Power Generation, IEE Conference on*, 1996, no. March, pp. 49–54.

[86] A. Gupta, D. K. Jain, and S. Dahiya, "Some Investigations on Recent Advances in Wind Energy Conversion Systems," 2012, vol. 28, pp. 47–52.

[87] M. D. Platzer, "US Wind Turbine Manufacturing: Federal Support for an Emerging Industry," 2012.

[88] R. D. Gowdar and M. C. Mallikarjune Gowda, "Reasons for wind turbine generator failures: a multi-criteria approach for sustainable power production," *Renewables Wind. Water, Sol.*, vol. 3, no. 1, p. 9, 2016.

[89] S. Sheng, "Report on Wind Turbine Subsystem Reliability - A Survey of Various Databases," 2013.

[90] P. Tavner, F. Spinato, G. van Bussel, and E. Koutoulakos, "Reliability of Different Wind Turbine Concepts with Relevance to Offshore Application," 2008.

[91] F. Carlsson, E. Eriksson, and M. Dahlberg, "Damage preventing measures for wind turbines Damage preventing measures for wind turbines Phase 1- Reliability data," 2010.

[92] B. Hahn, M. Durstewitz, and K. Rohrig, "Reliability of Wind Turbines," *Wind Energy*, pp. 1–4, 2007.

[93] U. Shipurkar, K. Ma, H. Polinder, F. Blaabjerg, and J. A. Ferreira, "A review of failure mechanisms in wind turbine generator systems," *2015 17th Eur. Conf. Power Electron. Appl. (EPE'15 ECCE-Europe)*, pp. 1–10, 2015.

[94] J. L. H. Silva and A. J. M. Cardoso, "Bearing failures diagnosis in three-phase induction motors by extended Park's Vector approach," in *IECON Proceedings (Industrial Electronics Conference)*, 2005, vol. 2005, pp. 2591–2596.

[95] IAS Motor Reliability Working Group, "Report of Large Motor Reliability Survey of Industrial and Commercial Installations Part 1," *IEEE Trans. Ind. Appl.*, vol. IA-4, July, no. 4, pp. 853–872, 1985.

[96] P. Albrecht, J. Appiarius, R. McCoy, E. Owen, and D. Sharma, "Assessment Of The Reliability Of Motors In Utility Applications - Updated," *IEEE Trans. Energy Convers.*, vol. EC-1, no. 1, pp. 39–46, 1986.

[97] M. Irfan, N. Saad, R. Ibrahim, and V. S. Asirvad, "Development of an n Intelligent Condition Monitoring System for AC C Induction Motors using g PLC," pp. 789–794, 2013.

[98] W. Yin, "Failure Mechanism of Winding Insulations in Inverter-Fed Motors," *IEEE Electrical Insulation Magazine*, pp. 18–23, Nov-1997.

[99]   A. H. Bonnett and G. C. Soukup, "Cause and Analysis of Stator and Rotor Failures in Three-Phase Squirrel Cage Induction Motors," *IEEE Trans. Ind. Appl.*, vol. 28, no. 4, 1992.

[100]   G. Gao and W. Chen, "Design challenges of wind turbine generators," *2009 IEEE Electr. Insul. Conf.*, no. June, pp. 146–152, 2009.

[101]   H. Li and R. Curiac, "Improvements in Energy Efficiency of Induction Motors," PCIC-2011-42, 2011.

[102]   H. de Swardt, "Electric Motor Failure Prevention: Wedge Failures," *Energizer*, 2007. [Online]. Available: http://www.mandc.co.za/pdfs/Electric_Motor_Failure_Wedges.pdf. [Accessed: 12-May-2016].

[103]   K. Alewine and C. Wilson, "Magnetic wedge failures in wind turbine generators," in *2013 IEEE Electrical Insulation Conference, EIC 2013*, 2013, no. June, pp. 244–247.

[104]   M. E. H. Benbouzid, "A Review of Induction Motors Signature Analysis as a Medium for Faults Detection," *Power*, vol. 47, no. 5, pp. 1950–1955, 1998.

[105]   IAS Motor Reliability Working Group, "Report of Large Motor Reliability Survey of Industrial and Commercial Installations Part 2," *IEEE Trans. Ind. Appl.*, vol. IA-21, Jul, no. 4, pp. 853–872, 1985.

[106]   J. L. Coetzee, *Maintenance*. Hatfield: Maintenance Publishers (Pty) Ltd, 1997.

[107]   L. R. Higgins, R. K. Mobley, and D. J. Wikoff, *Maintenance engineering handbook*, Seventh., vol. 6. McGraw-Hill Companies, 2002.

[108]   Z. Tian, T. Jin, B. Wu, and F. Ding, "Condition based maintenance optimization for wind power generation systems under continuous monitoring," *Renew. Energy*, vol. 36, no. 5, pp. 1502–1509, 2011.

[109]   K. K. Agrawal, G. N. Pandey, and K. Chandrasekaran, "Analysis of the condition based monitoring system for heavy industrial machineries," in *2013 IEEE International Conference on Computational Intelligence and Computing Research, IEEE ICCIC 2013*, 2013, pp. 1–4.

[110]   A. K. Jardine, D. Lin, and D. Banjevic, "A review on machinery diagnostics and prognostics implementing condition-based maintenance," *Mech. Syst. Signal Process.*, vol. 20, pp. 1483–1510, 2006.

[111]   F. Ding, Z. Tian, and T. Jin, "Maintenance modeling and optimization for wind turbine systems: A review," in *2013 International Conference on Quality, Reliability, Risk, Maintenance, and Safety Engineering (QR2MSE)*, 2013, pp. 569–575.

[112]   O. Thorsen and M. Dalva, "A survey of the reliability with an analysis of faults on variable frequency drives in the industry," *Conf. Power Electron. Appl.*, vol. 31, no. 5, 1995.

[113]   W. Yang, P. Tavner, J. Crabtree, Y. Feng, and Y. Qiu, "Wind turbine condition monitoring: technical and commercial challenges," *Wind Energy*, vol. 17, no. April 2013, pp. 657–669, 2014.

[114]   P. Tchakoua, R. Wamkeue, M. Ouhrouche, F. Slaoui-Hasnaoui, T. A. Tameghe, and G. Ekemb, "Wind turbine condition monitoring: State-of-the-art review, new trends, and future challenges," *Energies*, vol. 7, no. 4, pp. 2595–2630, 2014.

[115] P. Tchakoua, R. Wamkeue, T. A. Tameghe, and G. Ekemb, "A review of concepts and methods for wind turbines condition monitoring," *2013 World Congr. Comput. Inf. Technol.*, vol. 2, no. 1, pp. 1–9, 2013.

[116] F. P. García Márquez, A. M. Tobias, J. M. Pinar Pérez, and M. Papaelias, "Condition monitoring of wind turbines: Techniques and methods," *Renew. Energy*, vol. 46, pp. 169–178, 2012.

[117] Y. Ding, L. Ntaimo, and E. Byon, "Optimal Maintenance Strategies for Wind Turbine Systems Under Stochastic Weather Conditions," *IEEE Trans. Reliab.*, vol. 59, no. 2, pp. 393–404, 2010.

[118] H. Merabet, T. Bahi, and N. Halem, "Condition Monitoring and Fault Detection in Wind Turbine Based on DFIG by the Fuzzy Logic," *Energy Procedia*, vol. 74, pp. 518–528, 2015.

[119] C. Hellier, *Handbook of Nondestructive Evaluation*. McGraw-Hill, 2003.

[120] M. Schlechtingen and I. Ferreira, "Comparative analysis of neural network and regression based condition monitoring approaches for wind turbine fault detection," *Mech. Syst. Signal Process.*, vol. 25, no. 5, pp. 1849–1875, 2011.

[121] G. . Stone, E. . Boulter, I. Culbert, and H. Dhirani, *Electrical Insulation for Rotating Machines*. IEEE Press, 2004.

[122] W. Yang, R. Court, and J. Jiang, "Wind turbine condition monitoring by the approach of SCADA data analysis," *Renew. Energy*, vol. 53, pp. 365–376, 2013.

[123] C. S. Gray, F. Langmayr, N. Haselgruber, and S. J. Watson, "A Practical Approach to the Use of SCADA Data for Optimized Wind Turbine Condition Based Maintenance," in *EWEA Offshore*, 2011.

[124] K. Kim, G. Parthasarathy, O. Uluyol, W. Foslien, S. Sheng, and P. Fleming, "Use of SCADA Data for Failure Detection in Wind Turbines," in *Energy Sustainability Conference and Fuel Cell Conference*, 2011, no. October.

[125] P. Sun, J. Li, Y. Yan, X. Lei, and X. Zhang, "Wind Turbine Anomaly Detection Using Normal Behavior Models based on SCADA Data," in *High Voltage Engineering and Application (ICHVE)*, no. 1, pp. 1–4.

[126] M. Wilkinson, B. Darnell, T. Van Delft, and K. Harman, "Comparison of methods for wind turbine condition monitoring with SCADA data," *IET Renew. Power Gener.*, vol. 8, no. 4, pp. 390–397, 2014.

[127] J. Herp and E. Nadimi, "Wind Turbine Fault Detection based on Artificial Neural Networks Analysis of SCADA data," in *EWEA Offshore*, 2015, no. March, p. 2015.

[128] K. B. Abdusamad, D. W. Gao, and E. Muljadi, "A Condition Monitoring System for Wind Turbine Generator Temperature by Applying Multiple Linear Regression Model," in *North America Power Symposium (NAPS)*, 2013.

[129] B. Lu, Y. Li, X. Wu, and Z. Yang, "A Review of Recent Advances in Wind Turbine Condition Monitoring and Fault Diagnosis," 2012.

[130] W. Yang, P. Tavner, and M. Wilkinson, "Condition monitoring and fault diagnosis of a wind turbine synchronous generator drive train," *Renew. Power Gener. IET*, vol. 1, no. 1, pp. 10–16, 2007.

[131] Y. Amirat, M. E. H. Benbouzid, E. Al-Ahmar, B. Bensaker, and S. Turri, "A brief status on condition monitoring and fault diagnosis in wind energy conversion systems," *Renew. Sustain. Energy Rev.*, vol. 13, no. 9, pp. 2629–2636, 2009.

[132] S. Nandi, H. A. Toliyat, and X. Li, "Condition monitoring and fault diagnosis of electrical motors - A review," *IEEE Trans. Energy Convers.*, vol. 20, no. 4, pp. 719–729, 2005.

[133] Y. Han and Y. H. Song, "Condition monitoring techniques for electrical equipment-a literature survey," *IEEE Trans. Power Deliv.*, vol. 18, no. 1, pp. 4–13, 2003.

[134] S. Djurovic, S. Williamson, P. Tavner, and W. Yang, "Condition monitoring artefacts for detecting winding faults in wind turbine DFIGs," in *European Wind energy Conference and Exhibition*, 2009, no. April.

[135] C. Jeong, S. Lee, and J. Hur, "Early Detection Technique for Stator Winding Inter-Turn Fault in BLDC Motor using Input Impedance," pp. 4453–4459, 2013.

[136] T. Karthik and G. . Raju, "NEW CRITERION FOR STATOR INTER TURN FAULT DETECTION OF SYNCHRONOUS GENERATOR."

[137] M. R. Patel, *Wind and Solar Power System*, Second. CRC Press, 2006.

[138] O. Anaya-Lara, N. Jenkins, J. Ekanayake, P. Cartwright, and M. Hughes, *Wind Energy Generation*. John Wiley & Sons, Ltd, 2009.

[139] S. Heier, *Grid Integration of Wind Energy Conversion Systems*. John Wiley & Sons, Ltd, 2006.

[140] J. Pyrhonen, T. Jokinen, and V. Hrabovcova, *DESIGN OF ROTATING ELECTRICAL MACHINES*. John Wiley & Sons, Ltd, 2008.

[141] I. Boldea and S. Nasar, *The Induction Machine Handbook*. CRC Press, 2002.

[142] IEEE Machinery Committee, "IEEE Standard Test Procedure for Polyphase Induction Motors and," 2004.

[143] F. Iov, A. D. Hansen, P. Sørensen, and F. Blaabjerg, "Simulation Platform to Model , Optimize and Design Wind Turbines," 2004.

[144] D. Montgomery and G. Runger, *APPLIED STATISTICS AND PROBABILITY FOR ENGINEERS*, Sixth. Wiley, 2014.

[145] R. Walpole, R. Myers, S. Myers, and K. Ye, *Probability and Statistics for Engineers and Scientists*, Ninth. Prentice Hall, 2012.

[146] Andale, "How to draw a normal probablity plot," *Statistics How To*, 2013. [Online]. Available: http://www.statisticshowto.com/normal-probability-plot/. [Accessed: 14-Nov-2016].

[147] R. Darlington and A. Hayes, *Regression Analysis and Linear Models. Concepts, Applications and Implementation*. The Guilford Press, 2016.

[148] H. Douglas, P. Pillay, and P. Barendse, "The detection of interturn stator faults in doubly-fed induction generators," in *Conference Record - IAS Annual Meeting (IEEE Industry Applications Society)*, 2005, vol. 2, pp. 1097–1102.

[149] T. Bishop, "Understanding Motor Temperature Rise Limits," *Electro Mech. Auth.*, no. November, pp. 1–3, 2003.